Sari Agricultural & natural Resources University

Genetics and Agricultural Biotechnology Institute of Tabarestan

Journal of Plant Molecular Breeding

December 2022, Volume 10, Issue 2

ISSN: 2322-3332

Printed in January 2024

JPMB

Contact

Sari Agricultural Sciences and Natural Resources University, Genetics and Agricultural Biotechnology Institute of Tabarestan, Sari, P.O. Box: 578, Iran.
Tel: +98-11-33687577
Email: jpmbjournal@sanru.ac.ir
www.jpmb-gabit.ir

Message from the Editor-in-Chief

JPMB is an open-access journal that serves as an advanced forum for research findings in plant molecular genetics and breeding along with other related areas such as plant biology, physiology, taxonomy, stresses, and interactions with other organisms. The journal publishes original research articles, reviews, reports, conference proceedings (peer-reviewed full articles), and short communications. In original research papers, full experimental details must be provided. We also encourage the submission of lab protocols, data management protocols, and analytical procedures in sufficient detail on topics of interest to the plant research community.

Editorial Board

Aims and Scope

Journal of Plant Molecular Breeding | JPMB is an international, open-access, peer-reviewed, biannual scholarly publication that aims to offer comprehensive coverage of progress in the field of plant molecular breeding. It seeks to present findings to researchers, academics, and students, addressing the growing demand for applied plant improvement technologies, tools, and methodologies.

- Genetic engineering (transformation)
- Micropropagation and plant breeding
- Molecular markers and plant genetic diversity
- Plant functional genomics
- Germplasm assessments for genetic diversity
- Plant breeding technologies
- Plant mutation breeding
- Metabolomics and metabolites engineering in plant breeding
- Plant breeding for abiotic and biotic stresses
- Plant Molecular biology
- Plant Omics and Bioinformatics

Visit our main website https://www.jpmb-gabit.ir/ for more information including contact details.

Contents

2022 |
Volume 10 |
Issue 2

JPMB | Journal of Plant Molecular Breeding
Published by Genetics and Agricultural Biotechnology Institute of Tabarestan
2022 | Volume 10 | Issue 2

Genetic basis of drought tolerance in Iranian rice (*Oryza sativa* L.) recombinant lines at vegetative and reproductive stages

Original paper

Morteza Noryan [1], Islam Majidi Harvan [1], Hossein Sabouri *[2], Farokh Darvish Kojouri [1]

[1] Plant Breeding and Biotechnology Department, Science and Research Branch, Islamic Azad University, Tehran, Iran
[2] Department of Plant Production, Faculty of Agricultural and Natural resources Sciences, Gonbad Kavoos University, Iran

Abstract: To evaluate the genetic basis of drought tolerance in rice, an experiment was conducted using 120 recombinant inbred lines (RILs) derived from Neda × Ahlamitarom cross. A factorial experiment based on completely randomized design with three replications was used under greenhouse conditions setting at Gonbad Kavous University. In this study, Polyethylene Glycol (PEG) 6000 was employed to induce osmotic stress (at levels of −4.5 and −9 bar) during both vegetative and reproductive stages. In addition to assessing root and shoot morphological characters, genetic linkage map was constructed using Simple Sequence Repeat (SSR), Inter Primer Binding Site (iPBS), Inter-Retrotransposon Amplified Polymorphism (IRAP), and Inter Simple Sequence Repeats (ISSR) markers. Sixteen Quantitative Trait Loci (QTLs) were identified during vegetative growth stage, while twenty QTLs were identified during the reproductive stage. Through a comparative analysis of the three evaluated treatments, the qRN-12, qRS-11, and qRV-12 lines were determined as stable QTLs suitable for the selection of drought-tolerant lines at the vegetative stage under varying conditions. Several new alleles associated with drought-tolerant QTLs were identified in this study. Notably, in two distinct environmental conditions, crucial QTLs, such as qNTF-12 and qNL-3, related to the numbers of fertile tillers and leaves, were identified as stable QTLs at the reproductive stage. The QTLs identified at vegetative and reproductive stages in this study can serve as stable and major QTLs for selecting drought-tolerant lines in marker-assisted selection (MAS).

Keywords: major QTL, osmotic stress, quantitative trait loci, rice.

OPEN ACCESS

Edited by
Dr. Ahmad Arzani,
Isfahan University of Technology, Iran

Date
Received: 2 February 2023
Accepted: 22 May 2023
Published: 20 December 2023

Correspondence
Dr. Hossein Sabouri
hos.sabouri@gmail.com

Citation
Noryan, M., Majidi Harvan, I., Sabouri, H., and Darvish Kojouri, F. (2022). Genetic structure of drought tolerance in Iranian rice (*Oryza sativa*) recombinant lines at vegetative and reproductive stages. *J Plant Mol Breed* 10(2): 1-18. doi:10.22058/jpmb.2023.1989048.1270.

Introduction

Rice (*Oryza sativa* L.) is a staple food consumed regularly and plays a crucial role in ensuring the food security over half the world's population. Global rice production is projected to increase significantly, with estimates ranging from 58 to 567 million tons (Mt) by 2030 (Mohidem et al., 2022). Rice constitutes the primary food source for overhalf of the population in 60% of the world (Mohidem et al., 2022), with its derivatives contributing to 70% of their energy requirements.

Drought stands out as the major environmental constraint to rice production and yield stability in rainfed areas. Asia emerged as the most drought-affected region from 2003 to 2013, experiencing a 40% of total crop and livestock production resulting in losses totaling 28 billion USD (Rajurkar et al., 2021). The imperative to improve rice adaptation to drought and drought- resilient varieties is growing in significance, especially in light of the diminishing agricultural water resources worldwide (Pandey and Shukla, 2015). Drought is the foremost environmental factor that often negatively affects cereal yield. Therefore, improving drought tolerance becomes a crucial objective in cereal breeding programs (Aliyu et al., 2011; Giasi Oskoei et al., 2014). As outlined by Kramer and Boyer (1995), water scarcity can manifest during the early growing season or at any point from flowering to the grain filling, with stress severity contingent upon the duration and frequency of stress occurrences. A study indicates that stress application causes changes in plant roots, promoting increased water absorption. During drought stress exposure, water is typically scarce in the soil surface layer, prompting the the main plant root to grow deeper to cope with drought stress and enhance water absorption. On the other hand, lateral root development is inhibited under drought stress (Zhang et al., 2010).

The detrimental effect of drought stress is directly associated with reduced biomass production (Ji et al., 2012). Drought also caused significant reductions in seedling wet and dry weights. Jongdee (2001) observed that drought stress reduced leaf development and tillering, thereby lowering the photosynthetic rate and leaf surface area because of early aging. All these factors reduce grain yield in drought conditions (Price and Courtois, 1999; Fischer et al., 2012). Drought stress inflicts irreparable damage to rice at both vegetative and reproductive stages. Furthermore,, the genotype × environment (GE) relationship is a challenge for producers and has been reported to to hinder progress in quantitative trait selection. Due to the GE relationship, QTL that are important in an environment may not be important in phenotype determination in another environment (Sarayloo et al., 2015; Shirmohammadli et al., 2018). Accordingly, QTLs showing the quantitative GE relationship among a series of environments were reported to be appropriate in MAS programs (Zhang et al., 2010; Noryan et al., 2021). Three QTLs associated with yield, biomass, and reduced harvest index under drought stress were identified in pot experiments conducted over two consecutive years (Wang et al., 2007).

Multiple QTLs have been reported for rice yield and yield components under a variety of drought stress (Lilley et al., 1996; Price and Courtois, 1999; MacMillan et al., 2006). Drought tolerance is a complicated feature associated with many genes affected by the responses of interested components, which may be different in interaction with types, severity, and duration of water shortage. Furthermore, most crop traits are expressed differently in normal and stressful conditions and are influenced by environmental factors (Lilley et al., 1996; Aliyu et al., 2011; Babu et al., 2014). Until recently, breeding programs have focused on above-ground traits and direct selection for yield per se, while the crop's "hidden-half," i.e., the roots have been largely overlooked. Plant roots are important organs in determining grain productivity driven by water uptake and nutrient acquisition (Alahmad et al., 2019).

A qLA-4 for seed toxicity on chromosome 4 in a RIL produced from IR26/Jiucaiqing in drought stress and non-stress conditions detected (Price and Courtois, 1999; Zhang et al., 2010). Five stable QTLs among 24 cases were identified for drought-related traits at the reproductive stage of rice under the stress of PEG and flooded conditions (Sabouri, 2007).

Wang et al. (2005) identified stress-tolerant QTLs in rice mainly at the reproductive stage. However, limited reports are available on stress-tolerant QTLs

at the germination stage of rice seeds. MacMillan et al. (2006) found Six QTLs for root traits of rice in four different treatments. Most of the QTLs were the same for a single trait in four different environments. QTLs were reported for rice yield and yield components under various types of drought stress in numerous experiments. Babu et al. (2014) identified five QTLs for grain yield in a population of two CT9993/IR62266 varieties under drought stress in southern India.

The rise in abiotic stresses such as drought, salinity, and submergence significantly hinders increases in rice. Developing a rice variety with inherent tolerance against these major abiotic stresses will help achieve a sustained increase in rice production under unfavorable conditions (Muthu et al., 2020). The current study aimed to evaluate the drought tolerance of two genotypes derived from Neda × Ahlamitarom varieties, identify drought tolerance-related QTLs, and pinpoint the locations of molecular markers linked to QTLs controlling rice traits at vegetative and reproductive stages in drought stress and normal conditions.

Materials and Methods

Phenotypic evaluation

In this study, the plant material was 120 F_8 RILs derived from Neda × Ahlamitarom varieties (Ahlamitarum and Neda cultivars are tolerant and sensitive to salinity, drought stress, and deficiencies of some mineral elements. These cultivars were selected to undergo different biotic and abiotic stresses during different breeding programs of the Iranian *O. sativa* germplasm at Gonbad Kavous University.) to evaluate root and seedling morphological characters under osmotic stress treatment at the vegetative and reproductive stages. In the present study, two independent trials were carried out as follows. In the first experiment, the stress was applied until the end of the vegetative stage and before the reproductive stage, so the plants were harvested and the traits were recorded. In the second experiment, the plants were subjected to stress from the maximum tillering stage until ripening. Both experiments were conducted using a factorial experiment based on the completely randomized design with three replications in the greenhouse of Gonbad Kavous University. The two factors included in this study were lines and stress status.

During the vegetative stage, the grains of experimental lines initially germinated in Petri dishes. Subsequently, germinated seedlings were transferred to pots with 40 cm height and 30 cm diameter, with three seedlings planted per pot. Each line was evaluated in three replications of three treatments, control (EC = 0.850 dS/m) and two drought treatments (−4.5 and −9 bar). Osmotic stress was applied using a solution of water and PEG 6000. The PEG concentration used to produce the required potential was obtained from Eq. (Michel and Kaufmann, 1973).

$$\varphi = -(1.18 \times 10\text{-}2)\, C - (1.18 \times 10\text{-}4)\, C2 + (2.67 \times 10\text{-}4)\, CT + (8.39 \times 10\text{-}7)\, C2T$$

In this equation, φ is the osmotic potential, C is PEG 6000 concentration (g/l), and T is the temperature (°C).

During the reproductive stage, the seeds of experimental lines initially germinated in Petri dishes. Subsequently, germinated seedlings were transferred to pots, three seedlings planted per pot. Each line was evaluated in three replications of two treatments, control (EC = 0.850 dS/m) and drought treatments (−9 bar).

Both treatments underwent nutritional operations and the control of pests and diseases. Each pot was fed with 1 g of a rice-specific complete fertilizer (N:15%, P_2O_5 15%, K_2O 30%, Mg 1%, and Fe 1 mg with chelated Fe) three times at the beginning of growth, 3 weeks after planting seedlings, and the beginning of heading. Diazinon 10% G (1 g per pot) was used for pest control. Other crop operations, including fertilizing, weed control, and pest/disease control, were carried out at appropriate times. Plant morphologic traits were recorded from the beginning of the reproductive period. The studied traits were stem diameter, total panicle weight, flag leaf width, flag leaf length, fertile tiller number, total tiller number, panicle length, stem wet weight, root wet weight, root volume, drought number, root area, root area density in both stress and non-stress environments (Golesorkhy et al., 2016). Plant leaf chlorophyll content was measured three times by a chlorophyll content meter (CL-01). To compare osmotic stress tolerance in the lines, phenotypic scores were recorded after the application of stress conditions (Lanceras et al., 2004) every 4 days until

harvest time (Table 1). Final firing symptoms for leaf drought resistance at the vegetative stage (Loresto, 1981) were used for determination of plant reaction against osmotic stress. Collected data were analyzed using SAS Ver. 9.1 software.

Genotypic evaluation

DNA was extracted from fresh leaves of both lines and parents using the CTAB method (Saghai Maroof et al., 1994). SSR markers on chromosome 12 were specified from the related website (http://www.gramene.org). The polymerase chain reaction (PCR) at a volume of 10 µl was performed for each DNA sample (Zahedi et al., 2019). For this test, 2 µl of diluted genomic DNA was first partitioned in each PCR tube. Then, 8 µl of the PCR solution (other than genomic DNA) was added to each tube and shaken gently. To prepare the reaction mixture, double-distilled water, a stock solution (containing 0.04 unit/µl of *Taq* DNA polymerase, PCR buffer at 1xfinal concentration, 50 mM of $MgCl_2$, 10 mM of dNTPs, and 0.5-0.75 ng of diluted DNA), and 60 ng of each of forward and reverse primers were added to a 1.5 ml microtube. The reaction mixture was then centrifuged and partitioned in DNA-containing tubes. Finally, 4 µl of inorganic oil was poured into each tube to prevent the evaporation of contents. PCR tubes were placed in a thermocycler (iCycler, BIORAD, USA). Temperature cycles for SSR markers included initial denaturation (at 95 °C for 2.5 min), 35 cycles with denaturation (at 95 °C for 1 min), primer annealing at their specific temperatures (for 30 sec), elongation (at 72 °C for 30 sec), and final amplification (at 72 °C for 5 min). Temperature cycles for ISSR, iPBS and IRAP markers consisted of initial denaturation (at 95 °C for 5 min), denaturation (at 95 °C for 1 min), 10 cycles of primer annealing (at 42-54 °C for 1 min), elongation (at 72 °C for 1 min), 25 cycles of primer annealing at their specific temperatures (for 45 sec), and final amplification (at 72 °C for 5 min). PCR products were separated using 6% denaturing polyacrylamide gel electrophoresis. The bands were visualized by the rapid silver staining (Caetano-Anollés and Gresshoff, 1994).

Linkage map and analysis of QTLs

A genetic map obtained from SSR and ISSR markers was produced using QTXB17 Map Manager software (Shirmohammadli et al., 2018). The genetic map was constructed by genotyping 120 genotypes of the F_8 generation from the Neda and Ahlamitarom varieties using 30 SSR (McCouch, 1997) and 15 ISSR (Mohd Ikmal et al., 2021; Noryan et al., 2021) markers. An expected ratio of 1:1 was created for the segregation of tested lines for the employed markers using the χ^2 test by Map Manager Software. To assign each marker to the relevant chromosome, the obtained linkage groups were compared with genetic maps proposed Chen et al. (2007) and McCouch (1997). The recombinant ratios between the markers were converted to the map unit (cM) using a previous map function (Chen et al., 2007). QTLs were detected using composite interval mapping (CIM) with a LOD score threshold of 3.0 using QTL Cartographer (Noryan et al., 2021).

Table 1. Scores and firing symptoms for leaf drought resistance at the vegetative stage.

Scores	Reaction	Leaf firing
0	Highly resistant	No symptoms of stress
1	Resistant	Slight leaf tip drying
3	Moderately resistant	Leaf tip drying extended to ¼ in the top three leaves
5	Intermediate	Half of the younger leaf blades dried, and all lower leaves dried
7	Susceptible	¾ of younger leaf blade dried
9	Highly susceptible	All leaves dried

Results

ANOVA and correlations at the vegetative stage

The results of analysis of variance (ANOVA) at the vegetative stage under flooded conditions and osmotic stress levels of −4.5 and −9 bar indicated the significance of all studied traits at the 1% level (Table 2).

The maximum and minimum coefficients of variation (CV) for root volume (49.354) and root area (1.636), respectively, belonged to the −9 bar level. Different reactions of rice genotypes under osmotic stress were also investigated by some other researchers reported that most of the traits studied in osmotic stress and temperature conditions showed significant differences at the 1% level in ANOVA, indicating variation between studied lines for the measured traits (Lanceras et al., 2004; Iravani et al., 2008).

Table 2. Analysis of variance of the examined traits at the vegetative stage under normal and osmotic stress conditions.

Source of variation	df	Mean square					
		Chlorophyll content (mg/gr)	Stem length (cm)	Root length (cm)	Root number (cm)	Leaf length (cm)	Leaf width (cm)
Normal							
Line	119	0.058**	18.713**	11.694**	5.181**	31.564**	0.771**
Error	240	0.013	1.984	1.996	1.320	19.797	0.168
CV		44.517	7.410	15.699	17.818	30.527	13.471
-4.5 bar stress							
Line	119	0.252**	20.985**	11.213**	5.130**	21.852**	0.834**
Error	240	0.174	3.044	2.048	1.594	11.329	0.253
CV		25.998	8.798	15.394	18.834	22.296	19.199
-9 bar stress							
Line	119	0.361	56.622**	13.629**	6.645**	10.468**	0.581**
Error	240	0.332	45.487	2.123	0.895	1.738	0.0798
CV		17.536	37.119	16.013	17.307	9.571	13.519

Source of variation	df	Mean square						
		Stem wet weight	Root wet weight	Root volume	Drought number	Root area	Root area	Root area density
Normal								
line	119	0.001**	0.000**	0.001**	6.557**	0.027**	0.001**	1.020**
Error	240	0.000	0.000	0.000	0.022	0.006	0.000	0.164
CV		11.763	4.609	27.038	3.752	3.786	14.804	17.096
-4.5 bar stress								
Line	119	0.000**	0.000**	0.001**	10.105**	0.011**	0.000**	0.997**
Error	240	0.000	0.000	0.000	0.222	0.002	0.000	0.098
CV		12.233	4.835	6.908	7.834	2.375	7.549	8.222
-9 bar stress								
Line	119	0.000**	0.000**	0.0008**	6.595**	0.006**	0.000**	1.109**
Error	240	0.000	0.000	0.000	0.011	0.001	0.000	0.220
CV		33.607	6.166	49.354	4.299	1.636	20.291	23.723

*,**Significant at p = 0.05 and 0.01, respectively.

Baraty et al. (2014) found significant differences at the 1% level for the number of tillers, number of nodes, plant height, panicle length, awn length, flag leaf length, peduncle length, number of rows, 1000-grain weight, and yield between lines. Similarly, our data showed that the lines were significantly different for all traits at the 1% level, except for plant height, which corresponds to the aforementioned study, except for plant height.

Linkage map

The linkage map prepared based on 30 SSR and 15 ISSR markers (with 60 replicated polymorphic alleles) on 120 individuals of the F_8 population assigned the markers to 12 linkage groups belonging to 12 rice chromosomes with a map distance based on the Kosambi (1944) function equal to 1411.3 cM and an interval of 15.34 cM between two flanking markers. Maximum (156.3 cM) and minimum (81.3 cM) linkage lengths were determined on chromosomes 11 and 10, respectively.

QTLs identified under osmotic stress and normal conditions at the vegetative stage

Normal conditions

One QTL for the root number was located at the IRAP-5–RM111 marker distance on chromosome 12, with a LOD of 2.842, and could explain 10.3% of phenotypic changes. Our estimation revealed that the reducing additive effect was inherited from the Ahlamitarom. For the root area trait, one QTL was also found on chromosome 11 at the IRAP23-1 - IRAP23-7 genomic distance. qRS-11 was determined as a large-effect QTL with a coefficient of determination (R^2) of 13.

-4.5 bar stress conditions

To explain changes in the chlorophyll content trait, one QTL was identified on chromosome 2. An R^2 of 14.5 was obtained for qCL-2. The study of the additive effect of this QTL revealed that chlorophyll content was reduced by the Ahlamitarom alleles. For the stem length trait, three QTLs were located at ISSR21-2 – ISSR4-3, ISSR37-3 – ISSR8-6, and ISSR29-2 - IRAP17-1 genomic distances on chromosomes 5, 6, and 7. qSL-7 was detected as a large-effect QTL with a greater R^2 (13.4%) than the other QTLs. For the root volume trait, one QTL was located on chromosome 12 at ISSR15-3 - RM12 genomic distances. The additive effect and R^2 for this QTL were 0.01 and 13.6%, respectively. The positive additive effect and Neda alleles caused an increase in this trait. For the root diameter trait, two QTLs with additive effects were determined on chromosomes 2 and 5. Neda parental alleles contributed to the elevated root diameter trait. R^2 values for these two QTLs were 12.9% and 14%, respectively.

–9 bar stress conditions

For the traits evaluated under osmotic stress, seven QTL-containing distances were identified that controlled five traits (Table 3). Two QTLs for the root number were located on chromosome 12 in 50 and 32 positions at ISSR30-1 – RM277 and ISSR15-3 – RM12 genomic distances, respectively. The reducing additive effect for this trait was derived from the Ahlamitarom. R^2 values for these two QTLs were 12.8% and 13.2%, respectively.

For root wet weight, one QTL was recognized on chromosome 8 at the iPBS2074-3 – IRAP-4 genomic distance with an R^2 of 13.5%. For the root volume trait, two QTLs were identified on chromosome 12 in 32 and 50 positions at ISSR15-3 – RM12 and RM277 – IRAP-1 genomic regions, with R^2 values of 15.1% and 13.7%, respectively. For the root area trait, one QTL was also found on chromosome 11 at the IRAP23-1 - IRAP23-7 genomic region. The additive effect for this QTL was derived from the Neda. For the root diameter trait, one QTL was determined on chromosome 12 at the RM277 – IRAP-1 genomic distance with an R^2 value of 12.9%.

The descriptive statistical analysis of data in normal and low-irrigation conditions indicated the presence of variance required for multivariate analyses. The results showed the normal distribution of all evaluated traits. The average values of all traits are represented in Table 3.

Reproductive stage

Before any analysis, Bartlett's test results indicated the homogeneity of the test error variance. Accordingly, the results of ANOVA and correlation for the traits in osmotic stress and normal conditions are presented in Tables 4 and 5, respectively. According to the results, all evaluated traits were significantly different at the 1% level in the two experimental conditions at the reproductive stage.

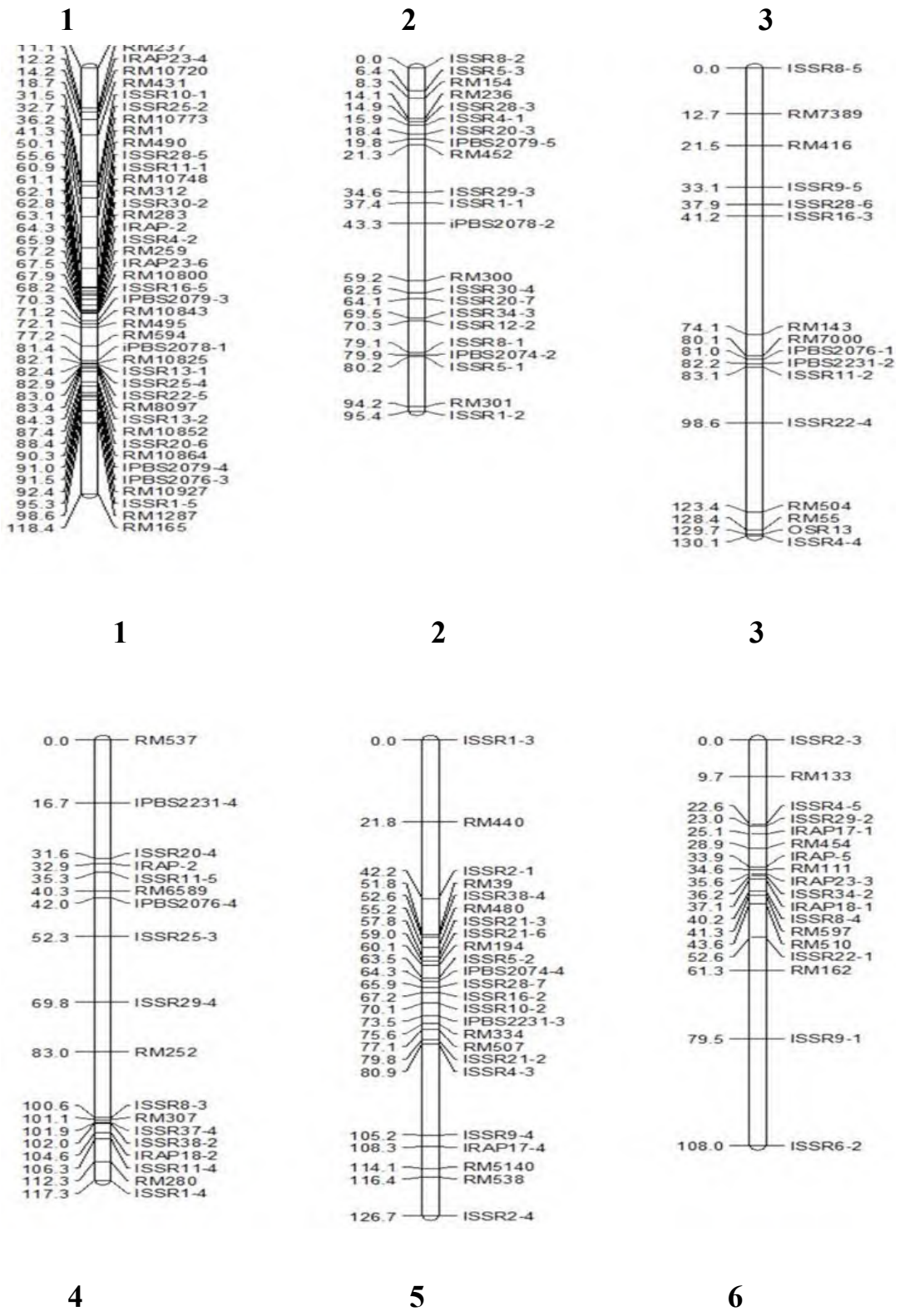

Figure 1. SSR, ISSR, iPBS and IRAP linkage map in the F8 population resulting from the crossing of Taremmahali and Neda. The names of the markers are shown on the right side of the linkage groups and the genetic distance between the markers based on the Kosambi (1944) function is shown on the left side.

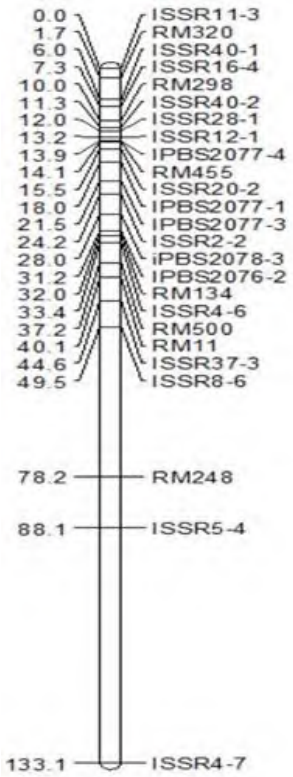
0.0 ISSR11-3
1.7 RM320
6.0 ISSR40-1
7.3 ISSR16-4
10.0 RM298
11.3 ISSR40-2
12.0 ISSR28-1
13.2 ISSR12-1
13.9 IPBS2077-4
14.1 RM455
15.5 ISSR20-2
18.0 IPBS2077-1
21.5 IPBS2077-3
24.2 ISSR2-2
28.0 iPBS2078-3
31.2 IPBS2076-2
32.0 RM134
33.4 ISSR4-6
37.2 RM500
40.1 RM11
44.6 ISSR37-3
49.5 ISSR8-6
78.2 RM248
88.1 ISSR5-4
133.1 ISSR4-7

7

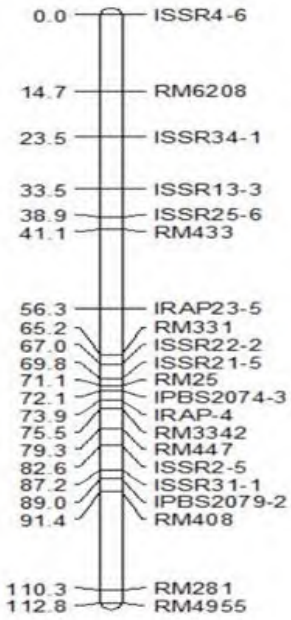
0.0 ISSR4-6
14.7 RM6208
23.5 ISSR34-1
33.5 ISSR13-3
38.9 ISSR25-6
41.1 RM433
56.3 IRAP23-5
65.2 RM331
67.0 ISSR22-2
69.8 ISSR21-5
71.1 RM25
72.1 IPBS2074-3
73.9 IRAP-4
75.5 RM3342
79.3 RM447
82.6 ISSR2-5
87.2 ISSR31-1
89.0 IPBS2079-2
91.4 RM408
110.3 RM281
112.8 RM4955

8

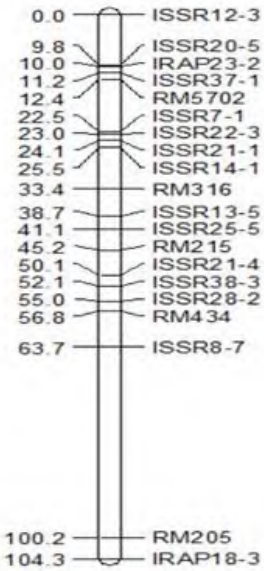
0.0 ISSR12-3
9.8 ISSR20-5
10.0 IRAP23-2
11.2 ISSR37-1
12.4 RM5702
22.5 ISSR7-1
23.0 ISSR22-3
24.1 ISSR21-1
25.5 ISSR14-1
33.4 RM316
38.7 ISSR13-5
41.1 ISSR25-5
45.2 RM215
50.1 ISSR21-4
52.1 ISSR38-3
55.0 ISSR28-2
56.8 RM434
63.7 ISSR8-7
100.2 RM205
104.3 IRAP18-3

9

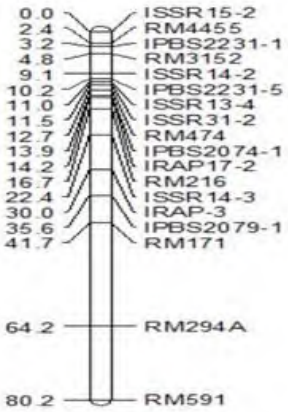
0.0 ISSR15-2
2.4 RM4455
3.2 IPBS2231-1
4.8 RM3152
9.1 ISSR14-2
10.2 IPBS2231-5
11.0 ISSR13-4
11.5 ISSR31-2
12.7 RM474
13.9 IPBS2074-1
14.2 IRAP17-2
16.7 RM216
22.4 ISSR14-3
30.0 IRAP-3
35.6 IPBS2079-1
41.7 RM171
64.2 RM294A
80.2 RM591

10

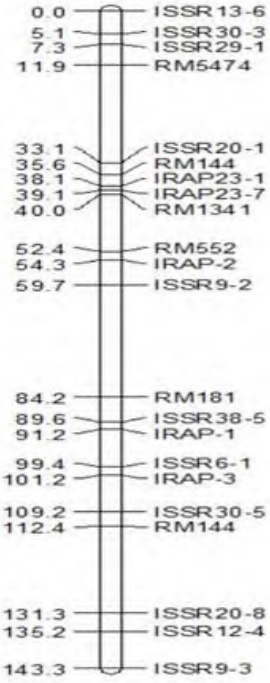
0.0 ISSR13-6
5.1 ISSR30-3
7.3 ISSR29-1
11.9 RM5474
33.1 ISSR20-1
35.6 RM144
38.1 IRAP23-1
39.1 IRAP23-7
40.0 RM1341
52.4 RM552
54.3 IRAP-2
59.7 ISSR9-2
84.2 RM181
89.6 ISSR38-5
91.2 IRAP-1
99.4 ISSR6-1
101.2 IRAP-3
109.2 ISSR30-5
112.4 RM144
131.3 ISSR20-8
135.2 ISSR12-4
143.3 ISSR9-3

11

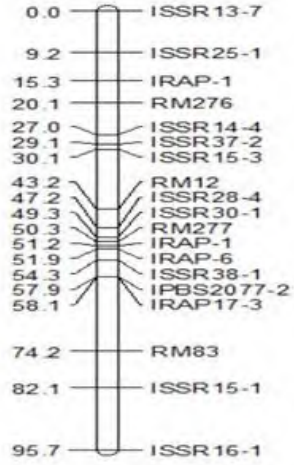
0.0 ISSR13-7
9.2 ISSR25-1
15.3 IRAP-1
20.1 RM276
27.0 ISSR14-4
29.1 ISSR37-2
30.1 ISSR15-3
43.2 RM12
47.2 ISSR28-4
49.3 ISSR30-1
50.3 RM277
51.2 IRAP-1
51.9 IRAP-6
54.3 ISSR38-1
57.9 IPBS2077-2
58.1 IRAP17-3
74.2 RM83
82.1 ISSR15-1
95.7 ISSR16-1

12

Table 3. Identified QTLs for investigated traits at the vegetative stage under normal and osmotic stress conditions (-4.5 and -9 bar stress).

Trait	QTL	Chromosome	Position (cM)	Flanking markers	LOD	Additive effect	R^2	Allele direction
Normal								
Root number	qRN-12	12	50	ISSR30-1 – RM277	2.842	-0.463	12.5	Ahlamitarom
Root area	qRS-11	11	76	IRAP23-1 – IRAP23-7	2.85	-0.248	13	Neda
-4.5 bar stress								
Chlorophyll content	qCL-2	2	80	iPBS2074-2 – ISSR5-1	3.468	-44.424	14.5	Ahlamitarom
Stem length	qSL-6	6	24	ISSR29-2 - IRAP17-1	3.302	45.18	12	Neda
	qSL-7	7	48	ISSR37-3 – ISSR8-6	2.841	-1.98	13.4	Ahlamitarom
	qSL-5	5	80	ISSR21-2 – ISSR4-3	2.746	-4.692	12	Ahlamitarom
Root volume	qRV-12	12	32	ISSR15-3 – RM12	2.950	0.01	13.6	Ahlamitarom
Root diameter	qRD-5	5	52	ISSR38-4 – RM480	2.913	0.003	14	Neda
	qRD-2	12	6	ISSR8-2 – ISSR5-3	2.841	0.039	12.9	Neda
-9 bar stress								
Root number	qRN-12	12	50	ISSR30-1 – RM277	2.712	-0.586	12.8	Ahlamitarom
	qRN-12	12	32	ISSR15-3 – RM12	2.315	-0.695	13.2	Ahlamitarom
Root wet weight	qRFW-8	8	72	iPBS2074-3 – IRAP-4	2.123	0.028	13.5	Neda
Root volume	qRV-12	12	32	ISSR15-3 – RM12	2.58	-0.007	15.1	Ahlamitarom
	qRV-12	12	50	RM277 – IRAP-1	2.068	-0.006	13.7	Ahlamitarom
Root area	qRL-11	11	38	IRAP23-1 – IRAP23-7	2.189	0.322	12.7	Neda
Root diameter	qRD-12	12	50	RM277 – IRAP-1	2.042	-0.006	12.9	Ahlamitarom

The statistically significant differences between the genotypes represent a high variance between the evaluated plant material and probably their different mechanisms in response to osmotic stress, which can be used in good genotype selection. The highest correlation (0.393**) was observed between the filled grain weight and flag leaf length under normal and stress conditions. Leaf area was positively and significantly correlated with total panicle weight (0.380**), stem diameter (0.265**), flag leaf length (0.275), and filled grain weight (0.356**). Positive and significant correlations were also observed between the number of fertile tillers, the number of total tillers (0.322**), and the number

of fertile tillers (0.388**). The main panicle weight was positively and significantly correlated with total panicle weight (0.319**) and full grain weight (0.334**). There were also positive and significant correlations between root dry weight (0.261**), leaf number (0.306**), and leaf area (0.379**).

QTLs identified under osmotic stress and normal conditions at the reproductive stage

The results of QTLs analyzed under osmotic stress and normal conditions are shown in Table 6.

One QTL was located for the number of total tiller trait on chromosome 12 in normal conditions, and 15.6% of the total phenotypic changes in this trait was explained by qNTT-12, which was positively affected by the Neda alleles.

In stress conditions, one QTL was determined for the number of fertile tiller trait on chromosome 12. qNTF-12 was recognized in similar stress and normal conditions and showed more effect in stress conditions. Similar QTLs at the ISSR16-1-ISSR15 distance could explain 12.7% and 12.8% of the phenotypic variance of these traits under stress and normal conditions. The QTLs also represented a dominant effect. One QTL was identified for the panicle weight trait on chromosome 6 in normal conditions. qLSP-6 was recognized with LOD 2.12 and 12.9% phenotypic variance. This trait was increased by the Neda alleles.

Table 4. Analysis of the variance of evaluated traits under normal and drought stress conditions at the reproductive stage.

Mean square							df	Source of variation
Stem diameter	Total panicle weight	Flag leaf width	Flag leaf length	Fertile tiller number	Total tiller number	Panicle length		
Normal								
1.654**	3.870**	12.321**	85.153**	2.360**	3.433**	74.332**	119	Line
0.191	1.769	0.631	2.089	0.394	39.359	26.927	240	Error
10.500	6.325	10.709	6.684	19.184	17.028	5.454		CV
Drought								
0.705**	21/752**	4.411**	86.868**	2.628**	0.818**	18.524	119	Line
0.115	2.645	0.421	3.886	0.460	0.764	25.055	240	Error
10.794	7.804	9.473	9.657	20.024	2557.1	5.739		CV

Continiued Table 4. Analysis of the variance of evaluated traits under normal and drought stress conditions at the reproductive stage

Mean square								df	Source of variation
Root dry weight	Leaf area	Filled grain weight	Number of filled grain	Main panicle weight	Total weight of panicles	Plant dry weight	Number of leaves		
Normal									
7.906**	55.687**	0.442	767.996**	0.414**	3.893**	10.477**	1.089**	119	Line
0.127	4.291	0.036	6.515	0.002	0.508	0.687	0.246	240	Error
8.688	17.422	24.066	23.602	4.673	27.573	15.764	10.936		CV
Drought									
7.337**	25.380**	3.219**	703.002**	0.411**	2.374**	13.436**	1.144**	119	Line
0.133	2.360	0.014	40.558	0.002	0.286	1.251	0.260	240	Error
7.740	14.883	11.455	31.040	6.701	32.680	21.254	9.896		CV

*,**Significant at p = 0.05 and 0.01, respectively.

Table 6. Putative QTLs for reproductive traits in F8 population under osmotic stress and non-stress conditions.

Trait	QTL	Markers interval [a]	Chr.	Position (cM) [b]	LOD	Additive effect(A)	R^2 (%)[c]	DPE[d]
Non-stress								
Total number of tillers	qNTT-12	ISSR15-1-ISSR16-1	12	82	2.99	-2.072	15.6	Neda
Number of fertile tillers	qNTF-12	ISSR16-1-ISSR15-1	12	110	2.13	-0.38	12.7	Ahlamitarom
Panicle length	qLSP-6	IRAP-5 – RM454	6	32	2.12	-0.022	12.9	Neda
Main panicle weight	qWSPM-8	ISSR4-6-RM6208	8	8	2.18	-0.18	13	Ahlamitarom
Number of leaves	qNL-3	ISSR11-2–ISSR22-4	3	86	2.428	0.156	12.9	Neda
Root dry weight	qWDR-5	ISSR21-6 – ISSR21-3	5	58	2.288	-0.988	13.2	Ahlamitarom
	qWDR-9	ISSR28-2 – ISSR38-3	9	54	2.708	-0.359	14.8	Neda
Osmotic stress								
Flag leaf length	qLLF-1	RM165- RM1287	1	112	2.328	0.117	13	Neda
Number of fertile tillers	qNTF-12	ISSR16-1-ISSR15-1	12	76	2.434	-0.444	12.8	Ahlamitarom
Flag leaf width	qWLF-8	ISSR4-6-RM6208	8	2	2.23	-0.62	13.2	Ahlamitarom
Stem diameter	qSTD-11	ISSR20-8-ISSR12-4	11	134	2.121	-0.464	11.8	Neda
Number of leaves	qNL-3	ISSR11-2–ISSR22-4	3	62	2.428	-0.958	12.5	Ahlamitarom
Plant dry weight	qWDP-8	RM447 – ISSR2-5	8	82	2.686	0.191	11.3	Neda
	qWDP-1	IRAP2-RM283	1	64	2.157	1.153	10.8	Neda
Total weight of panicles	qWTS-12a	ISSR15-1 – ISSR16-1	12	72	3.254	-0.113	13.1	Neda
	qWTS-12b	IRAP17-3-RM83	12	64	2.617	-0.804	12	Neda
	qWTS-2	RM154-RM236	2	12	2.115	-0.361	11.5	Neda
Filled grain weight	qWGRF-9	ISSR22-3 – ISSR21-1	9	24	2.123	-2.28	13.2	Neda
Leaf area	qLA-1	RM1287-RM165	1	110	2.481	1.446	11	Neda
	qLA-8	ISSR4-6-RM6208	8	0	2.371	-1.757	11.7	Ahlamitarom

[a] Underlined markers are more closer to QTL; [b] QTL position from the nearest flanking marker (cM); [c] Phenotypic variance explained by each QTL. [d] DPE, Direction of phenotypic effect.

In normal conditions, one QTL was detected for the main panicle weight trait on chromosome 8. qWSPM-8 represented 13% of the total phenotypic variance. Neda alleles positively influenced qGN13-8. In stress conditions, one QTL was identified for the number of leaves trait on chromosome 3. In normal conditions, qNL-3 between ISSR11-2 and ISSR22-4 on chromosome 3 could explain 12.9% of the total phenotypic variance. The additive allele of these QTLs could be explained by the Ahlamitarom variety.

In normal conditions, two QTLs for root dry weight were determined on chromosomes 5 (ISSR21-6 - ISSR21-3) and 9 (ISSR28-2 - ISSR38-3), representing 13.2% and 14.8% of the total phenotypic variance, respectively. This trait was increased by Ahlamitarom alleles on chromosome 5 while Neda alleles on chromosome 9 reduced this trait. In stress conditions, one QTL was located for the flag leaf length trait on chromosome 1. The phenotypic variance of this trait (13%) was explained by qLLF-1 with a loading level of 2.328. This increase was mediated by the Neda parental effect. In osmotic stress conditions, one QTL was recognized for the flag leaf width trait on chromosome 8 (ISSR4-6-RM6208), which explained 13.2% of the total phenotypic variance. In normal conditions, one QTL was detected for the stem diameter trait on chromosome 11 located between ISSR20-8 and ISSR12-4 markers, explaining 11.8% of the total variance. In osmotic stress conditions, two QTLs were found for the panicle dry weight trait on chromosomes 8 and 1. One QTL was located on chromosome 8 at the RM447 - ISSR2-5 distance, which explained 11.3% of the total phenotypic variance. Neda alleles caused the increase in this trait. In osmotic stress conditions, three QTLs for the total panicle weight trait were discovered on chromosomes 12 and 2. Two QTLs (qWTS-12a and qWTS-12b with LOD values of 3.254 and 2.617) on chromosome 12 explained 13.1% and 12% of the phenotypic variance, respectively. The increasing effect of the alleles in these QTLs was attributed to the Neda parent. In osmotic stress conditions, one QTL for the filled grain weight trait was found on chromosome 9 (ISSR22-3 - ISSR21-1) and explained 13.2% of the total phenotypic variance. The increasing effect of the allele in this QTL could be explained by the Neda parent. In osmotic stress conditions, two QTLs for the leaf area trait were identified on chromosomes 1 (RM1287-RM165) and 8 (ISSR4-6-RM6208), which explained 11% and 11.7% of the total phenotypic variance. Neda parental alleles were effective in increasing the QTL on chromosome 1 whereas Ahlamitarom alleles in the QTL on chromosome 8 reduced this trait.

4. Discussion

Based on the results, all evaluated traits at the vegetative stage were significantly different at the 1% level in the three experimental conditions at the reproductive stage. Paralleled to our findings, Bhandari et al. (2023) reported that drought stress negatively impacts the general morphology of rice plants, including plant growth, plant biomass, yield, roots, and grain development.

In terms of morphology (Mohd Ikmal et al., 2021), plants under water stress exhibit decreased germination, leaf size, leaf area, leaf number, biomass, cell growth, and elongation due to low or insufficient water flow onto the xylem or neighboring cell. The statistically significant differences between the genotypes indicate a high variance between the evaluated plant material and probably their different mechanisms in reaction to osmotic stress, which can be used in the selection of good genotypes. The comparison of QTLs located in three flooded, −4.5 bar, and −9 bar conditions showed that two, seven, and seven QTLs were respectively identified in these treatments. In −4.5 bar osmotic stress conditions, two large-effect QTLs (qCL-2 and qRD-5) for chlorophyll content and root diameter were found on chromosomes 2 and 12, compared to one large-effect QTL (qRV-12) detected on chromosome 12 in −9 bar osmotic stress. Among rice chromosomes, most of the traits were identified on chromosome 12 and its genomic regions. According to the comparison of three treatments, qRN-12 and qRS-11 on chromosomes 12 and 11 in flooded conditions and −9 bar osmotic stress, respectively, as well as qRV-12 on chromosome 12 in −4.5 and −9 bar osmotic stress, were jointly located regarding the chromosome and genomic loci. These QTLs are stable and are not influenced by environmental factors. The mentioned QTLs controlled root number, root area, and root volume traits, playing an important role in these traits. Kamoshita et al. (2002) found only two stable QTLs among 31 cases identified for seven traits related to root morphology in two non-stress and −6 bar conditions. These results demonstrate that the identified QTLs and the large-effect QTL with a high R^2 can be jointly effective in two different conditions without environmental effects using the MAS method to produce and improve drought-tolerant rice varieties. Similar to our results, Lilley et al. (1996), Zhang et al. (2005), and Kato et al. (2007) identified QTLs mostly associated with root

traits (length, area, volume, and dry weight) at the vegetative stage.

Horii et al. (2006) recognized two QTLs on chromosomes 1 and 9 (marker intervals RM243-RM23 and RM257-RM258, respectively) for root diameter at the rice vegetative stage; these QTLs do not match with those identified in the present study. Babu et al. (2003) investigated the relationship between the secondary traits and yield of the rice plant using the QTL analysis in osmotic stress conditions. They found 47 QTLs for different traits that explained 5-59% of changes. Regions on chromosome 4 included a large-effect QTL controlling plant height and root traits, which does not correspond to our results. The present findings are in line with those of Sabouri (2007), who determined two QTLs on chromosomes 1 and 8 for rice root wet weight in osmotic stress conditions. They reported additive effects (−1.01 and −1.04) and phenotypic explanations (22.44 and 22.97) for the located QTLs.

Mardani et al. (2014) detected QTLs associated with drought tolerance in an $F_{2:4}$ population by employing 105 AFLP and 131 microsatellite markers, during germination and vegetative stages in rice. They located three, two, and two QTLs for germination rate, germination percentage, and root number, respectively, on chromosome 12. Long-Zhi et al. (2006) studied QTLs controlling root wet and dry weights in a population derived from an Indica and Japonica rice cross under salinity and osmotic stress. They determined QTLs on chromosomes 8 and 12 for root wet weight, which explained total phenotypic variance with R^2 values of 21 and 12.3%, which is inconsistent with our results. Consistent with this study, Khalili et al. (2017) discovered four loci on chromosomes 1H, 2H, 5H, and 6H for leaf chlorophyll content. The discrepant results obtained in the present and other investigations may be attributed to the number and type of evaluated markers, population type, the number of individuals in the population, the type of examined parents, and environmental conditions.

In this research, QTLs were recognized at the reproductive stage, and genetic relationships between traits were compared in two different conditions. Of 20 QTLs detected in both conditions, 13 and 7 QTLs were associated with osmotic stress and normal conditions. Under osmotic stress, three large-effect QTLs (qNTF-12, qWTS-12a, and qWDP-8) were found on chromosomes 8 and 12 in comparison to two large-effect QTLs (qNNT-12 and qWDR-9) identified on chromosomes 9 and 12 in normal conditions. In the comparison of the two treatments, only two QTLs (qNTF-12 and qNL-3) on chromosomes 3 and 12 were determined in osmotic stress and normal conditions. The mentioned QTLs are stable and are not affected by environmental factors. In this investigation, qNTF-12 and qNL-3 QTLs were found for NTF and NL under both conditions, which may play an important role in NTF and NL. The QTLs were located at intervals of ISSR15-1 and ISSR11-2 markers on chromosomes 3 and 12. Wang et al. (2007) determined seven QTLs for these traits on chromosomes 3, 7, and 10 using a RIL (F2:9) population, and qNL-3 with LOD = 2.6, which explained 9% of the total phenotypic variance, is similar to the QTL recognized in our study. The regional and phenotypic variance with the explained QTL (qNL-3) is also similar to QTLs identified by Teng et al. (2001).

In the current study, two QTLs for plant dry weight (WDP) on chromosomes 1 and 8 were found in normal conditions, which disagrees with other studies (Redona and Mackill, 1996; Zhang et al., 2005). They studied different traits and phenotypic methods. One QTL for WDP on a similar region on chromosome 8 was reported in normal conditions by Ji et al. (2012). Similarly, the ISSR16-1-ISSR15-1 area on chromosome 12 contains one QTL for NTF, which was reported earlier by many researchers. For example, drought-tolerance QTLs in the same area were reported by Price and Courtois (1999), Lafitte et al. (2002), and Wang et al. (2007). Therefore, this region seems to be a good candidate for improving drought-tolerant varieties through marker selection as well as map saturation and local gene formation. The current investigation is the first to identify three QTLs for the WTS trait on chromosomes 2 and 12, which is not in agreement with other studies. Some of the 20 identified QTLs are reported for the first time. In this study, most of the identified QTLs show a wide range of inadequate effects, suggesting the complexity of the studied traits. In our investigation, the F8 population derived from an Ahlamitarom × Neda cross is a new source of novel drought-tolerant QTLs. These results demonstrate that these QTLs

were effective for the production and improvement of drought-tolerant rice varieties using the MAS technique. Such varieties provide yield sustainability to farmers in regions impacted by drought and submergence (Mohd Ikmal et al., 2021) while serving as important genetic materials for future breeding programs.

Conclusion

In this study, we identified QTLs associated with drought-tolerance particularly on chromosome 12. Our findings underscore the variability of rice RILs across all traits in both environments. In drought stress conditions, the F8 population derived from the Ahlamitarom × Neda cross serves as a novel reservoir of identified QTLs at both vegetative and reproductive growth stages. Thus, these QTLs can be effectively utilized as reliable and stable QTLs for the identification of drought-tolerant lines at all stages of plant growth using the MAS approach.

Supplementary Materials

No supplementary material is available for this article.

Author Contributions

Conceptualization, M.N. and H.S.; methodology, M.N.; software, H.S; validation, M,N., H.S., and I.M.H; formal analysis, M.N.; investigation, M.N.; resources, H.S.; data curation, M.N.; writing—original draft preparation, M.N.; writing—review and editing, H.S.; visualization, M.N.; supervision, H.S. ; I.M.H; and F.D.K project administration, H.S.; funding acquisition, H.S. All authors have read and agreed to the published version of the manuscript.

Funding

This research was funded by Gonbad Kavous University and Azad Islamic University Since and Research Branch.

Acknowledgments

We are grateful to the Department of Plant Production at Gonbad Kavous University for providing us with the resources and support we needed to complete this project.

Conflicts of Interest

The authors declare no conflict of interest.

References

Alahmad, S., El Hassouni, K., Bassi, F.M., Dinglasan, E., Youssef, C., Quarry, G., Aksoy, A., Mazzucotelli, E., Juhasz, A., Able, J.A., Christopher, J., Voss-Fels, K.P., and Hickey, L.T. (2019). A major root architecture QTL responding to water limitation in durum wheat. *Front Plant Sci* 10: 436. doi: 10.3389/fpls.2019.00436.

Aliyu, R., Adamu, A., Muazu, S., Alonge, S., and Gregorio, G. (2011). "Tagging and validation of SSR markers to salinity tolerance QTLs in rice (*Oryza* spp)", in: *International conference on biology, environment and chemistry IPCBEE.* (Singapore: IACSIT Press).

Babu, N.N., Vinod, K., Krishnan, S.G., Bhowmick, P., Vanaja, T., Krishnamurthy, S., Nagarajan, M., Singh, N., Prabhu, K., and Singh, A. (2014). Marker based haplotype diversity of Saito/QTL in relation to seedling stage salinity tolerance in selected genotypes of rice. *Indian J Genet Plant Breed* 74(01): 16-25.

Babu, R.C., Nguyen, B.D., Chamarerk, V., Shanmugasundaram, P., Chezhian, P., Jeyaprakash, P., Ganesh, S., Palchamy, A., Sadasivam, S., and Sarkarung, S. (2003). Genetic analysis of drought resistance in rice by molecular markers: association between secondary traits and field performance. *Crop Sci* 43(4): 1457-1469.

Baraty, M., Amiri, R., Ebrahimi, M., Naghavi, M.R., and Nikkhah, H.R. (2014). Study of genetic diversity in some agronomic traits of barley using recombinant inbred lines. *Appl Field Crops Res* 27(102): 61-70.

Bhandari, U., Gajurel, A., Khadka, B., Thapa, I., Chand, I., Bhatta, D., Poudel, A., Pandey, M., Shrestha, S., and Shrestha, J. (2023). Morpho-physiological and biochemical response of rice (*Oryza sativa* L.) to drought stress: A review. *Heliyon* 9(3): e13744. doi: 10.1016/j.heliyon.2023.e13744.

Caetano-Anollés, G., and Gresshoff, P.M. (1994). Staining nucleic acids with silver: an alternative to radioisotopic and fluorescent labeling. *Promega Notes* 45: 13.

Chen, H., An, R., Tang, J.-H., Cui, X.-H., Hao, F.-S., Chen, J., and Wang, X.-C. (2007). Over-expression of a vacuolar Na+/H+ antiporter gene improves salt tolerance in an upland rice. *Mol Breed* 19: 215-225.

Fischer, K.S., Fukai, S., Kumar, A., Leung, H., and Jongdee, B. (2012). Field phenotyping strategies and breeding for adaptation of rice to drought. *Front Physiol* 3: 282. doi: 10.3389/fphys.2012.00282.

Giasi Oskoei, M., Farahbakhsh, H., and Mohamadinejad, G. (2014). Evaluation of rice cultivars in drought and normal conditions based on sensitive and tolerance indices. *J Crop Prod* 6(4): 55-75.

Golesorkhy, M., Biabani, A., Sabouri, H., and Esmaeili, M.M. (2016). Studying the relationship between agronomy traits of rice under flooding and drought stress conditions. *Environmental Stresses Crop Sci* 8(2): 191-204 (In persian).

Horii, H., Nemoto, K., Miyamoto, N., and Harada, J. (2006). Quantitative trait loci for adventitious and lateral roots in rice. *Plant Breed* 125(2): 198-200.

Iravani, M., Solouki, M., Rezai, A., Siasar, B., and Kohkan, S. (2008). Investigating the diversity and relationship between agronomical traits and seed yield in barley advanced lines using factor analysis. *J Crop Prod Proc* 12(45): 137-145 (In persian).

Ji, K., Wang, Y., Sun, W., Lou, Q., Mei, H., Shen, S., and Chen, H. (2012). Drought-responsive mechanisms in rice genotypes with contrasting drought tolerance during reproductive stage. *J Plant Physiol* 169(4): 336-344. doi: 10.1016/j.jplph.2011.10.010.

Jongdee, B. (2001). "New rice-breeding methods for the rainfed lowlands of North and Northeast Thailand", in: *Increased lowland rice production in the Mekong Region: Proceedings of an International Workshop held in Vientiane, Laos, 30 October-2 November 2000.* (Vientiane: Australian Centre for International Agricultural Research (ACIAR)).

Kamoshita, A., Zhang, J., Siopongco, J., Sarkarung, S., Nguyen, H.T., and Wade, L.J. (2002). Effects of phenotyping environment on identification of quantitative trait loci for rice root morphology under anaerobic conditions. *Crop Sci* 42(1): 255-265. doi: 10.2135/cropsci2002.2550.

Kato, Y., Kamoshita, A., Yamagishi, J., Imoto, H., and Abe, J. (2007). Growth of rice (*Oryza sativa* L.) cultivars under upland conditions with different levels of water supply 3. Root system development, soil moisture change and plant water status. *Plant Prod Sci* 10(1): 3-13.

Khalili, M., Javaheri Kashani, F., and Ebrahimi, M. (2017). Evaluation of genetic diversity and identification of QTL controlling seed germination and seedling establishment traits in wheat. *Iran Dry Agron J* 6(1): 121-138 (In persian).

Kosambi, D. (1944). Efficient mapping of a female sterile gene in wheat (*Triticum aestivum* L.). *Ann Eugenics* 12: 172-175.

Kramer, P.J., and Boyer, J.S. (1995). *Water relations of plants and soils.* Academic Press.

Lafitte, H., Courtois, B., and Arraudeau, M. (2002). Genetic improvement of rice in aerobic systems: progress from yield to genes. *Field Crops Res* 75(2-3): 171-190.

Lanceras, J.C., Pantuwan, G., Jongdee, B., and Toojinda, T. (2004). Quantitative trait loci associated with drought tolerance at reproductive stage in rice. *Plant Physiol* 135(1): 384-399.

Lilley, J., Ludlow, M., McCouch, S., and O'toole, J. (1996). Locating QTL for osmotic adjustment and dehydration tolerance in rice. *J Exp Bot* 47(9): 1427-1436.

Long-Zhi, H., Zhang, Y.-Y., Yong-Li, Q., Gui-Lan, C., Zhang, S.-Y., Jong-Hwan, K., and Hee-Jong, K. (2006). Genetic and QTL analysis for low-temperature vigor of germination in rice. *Acta Genet Sin* 33(11): 998-1006.

Loresto, G. (1981). Decimal scroing systems for drought reactions and recovery ability in screening nurseries of rice. *Int. Rice. Res. Newsl.* 6: 9-10.

MacMillan, K., Emrich, K., Piepho, H.P., Mullins, C.E., and Price, A.H. (2006). Assessing the importance of genotype x environment interaction for root traits in rice using a mapping population II: conventional QTL analysis. *Theor Appl Genet* 113(5): 953-964. doi: 10.1007/s00122-006-0357-4.

Mardani, Z., Rabiei, B., Sabouri, H., and Sabouri, A. (2014). Identification of molecular markers linked to salt - tolerant genes at germination stage of rice. *Plant Breed* 133(2): 196-202.

McCouch, S.R. (1997). Report on QTL nomenclature. *Rice Genet. Newsl.* 14: 11-13.

Michel, B.E., and Kaufmann, M.R. (1973). The osmotic potential of polyethylene glycol 6000. *Plant Physiol* 51(5): 914-916. doi: 10.1104/pp.51.5.914.

Mohd Ikmal, A., Noraziyah, A.A.S., and Wickneswari, R. (2021). Incorporating drought and submergence tolerance QTL in Rice (*Oryza sativa* L.)—the effects under reproductive stage drought and vegetative stage submergence stresses. *Plants* 10(2): 225.

Mohidem, N.A., Hashim, N., Shamsudin, R., and Che Man, H. (2022). Rice for food security: Revisiting its production, diversity, rice milling process and nutrient content. *Agriculture* 12(6): 741.

Muthu, V., Abbai, R., Nallathambi, J., Rahman, H., Ramasamy, S., Kambale, R., Thulasinathan, T., Ayyenar, B., and Muthurajan, R. (2020). Pyramiding QTLs controlling tolerance against drought, salinity, and submergence in rice through marker assisted breeding. *PLoS One* 15(1): e0227421.

Noryan, M., Hervan, I.M., Sabouri, H., Kojouri, F.D., and Mastinu, A. (2021). Drought resistance loci in recombinant lines of iranian Oryza sativa L. in germination stage. *BioTech (Basel)* 10(4): 26. doi: 10.3390/biotech10040026.

Pandey, V., and Shukla, A. (2015). Acclimation and tolerance strategies of rice under drought stress. *Rice Sci* 22(4): 147-161.

Price, A., and Courtois, B. (1999). Mapping QTLs associated with drought resistance in rice: progress, problems and prospects. *J Plant Growth Regul* 29: 123-133.

Rajurkar, A.B., Muthukumar, C., Ayyenar, B., Thomas, H.B., and Chandra Babu, R. (2021). Mapping consistent additive and epistatic QTLs for plant production traits under drought in target populations of environment using locally adapted landrace in rice (*Oryza sativa* L.). *Plant Prod Sci* 24(3): 388-403.

Redona, E., and Mackill, D. (1996). Genetic variation for seedling vigor traits in rice. *Crop Sci* 36(2): 285-290.

Sabouri, H. (2007). *Evaluation of genetic diversity of Iranian rice germplasm for drought tolerance and locating its related QTLs.* PhD Dissertation, Isfahan University of Technology.

Saghai Maroof, M.A., Biyashev, R.M., Yang, G.P., Zhang, Q., and Allard, R.W. (1994). Extraordinarily polymorphic microsatellite DNA in barley: species diversity, chromosomal locations, and population dynamics. *Proc Natl Acad Sci USA* 91(12): 5466-5470. doi: 10.1073/pnas.91.12.5466.

Sarayloo, M., Sabouri, H., and Dadras, A.R. (2015). Assessing genetic diversity of rice genotypes using microsatellite markers and their relationship with morphological characteristics of seedling stage under non-and drought-stress conditions. *Cereal Res* 5(1): 1-15.

Shirmohammadli, S., Sabouri, H., Ahangar, L., Ebadi, A.A., and Sajjadi, S.J. (2018). Genetic diversity and association analysis of rice genotypes for grain physical quality using iPBS, IRAP, and ISSR markers. *J Genet Resour* 4(2): 122-129.

Teng, S., Zeng, D., Qian, Q., Kunihifo, Y., Huang, D., and Zhu, L. (2001). QTL analysis of rice low temperature germinability. *Chin Sci Bull* 46: 1800-1803.

Wang, S., Basten, C., Gaffney, P., and Zeng, Z. (2007). Windows QTL Cartographer 2.0. North Carolina State University. *Bioinformatics Research Center*.

Wang, X.S., Zhu, J., Mansueto, L., and Bruskiewich, R. (2005). Identification of candidate genes for drought stress tolerance in rice by the integration of a genetic (QTL) map with the rice genome physical map. *J Zhejiang Univ Sci B* 6(5): 382-388. doi: 10.1631/jzus.2005.B0382.

Zahedi, Z., Nabipour, A., and Ebrahimi, A. (2019). Effectiveness of molecular markers for improving grain quality in Iranian rice. *J Plant Mol Breed* 7(1): 22-30.

Zhang, Z., Ersoz, E., Lai, C.Q., Todhunter, R.J., Tiwari, H.K., Gore, M.A., Bradbury, P.J., Yu, J., Arnett, D.K., Ordovas, J.M., and Buckler, E.S. (2010). Mixed linear model approach adapted for genome-wide association studies. *Nat Genet* 42(4): 355-360. doi: 10.1038/ng.546.

Zhang, Z.H., Qu, X.S., Wan, S., Chen, L.H., and Zhu, Y.G. (2005). Comparison of QTL controlling seedling vigour under different temperature conditions using recombinant inbred lines in rice (*Oryza sativa*). *Ann Bot* 95(3): 423-429. doi: 10.1093/aob/mci039.

JPMB
Journal of Plant Molecular Breeding
Published by Genetics and Agricultural Biotechnology Institute of Tabarestan
2022 | Volume 10 | Issue 2

مقاله پژوهشی

ساختار ژنتیکی تحمل به خشکی در لاین‌های نوترکیب برنج ایرانی (*Oriza sativa*) در مراحل رویشی و زایشی

مرتضی نوریان [۱]، اسلام مجیدی هاروان [۱]، حسین صبوری *[۲]، فرخ درویش کجوری [۱]

[۱] گروه اصلاح نباتات و بیوتکنولوژی، واحد علوم و تحقیقات، دانشگاه آزاد اسلامی، تهران، ایران
[۲] گروه تولیدات گیاهی، دانشکده علوم کشاورزی و منابع طبیعی، دانشگاه گنبد کاووس، ایران

چکیده: به منظور بررسی ساختار ژنتیکی تحمل به خشکی در برنج، آزمایشی با استفاده از ۱۲۰ لاین نوترکیب (ندا × اهلمی طارم) به صورت فاکتوریل در قالب طرح کاملاً تصادفی با سه تکرار در گلخانه دانشگاه گنبدکاووس انجام شد. در این تحقیق برای القای تنش اسمزی (۴/۵- و ۹- بار)، از PEG 6000 در مراحل رویشی و زایشی استفاده شد. علاوه بر اندازه‌گیری صفات مورفولوژیکی ریشه و اندام هوایی، از نشانگرهای SSR، iPBS، IRAP و ISSR برای ایجاد نقشه پیوستگی ژنتیکی استفاده شد. به ترتیب در مراحل رویشی و زایشی ۱۶ و ۲۰ QTL شناسایی شدند. در مقایسه سه تیمار ارزیابی شده، qRN-12، qRS-11، و qRV-12 به عنوان QTLهای پایدار مناسب برای انتخاب لاین‌های متحمل به خشکی در مرحله رویشی در شرایط مختلف تعیین شدند. چندین آلل جدید مرتبط با QTLهای تحمل به خشکی در این مطالعه شناسایی شدند. در دو شرایط محیطی، QTLهای مهم شناسایی شده، مانند qNTF-12 و qNL-3، متعلق به تعداد پنجه‌های بارور و برگ‌ها بودند که به عنوان QTL های پایدار در مرحله زایشی تعیین شدند. در این مطالعه، QTLهای شناسایی شده در مراحل رویشی و زایشی می‌توانند به عنوان QTLهای پایدار و اصلی برای انتخاب لاین‌های متحمل به خشکی در انتخاب به کمک نشانگر مورد استفاده قرار گیرند.

کلمات کلیدی: QTL بزرگ اثر، تنش اسمتیک، مکان های ژنی کنترل کننده صفات کمی، برنج.

ویراستار علمی
دکتر احمد ارزانی،
دانشگاه صنعتی اصفهان، ایران

تاریخ
دریافت: ۱۳ بهمن ۱۴۰۱
پذیرش: ۱ خرداد ۱۴۰۲
چاپ: ۲۹ آذر ۱۴۰۲

نویسنده مسئول
دکتر حسین صبوری
hos.sabouri@gmail.com

ارجاع به این مقاله
Noryan, M., Majidi Harvan, I., Sabouri, H., and Darvish Kojouri, F. (2022). Genetic structure of drought tolerance in Iranian rice (*Oryza sativa*) recombinant lines at vegetative and reproductive stages. *J Plant Mol Breed* 10(2): 1-18. doi:10.22058/jpmb.2023.1989048.1270

JPMB | Journal of Plant Molecular Breeding
Published by Genetics and Agricultural Biotechnology Institute of Tabarestan
2022 | Volume 10 | Issue 2

In vitro asymbiotic germination of mature seed of medicinal orchid (*Orchis simia* Lam.)

Zeinab Masoudi Jozchal *[1], Nadali Bagheri [1], Nadali Babaeian Jelodar [1], Gholamali Ranjbar [1], Jamshid Farmani [2]

[1.] Department of Genetics and Plant Breeding, Sari Agricultural Sciences & Natural Resources University, Sari, Iran
[2.] Department of Food Science, Sari Agricultural Sciences &Natural Resources University, Sari, Iran

Original paper

OPEN ACCESS

Edited by

Dr. Seyyed Kamal Kazemitabar,
Sari Agricultural Sciences & Natural Resources University, Iran

Date

Received: 21 June 2023
Accepted: 13 October 2023
Published: 01 january 2024

Correspondence

Zeinab Masoudi Jozchal
Zeinab.Masoodi3271@gmail.com

Citation

Masoudi Jozchal, Z., Bagheri, N., Babaeian Jelodar, N., Ranjbar, Gh. and Farmani, J. (2022). *In vitro* asymbiotic germination of mature seed of medicinal orchid (*Orchis simia* Lam.). *J Plant Mol Breed* 10(2): 19-30. doi:10.22058/JPMB.2023.2005284.1276

Abstract: The sexual reproduction of orchids is a notably slow process. This is due to their seeds lacking endosperm, which necessitates a fungal elicitor for germination in natural conditions. In the current study, we evaluated seed germination and the initial development of the protocorm of *Orchis simia*, an important medicinal orchid species, using a completely randomized design with three replications. The tetrazolium test revealed that 35% of the seeds were viable. Subsequently, we investigated the influence of casein, activated charcoal, indole acetic acid (IAA), photoperiod, and temperature on the germination of *O. simia* seeds. The analysis of variance demonstrated varying responses in terms of seed germination percentages, with photoperiod and temperature treatments having a more pronounced impact on germination. The optimal conditions for asymbiotic orchid seed germination in this experiment were achieved using Murashige and Skoog's (MS) medium supplemented with one-fifth of nitrate concentration, casein (2.0 g/l), activated charcoal (2.0 g/l), and an IAA growth regulator (1.0 mg/l), resulting in a germination rate of 31%. After a three-month period, the nodes underwent transformation into protocorms. The findings presented in this report can serve as valuable insights for the production of orchid plants and the conservation of this medicinal species.

Keywords: germination factors, growth regulator, orchid, protocorm.

Introduction

The Orchidaceae family stands out as one of the largest and most diverse families of flowering plants, encompassing an impressive 28237 species (Willis, 2017). These orchids are found in various regions, including the tropical humid forests of India, Sri Lanka, South Asia, South and Central America, and Mexico (Singh et al., 2019). Notably, the Orchidaceae family is included in the International Union for Conservation of Nature (IUCN) list of endangered plants, highlighting their ecological significance.

Within the realm of monocots, orchids represent one of the most advanced families, boasting around 850 genera (Stewart and Griffiths, 1995; Gutiérrez, 2010). Orchids are valued not only for their aesthetic beauty but also for their medicinal properties attributed to the presence of alkaloids, flavonoids, glycosides, and various other plant compounds (Gutiérrez, 2010). Owing to the persistent destruction of their natural habitats, excessive harvesting for medicinal applications, illegal trade, and overzealous cultivation by orchid farmers, orchid populations are facing a rapid and alarming decline. Additionally, the premature harvesting of orchids during their flowering stage, before the physiological ripening of seeds, underscores the need for mass *in vitro* propagation of this plant.

Micro orchid seeds face a natural limitation as they lack the ability to germinate independently. However, the germination process in these plants can be accelerated by a range of biotic and abiotic factors. Understanding the ecology of orchid reproduction, including issues such as non-germination or seed dormancy in natural conditions, represents a significant aspect of orchid growth characteristics in temperate climates (Butcher and Marlow, 1989). The seeds of terrestrial orchids have a special form of morphophysiological dormancy, which consists of morphological (the presence of an undifferentiated embryo and a strong seed coat) and physiological factors (the embryo does not have enough growth potential to penetrate the seed coat and germinate). In addition, seeds do not have endosperm, and the nutrients of mature seeds are concentrated in the embryo cells. Nutrients in seeds include lipids, proteins, and carbohydrates, and their amounts vary from species to species (Rasmussen, 1995). Although the seed embryo in these plants contains carbohydrates, the amount of sugar in the embryo is not usually enough to support germination completely or even to initiate germination (Manning and Van, 1987). In their natural habitat, orchid seed germination hinges on a specific symbiotic relationship with mycorrhizal fungi (Marks et al., 2013). This dependence poses a challenge to the sustainability of viable plant populations, particularly in regions grappling with habitat loss caused by forest degradation (Tremblay et al., 2005).

Advancements in orchid seed germination techniques, particularly *in vitro* germination, have significantly enhanced the reliability of germination and the propagation of numerous orchid species. This approach offers an ideal system for investigating the growth and development of orchid seeds and seedlings (Kauth et al., 2008). Propagation of orchids using tissue culture methods is suitable because there is a good opportunity to improve and increase the number of seedlings through mass propagation of important orchids, hybrids, and or a new variety in a short period of time (Goh and Wong, 1990; Chen and Chang, 2000; Pathak et al., 2001; Chen et al., 2004; Bhattacharjee and Hossain, 2015; Borah et al., 2015; Sibin and Gangaprasad, 2016; Bhatti et al., 2017; Mohanty and Salam, 2017; Decruse and Gangaprasad, 2018). One of the major obstacles to the mass propagation of economically important orchids for commercial purposes and to prevent the risk of extinction is the unavailability of efficient and reliable instructions for the germination of this plant species. In general, the biology of seed germination is the same for all orchid species and includes two developmental stages-embryo swelling and protocorm formation. However, several factors such as seed maturity, seed dormancy, seed sterilization, composition and content of the nutrient medium, light, and temperature have a great influence on seed germination (Arditti, 1967; Kauth et al., 2008; Zeng et al., 2014; Dulić et al., 2019). Hence, it is imperative to develop specific guidelines for each orchid species to expedite and optimize the germination and growth of these plants.

In the case of most terrestrial orchids, the inclusion of organic additives rich in amino acids within nutrient media significantly influences seed

germination. Commonly employed organic additives in *in vitro* culture include coconut water, banana powder, peptone, hydrolyzed casein, yeast extract, and pineapple juice. Notably, the organic content of casein has been found to have a beneficial impact on the germination rate of medicinal orchid seeds, such as those of *Eulophia nuda*, which face extinction (Nanekar et al., 2014). *Rhynchostylis retusa*, *Cymbidium elegans*, *Cypripedium calceolus*, and *Epipactis helleborine* species also showed higher germination speed and shorter period length for germination in a casein-enriched nutrient medium (Nandi et al., 1999).

In order for symbiotic and asymbiotic orchid seed germination to be effective, many conditions such as photoperiod, temperature, and nutrition should be considered. Lighting is one of the most important environmental factors in orchid seed germination, which was less studied. In most orchid species, light has an inhibitory effect on seed germination. However, there are species whose seeds germinate under light conditions, and *in vitro* culture, germination responses to the length of the light period often depend on the type of species (Arditti et al., 1981; Kauth et al., 2008). However, germination responses to photoperiods is often species-specific, regardless of growth habit (Kauth et al., 2008). darkness is often considered to stimulant germination of terrestrial orchids. For example, seeds of terrestrial orchids may not germinate until do not be under the soil (Rasmussen and Rasmussen, 1991). Also, many terrestrial orchids grow in shadow environments better than their epiphytic counterparts (Rasmussen, 1995), While the light may not reach the floor of the habitat easily (Rasmussen and Rasmussen, 1991). Van Waes and Debergh (1986) reported that even a small increase in light intensity from complete darkness to 1.2 µmol/m2/s reduced the germination of several European terrestrial orchids. Asymbiotic germination of *Cypripedium acaule*, a North American terrestrial orchid, was lower when seeds were incubated in a photoperiod of 16 h (6.7% germination) compared to complete darkness (96.7%) (ST-ARNAUD, 1992).

The use of growth regulators stimulates the zygote embryo to form protocorms that grow into seedlings (Pant and Gurung, 2005). Cytokinin treatments showed increased asymbiotic germination in many orchid species. Miyoshi and Mii (1988), and Stewart and Kane (2006) also reported increased germination levels of several terrestrial orchids.

Vegetative propagation is a time-consuming process for generating a substantial quantity of orchid clones. Consequently, tissue culture represents an alternative method for mass-scale propagation and conservation of rare and endangered orchids. This technique can significantly expedite the identification and protection of new plant species. The current study seeks to explore the *in vitro* asymbiotic germination of medicinal orchid seeds. It investigates the influence of factors such as light conditions, temperature, casein, activated carbon, and plant growth regulators to accelerate the germination and propagation of this plant within a shorter timeframe compared to natural conditions.

Materials and Methods

Plant materials

Orchid seedlings (*Orchis simia* Lam.) were collected from the Ramyan region in Golestan province, Iran, during flowering stage. These seedlings were transplanted into pots, with soil carefully placed around their roots, and they were nurtured until the formation of capsules. By the end of May, mature capsules were harvested and stored in a refrigerator at 5°C, awaiting tissue culture.

Tetrazolium viability test

Seed viability was evaluated using 2, 3, 5-triphenyltetrazolium chloride solution. A small sample of seeds (5 mg) was pretreated with 10% sucrose solution for 24 h at room temperature. Then the solution was drained with a sampler, 0.1% tetrazolium solution was added, and the tubes were incubated in the dark for 24 h in a 40°C water bath, according to the method described by Hosomi et al. (2011). Seed viability was assessed using a light microscope with 100 seeds replicated three times. Red seeds were considered alive and brown seeds or no embryos were considered dead. The percentage of live seeds was calculated by dividing the number of live embryos by the total number of tested embryos.

Surface sterilization of capsules

Initially, the capsules underwent surface disinfection using a 70% ethanol solution for 1 minute, followed by rinsing with sterile distilled water. Subsequently, they were disinfected in a 20% sodium hypochlorite solution for 15 minutes, after which they were transferred within a laminar hood and subjected to two additional washes with sterile distilled water.

Culture media

MS culture media (control), MS plus 0.2% casein, $MS_{N_{\frac{1}{5}}}$ (MS culture medium containing one-fifth of nitrate plus 0.2% casein), and $MS_{N_{\frac{1}{5}}}$ supplemented with (0.2% casein and 1.0 mg/l IAA) were employed for the cultivation and germination of orchid seeds. In addition, all these cultures contained 0.2% activated charcoal. The pH of the culture medium was adjusted to 5.8 by adding 1 N NaOH or 1 N HCl and then it was autoclaved at 121 °C with a pressure of 1.2 kPa for 20 min. The sterilized culture medium was transferred to the culture chamber (laminar hood) and 25 ml of culture medium was poured into 100 ml sterile flasks.

Cultivation of seeds

The sterilized capsules inside the laminar airflow hood, after washing with sterile distilled water and drying with sterile filter paper, were transferred to a sterilized Petri dish, and using a sterilized scalpel, a longitudinal slit was given to the capsules and the seeds were placed on the culture medium. About 200 seeds were cultivated in each culture container containing 25 ml of culture medium. The cultivated seeds were kept in the incubator under different light conditions (darkness and light/darkness 12/12 h) and temperature (20 and 25 °C).

Statistical method

The treatments studied include casein (2.0 g/l), activated charcoal (2.0 g/l), indole acetic acid (1.0 mg/l). The data relating to the germination percentage of mature seeds and the number of days until germination were analyzed using SPSS statistical software in a completely randomized design with 3 replications and mean comparison was done by Duncan's multi-range test method at 5% probability level.

Results

The mature seeds of *Orchis simia* used in this experiment as explants have a brown color and the embryos consist of a concentrated mass with a seed coat (Figure 2A). Physiological developmental stages from seed to early protocorm development are given in Figure 2. The tetrazolium (TZ) test before sterilizing the seeds showed that 35% of the seeds were alive, 40% of the seeds were without embryos, and 25% of the seeds were dead (Figure 2B). The effects of culture medium with different conditions on germination were evaluated. The results of the TZ test of *O. Simia* seeds confirmed the results of their *in vitro* germination in MS medium (N1/5) + IAA+ casein (31%) medium. Studies have questioned the use of the TZ test alone as an indicator of seed germination and show the importance of confirming *in vitro* germination results, as we determined. The TZ test showed that seed viability was significantly higher than the observed maximum germination. This discrepancy can be explained by the fact that the nutrients or other components required by the explant are not present or are not in the optimal concentration in the culture medium (Lauzer et al., 2007). The results of the analysis of variance showed that the percentage of germination of orchid seeds of *Orchis simia* in different culture media has a significant difference at the level of 1% (Table 1).

The comparison of the means shows the importance of the organic matter and growth regulator IAA in the germination of the desired orchid seed. MS culture medium together with one-fifth of nitrate and having casein organic matter 2 g/L plus IAA 1 mg/L was the most suitable culture medium ($\bar{Y}$= 31%) for the germination of these seeds (Figure 1A). About 4 weeks after placing the cultures in the incubator at a temperature of 20°C in the dark, some of the seeds swelled and formed small white dots with thin threads, and about two months later, they started to form protocorms (Figure 2D). Also, MS culture medium (control) showed the lowest percentage of seed germination ($\bar{Y}$= 8.66 %). The number of days until seed germination in MS medium (control) took longer than in other culture mediums ($\bar{Y}$= 31.66 days). There was no significant difference in the number of days until germination for other culture mediums, and the length of culture was about 25 days. By adding casein organic

material to the MS medium, the germination percentage increased by 19.33% compared to the MS medium (control), and the germination time decreased to 25 days (Figure 1B). The incubator temperature of 20°C and dark conditions played a very important role in seed germination so under the mentioned conditions, seed germination was observed after one month, but in the seeds incubated at 20°C and light conditions, seed germination was not observed. This indicates the importance of dark conditions for *orchis simia* seeds germination. Also, no seed germination was observed in the seeds incubated in the dark at 25°C. Therefore, dark conditions and a temperature of 20°C are very important for germination in this plant. The results of the mean comparison showed that among the tested culture mediums, MS medium (N1/5) + casein + IAA with the highest percentage of germination and the lowest number of days to germination was the most suitable medium compared to other tested mediums. Based on the obtained results, IAA growth regulator and casein had a positive and significant effect on the percentage of germination and the number of days until germination.

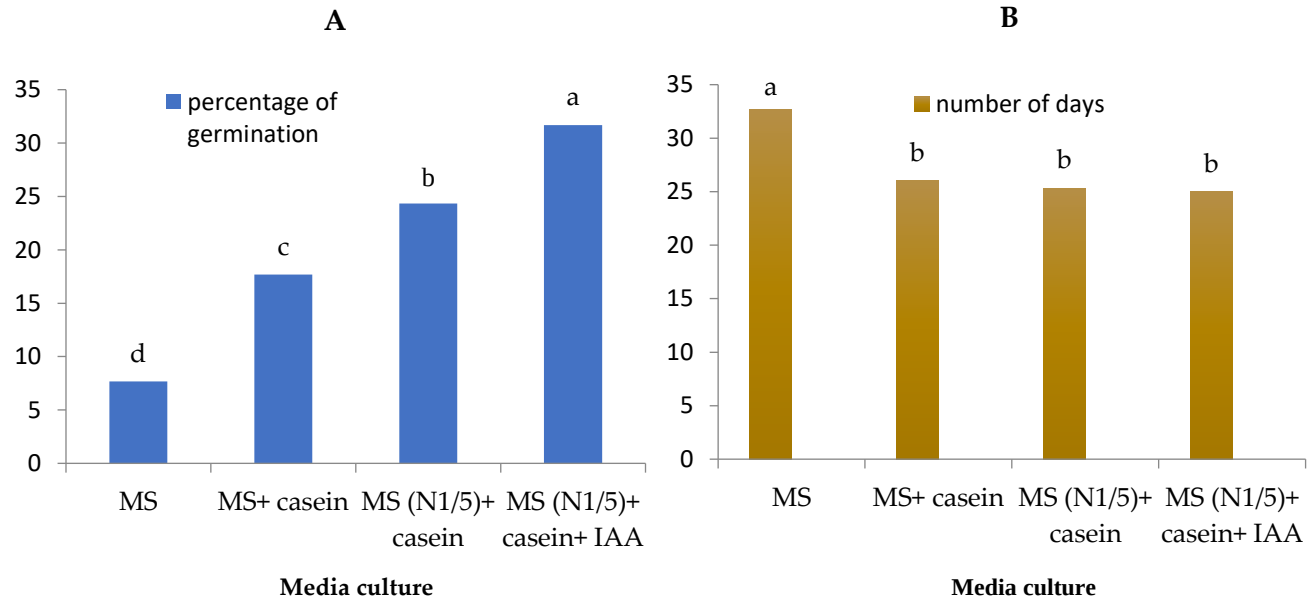

Figure 1- Comparison of the means percentage of germination (A) and the number of days to initial germination (B) in different culture media by Duncan's multi-range test method.

Table 1. Analysis of variance of studied orchid traits in different culture media

Sources of variation	Degree of freedom	Mean square	
		Germination %	Number of days until germination
Treatment	3	265.89**	29.56 **
Residual	8	1.75	1.67
Coefficient of variation (%)		6.35	4.78

** ؛Significant at the 1% probability level

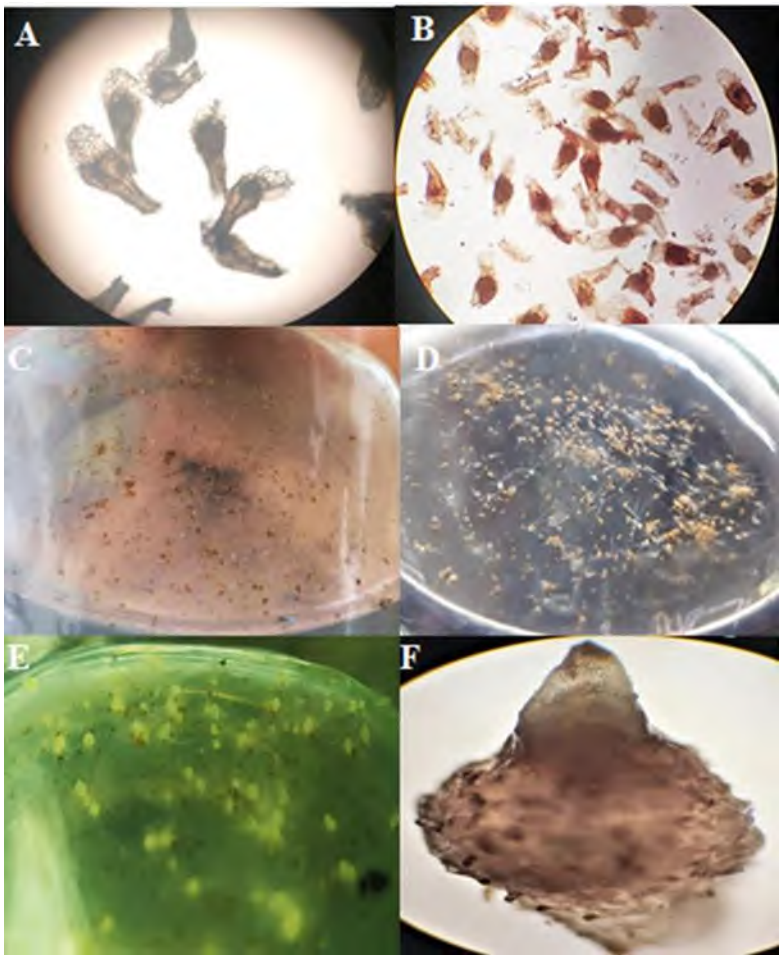

Figure 2. *In vitro* germination of *orchis simia*. A. Mature seeds. B. Seeds subjected to tetrazolium test. C. Seed germination in MS + casein medium. D. Seeds germinated in MS medium (N1/5) + IAA + casein. E. Protocorm formation. F. Protocorm with 10 x magnification

4. Discussion

Due to their unique characteristics, orchids do not reproduce via seeds in the same manner as other crops. Orchid seeds are incredibly small, almost microscopic in size, and they lack essential components such as endosperm, cotyledon, and a primary root. Their germination and initial growth depend on a symbiotic relationship with fungi (Seaton et al., 2013). Furthermore, orchid seeds contain an undifferentiated embryo that lacks the necessary enzymes for metabolizing polysaccharides and lipids. Despite the presence of sugars like sucrose, fructose, maltose, rhamnose, and glucose in the orchid embryo, these sugars are often insufficient for sustaining germination. Consequently, the presence of symbiotic fungi is crucial during the initial stages of seed germination, as they provide the embryo with essential resources such as water, carbohydrates, vitamins, and minerals after penetrating the embryo (Kauth et al., 2008). In nature, from the thousands to millions of microscopic seeds produced by an orchid pod, only a mere 2-3% of them undergo germination (Dutta et al., 2011). Vegetative propagation of this plant is very slow and time-consuming (Pradha and Pant, 2009). Therefore, this reproduction method cannot meet the needs of the people, the market, and different pharmaceutical companies (Basker and Bai, 2010). The *in vitro* culture method will solve these problems by reducing the time required for seed germination as well as plant propagation on a large scale (Pradha and Pant, 2009). Tissue culture has become a standard propagation method for orchid conservation. Seed germination *in vitro* is an advance in orchid propagation (Fay, 1996). In this

study, different MS media were used for the germination of mature orchid seeds. According to the observations, germination was seen in all investigated media, but the percentage of germination was different (Lal et al., 2020), in the study of the germination of mature seeds of two orchid species, observed the first germination in 4 weeks after sowing, and protocorm development was observed 7-9 weeks after sowing. Also, in the study of the germination of immature orchid seeds by Jain and Saxena (2009), the seeds started to germinate in Mitra medium with peptone in dark conditions for one week and formed protocorms in 6 weeks, and about 90% of the germinated seeds started to form a protocorm. In the study of Fatahi et al. (2022), the characteristics of asymbiotic seed germination and seedling growth *in vitro* conditions were significantly ($P<0.05$) influenced by two main types of organic compounds and nitrogen sources. So the seeds cultivated in media containing pineapple juice (PJ) and casein hydrolyzed (CH) had the highest germination percentage. In addition, germination was the most frequent in the MS medium with casein organic matter and indole acetic acid growth regulator. In the present study and the comparisons made, it is possible to understand the application and importance of cytokinin growth regulators on the germination rate of *Orchis Simia* orchids. The role of plant growth regulators (PGRs) in orchid germination is unclear and the response of growth regulators is often species-specific. A major obstacle in understanding the role of exogenous and endogenous PGRs in promoting/inhibiting orchid seed germination may be the small size of the seeds and the possible low levels of PGRs in the embryo. Research on the concentration of endogenous PGRs in orchid seeds, as well as when PGRs are active at germination, will greatly increase the knowledge of how PGRs affect orchid seed germination (Kauth et al., 2008).

Through an examination of the *in vitro* multiplication of mature seeds from *Orchis coriophora* L and the evaluation of various PGRs on their germination, the highest observed germination rate (44.2%) was achieved in the Orchimax culture medium supplemented with activated charcoal and 1 mg/liter of indole-3-acetic acid (Bektaş et al., 2013). Castillo-Pérez et al. (2021) investigated the germination of mature seeds of the orchid *Stanhopea tigrina* in Morashig and Skoog medium and the auxins indole-3-acetic acid (IAA) and indole-3-butyric acid singly or in combination with salicylic acid or coconut water were tested for rooting, and the combination of coconut water (100 ml/L) alone or in combination with indole-3-acetic acid (2.5 or 5 mg/L) was the best treatment. Based on the obtained results, the IAA growth regulator and casein had a positive and significant effect on the percentage of germination and the number of days until germination. Therefore, orchid seeds can germinate better in a medium with organic matter and IAA growth regulators. For many plant species, temperature is a major factor in initiating and breaking physiological seed dormancy (Baskin et al., 2004). Baskin et al. (2006) recommended an alternating temperature range to study the germination ecology of all seeds because constant temperatures are not common *in nature*. However, orchid seeds often germinate *in vitro* at a constant temperature. In the medicinal orchid species *Orchis simia*, mature seeds germinated at a constant temperature of 20°C, but no germination was observed at a temperature of 25 °C.

There are several valuable studies on orchid seed germination and temperature. Like many other species, orchid seeds germinate within a certain temperature range, but maximum germination occurs at a certain temperature. *Dactylorhiza majalis* seeds germinate between 10 and 30°C, but the optimum temperature range seems to be between 23 and 24.5°C (Rasmussen et al., 1990). The percentage of germination decreased below 15°C and above 27°C (Rasmussen and Rasmussen, 1991; Pradha and Pant, 2009). The effect of light and darkness on the germination of orchid seeds is debatable. Zettler and Hofer (1997) reported a significant reduction in germination when *S. odorata* seeds were exposed to a short light period. Germination in complete darkness for three weeks was higher than the germination of seeds that were exposed to 7 days of 12.12 and 16/8 h light period and then in darkness for 2 weeks. Stewart and Kane (2006) reported that light inhibited asymbiotic germination and the development of *Habenaria macroceratitis*. The aforementioned terrestrial orchids all grow in shady areas. If the orchid studied in this research also grows in shady areas. In the study of the seed germination of the orchid

species called Spiranthes by Zale et al. (2022), the seedlings in light/dark periods of 0/24 h and light/darkness of 16/8 h had significantly more fresh weight than the dark treatment group, and therefore for optimal growth need light. The impact of light and darkness on orchid seed germination remains a subject of debate. In line with our findings, another study reported the highest germination rate for *Cyrtopodium punctatum* seeds under continuous darkness (0/24 h) (Dutra et al., 2009).

Conclusion

In this study, the MS (N1/5) + casein + IAA medium emerged as the most favorable culture medium for the germination of mature seeds. Notably, germination was observed four weeks after cultivation, with protocorms appearing within two months after seed cultivation. Dark conditions were found to be significantly conducive to the germination of the tested orchid species, as no germination occurred under bright conditions. It is advisable to explore the use of additional organic compounds such as coconut water and peptone to potentially enhance germination results. Furthermore, investigating the impact of varying IAA concentrations on the duration and germination percentage of the target orchid seeds would be a valuable avenue for future research.

Supplementary Materials:

No supplementary material is available for this article.

Author Contributions:

Conceptualization, Z.M.J. and N.B.; methodology, Z.M.J. and N.B.; software, N.B.; validation, Z.M.J.; N.B., N.B.J., G.R. and J.F.; formal analysis, Z.M.J. and N.B.; investigation, Z.M.J.; resources, Z.M.J.; data curation, Z.M.J and N.B.; writing—original draft preparation, Z.M.J. and N.B.; writing—review and editing, Z.M.J., N.B., and G.R.; visualization, N.B.J. and N.B.; supervision, Z.M.J. and N.B.; project administration, Z.M.J. and N.B.; funding acquisition, N.B., N.B.J., G.R. and J.F. All authors have read and agreed to the published version of the manuscript.

Funding:

This research did not receive any external funding.

Acknowledgments:

Thanks for the support of Biotechnology Laboratory of Sari University of Agricultural Sciences and Natural Resources, Iran.

Conflicts of Interest:

The authors declare no conflict of interest.

References

Arditti, J. (1967). Factors affecting the germination of orchid seeds. *Bot Rev* 33(1): 1-97.

Arditti, J., Michaud, J.D., and Oliva, A.P. (1981). Seed germination of North American orchids. I. native California and related species of *Calypso*, *Epipactis, Goodyera, Piperia*, and *Platanthera*. *Bot Gaz* 142(4): 442-453.

Basker, S., and Bai, V.N. (2010). In vitro propagation of an epiphytic and rare orchid *Eria bambusifolia* Lindl. *Res J Biotechnol* 1(1): 15-20.

Baskin, C.C., Baskin, J.M., Guerrant, E., Havens, K., and Maunder, M. (2004). Determining dormancy-breaking and germination requirements from the fewest seeds. *Ex situ plant conservation: supporting species survival in the wild*: 162-179.

Baskin, C.C., Thompson, K., and Baskin, J.M. (2006). Mistakes in germination ecology and how to avoid them. *Seed Sci Res* 16(3): 165-168.

Bektaş, E., Cüce, M., and Sökmen, A. (2013). In vitro germination, protocorm formation, and plantlet development of *Orchis coriophora* (*Orchidaceae*), a naturally growing orchid species in Turkey. *Turk J Bot* 37(2): 336-342.

Bhattacharjee, D., and Hossain, M. (2015). Effect of plant growth regulators and explants on propagation on a monopodial and sympodial orchid: A study in vitro. *J Orchid Soc India* 29: 91-102.

Bhatti, S.K., Verma, J., Sembi, J.K., and Pathak, P. (2017). Symbiotic seed germination of *Aerides multiflora* Roxb.-A study in vitro. *J Orchid Soc India* 31: 85-91.

Borah, N., Chakraborty, S., Choudhary, S.R., and Dutta, B. (2015). In vitro propagation of *Paphiopedilum spicerianum* (Reichb. F.) Pfitz.-A rare and endangered orchid species from NorthEast India. *J Orchid Soc India* 29: 85-90.

Butcher, D., and Marlow, S. (1989). "Asymbiotic germination of epiphytic and terrestrial orchids", in: *Modern methods in orchid conservation: the role of physiology, ecology and management.* (Berlin Heidelberg: Springer).

Castillo-Pérez, L.J., Martínez-Soto, D., Fortanelli-Martínez, J., and Carranza-Álvarez, C. (2021). Asymbiotic seed germination, in vitro seedling development, and symbiotic acclimatization of the Mexican threatened orchid *Stanhopea tigrina*. *Plant Cell Tissue Organ Cult* 146: 249-257.

Chen, J.-T., and Chang, W.-C. (2000). Efficient plant regeneration through somatic embryogenesis from callus cultures of *Oncidium* (*Orchidaceae*). *Plant Sci* 160(1): 87-93.

Chen, T.-Y., Chen, J.-T., and Chang, W.-C. (2004). Plant regeneration through direct shoot bud formation from leaf cultures of *Paphiopedilum orchids*. *Plant Cell Tissue Organ Cult* 76: 11-15.

Decruse, S.W., and Gangaprasad, A. (2018). Restoration of *Smithsonia maculata* (Dalz.) Saldanha, an endemic and vulnerable orchid of Western Ghats through in vitro propagation. *J Orchid Soc India* 32: 25-32.

Dulić, J., Ljubojević, M., Ognjanov, V., Barać, G., and Dulić, T. (2019). In vitro germination and seedling development of two European orchid species, *Himantoglossum jankae Somlyay, Kreutz* & Óvári and *Spiranthes spiralis* (L.) Chevall. *In Vitro Cell Dev Biol Plant* 55(4): 380-391.

Dutra, D., Kane, M.E., and Richardson, L. (2009). Asymbiotic seed germination and in vitro seedling development of *Cyrtopodium punctatum:* a propagation protocol for an endangered Florida native orchid. *Plant Cell Tissue Organ Cult* 96(3): 235-243.

Dutta, S., Chowdhury, A., Bhattacharjee, B., Nath, P., and Dutta, B. (2011). In vitro multiplication and protocorm development of *Dendrobium aphyllum* (Roxb.) CEC Fisher. *Assam Univ J* 7(1): 57-62.

Fatahi, M., Vafaee, Y., Nazari, F., and Tahir, N.A.-r. (2022). In vitro asymbiotic seed germination, protocorm formation, and plantlet development of *Orchis simia* Lam.: A threatened terrestrial orchid species. *S Afr J Bot* 151: 156-165.

Fay, M. (1996). Micropropagation as a tool in plant conservation. *Plant Talk* 4: 22-23.

Goh, C., and Wong, P. (1990). Micropropagation of the monopodial orchid hybrid *Aranda* 'Deborah'using inflorescence explants. *Sci Hortic* 44(3-4): 315-321.

Gutiérrez, R.M.P. (2010). Orchids: A review of uses in traditional medicine, its phytochemistry and pharmacology. *J Med Plants Res* 4(8): 592-638.

Hosomi, S., Santos, R., Custodio, C., Seaton, P., Marks, T., and Machado-Neto, N. (2011). Preconditioning *Cattleya* seeds to improve the efficacy of the tetrazolium test for viability. *Seed Sci Technol* 39(1): 178-189.

Jain, S.M., and Saxena, P.K. (2009). *Protocols for in vitro cultures and secondary metabolite analysis of aromatic and medicinal plants.* Springer.

Kauth, P.J., Dutra, D., Johnson, T.R., Stewart, S.L., Kane, M.E., and Vendrame, W. (2008). Techniques and applications of in vitro orchid seed germination. *Floric Ornam* 5: 375-391.

Lal, A., Pant, M., Palni, L.M.S., and Kumar, A. (2020). Development of rapid micropropagation protocol for germplasm conservation of two orchid species–*Aerides multiflora* Roxb. And *Rhynchostylis retusa* (L.) Blume. *Asian J Conserv Biol* 9(2): 341-347.

Lauzer, D., Renaut, S., St-Arnaud, M., and Barabé, D. (2007). In vitro asymbiotic germination, protocorm development, and plantlet acclimatization of *Aplectrum hyemale* (Muhl. ex Willd.) Torr.(*Orchidaceae*). *J Torrey Bot Soc* 134(3): 344-348.

Manning, J., and Van, S.J. (1987). The development and mobilisation of seed reserves in some African orchids. *Aust J Bot* 35(3): 343-353.

Marks, T.R., Seaton, P., Pritchard, H.W., Kendon, J.P., and Puspitaningtyas, D.M. (2013). Orchid conservation: the next ten years. *Lankesteriana Int J Orchidol* 13(1-2): 93-101.

Miyoshi, K., and Mii, M. (1988). Ultrasonic treatment for enhancing seed germination of terrestrial orchid, *Calanthe discolor*, in asymbiotic culture. *Sci Hortic* 35(1-2): 127-130.

Mohanty, C., and Salam, P. (2017). In vitro seed culture studies in *Dendrobium* orchid cv. Banyat Pink. *J Orchid Soc India* 31: 93-96.

Nandi, S., Palni, L., and Kumar, A. (1999). "Role of plant tissue culture in biodiversity conservation and economic development," in *Curr Sci*. (Prakashan: Gyanodaya), 1229-1231.

Nanekar, V., Shriram, V., Kumar, V., and Kishor, P. (2014). Asymbiotic in vitro seed germination and seedling development of *Eulophia nuda* Lindl., an endangered medicinal orchid. *Proc Natl Acad Sci India Sect B Biol Sci* 84(3): 837-846.

Pant, B., and Gurung, R. (2005). In vitro seed germination and seedling development in *Aerides odorata* Lour. *J Orchid Soc India* 19(1&2): 51-55.

Pathak, P., Mahant, K., and Gupta, A. (2001). In vitro propagation as an aid to conservation and commercialization of Indian orchids: seed culture. *Orchids: science and commerce*: 319-362.

Pradha, S., and Pant, B. (2009). In vitro seed germination in *Cymbidium elegans* Lindl. and *Dendrobium densiflorum* Lindl. ex Wall.(*Orchidaceae*). *Botanica Orientalis: J Plant Sci* 6: 100-102.

Rasmussen, H., Andersen, T.F., and Johansen, B. (1990). Temperature sensitivity of in vitro germination and seedling development of *Dactylorhiza majalis* (*Orchidaceae*) with and without a mycorrhizal fungus. *Plant Cell Environ* 13(2): 171-177.

Rasmussen, H.N. (1995). *Terrestrial orchids: from seed to mycotrophic plant.* Cambridge University Press.

Rasmussen, H.N., and Rasmussen, F.N. (1991). Climactic and seasonal regulation of seed plant establishment in *Dactylorhiza majalis* inferred from symbiotic experiments in vitro. *Lindleyana* 6(4): 221-227.

Seaton, P., Kendon, J.P., Pritchard, H.W., Puspitaningtyas, D.M., and Marks, T.R. (2013). Orchid conservation: the next ten years. *Lankesteriana Int J Orchidol* 13(1-2): 93-101.

Sibin, N., and Gangaprasad, A. (2016). Development of in vitro propagation protocol for rapid and mass propagation of *Coelogyne nervosa* A. Rich., an endemic orchid of the Southern Western Ghats using immature seeds. *J Orchid Soc India* 30: 37-41.

Singh, S., Agarwala, D., Jalal, J., Dash, S., Mao, A., and Singh, P. (2019). Orchids of India, a pictorial guide, botanical survey of India. *Kolkata* 548.

ST-ARNAUD, M. (1992). In vitro germination and early growth of seedlings of *Cypripedium acaule* (*Orchidaceae*). *Lindleyana* 7: 22-27.

Stewart, J., and Griffiths, M. (1995). *Manual of orchids.* Timber Press New York.

Stewart, S.L., and Kane, M.E. (2006). Asymbiotic seed germination and in vitro seedling development of *Habenaria macroceratitis* (*Orchidaceae*), a rare Florida terrestrial orchid. *Plant Cell Tiss Organ Cult* 86: 147-158.

Tremblay, R.L., Ackerman, J.D., Zimmerman, J.K., and Calvo, R.N. (2005). Variation in sexual reproduction in orchids and its evolutionary consequences: a spasmodic journey to diversification. *Biol J Linn Soc Lond* 84(1): 1-54.

Van Waes, J., and Debergh, P. (1986). In vitro germination of some Western European orchids. *Physiol Plant* 67(2): 253-261.

Willis, K. (2017). *State of the world's plants 2017.* Royal Botanics Gardens Kew.

Zale, P.J., Clayton, A., Nix, J., and Taylor, M. (2022). Asymbiotic in vitro seed germination, in vitro seedling development, and ex vitro acclimatization of *Spiranthes*. *Appl Plant Sci* 10(5): e11494. doi: 10.1002/aps3.11494.

Zeng, S., Zhang, Y., Teixeira da Silva, J.A., Wu, K., Zhang, J., and Duan, J. (2014). Seed biology and in vitro seed germination of *Cypripedium*. *Crit Rev Biotechnol* 34(4): 358-371. doi: 10.3109/07388551.2013.841117.

Zettler, L.W., and Hofer, C.J. (1997). Sensitivity of *Spiranthes odorata* seeds to light during in vitro symbiotic seed germination. *Lindleyana* 12(1): 26-29.

JPMB
Journal of Plant Molecular Breeding
Published by Genetics and Agricultural Biotechnology Institute of Tabarestan
2022 | Volume 10 | Issue 2

مقاله پژوهشی

جوانه‌زنی غیرهمزیستی بذر بالغ ارکیده دارویی (*Orchis simia* Lam.) در شرایط آزمایشگاهی

زینب مسعودی جوزچال*[1]، نادعلی باقری[1]، نادعلی بابائیان جلودار[1]، غلامعلی رنجبر[1]، جمشید فرمانی[2]

[1] گروه ژنتیک و اصلاح نباتات، دانشگاه علوم کشاورزی و منابع طبیعی ساری، ساری، ایران
[2] گروه صنایع غذایی، دانشگاه علوم کشاورزی و منابع طبیعی ساری، ساری، ایران

چکیده: تکثیر جنسی ارکیده‌ها به دلیل فاقد آندوسپرم بودن بذرهای آن از روند کندی برخوردار بوده، ضمن اینکه جوانه‌زنی آنها در طبیعت نیز نیازمند به محرک‌های قارچی می‌باشد. در مطالعه حاضر، جوانه‌زنی بذر و توسعه اولیه پروتوکورم گونه *Orchis simia* ،یک ارکیده مهم دارویی، در قالب طرح کاملا تصادفی با سه تکرار مورد ارزیابی قرار گرفت. آزمایش تترازولیوم نشان داد ۳۵ درصد از بذرها زنده بودند. متعاقبا اثر کازئین، زغال فعال، ایندول استیک اسید، دوره نوری و دما بر جوانه‌زنی بذور *O. simia* بررسی شد. تجزیه و تحلیل واریانس پاسخ‌های متفاوتی از نظر درصد جوانه‌زنی بذر نشان داد، بطوری‌که تیمارهای دوره نوری و دما تاثیر بارزتری بر جوانه‌زنی داشتند. شرایط بهینه در این آزمایش برای جوانه‌زنی بذر گیاه ارکیده به صورت غیرهمزیست، محیط کشت موراشیگ و اسکوگ (MS) با یک پنجم نیترات همراه با کازئین (۲ گرم در لیتر)، زغال فعال (۲ گرم در لیتر) و تنظیم کننده رشد IAA (یک میلی‌گرم در لیتر) بوده، که در نتیجه آن سرعت جوانه‌زنی ۳۱٪ بدست آمد. پس از یک دوره سه ماهه، گویچه‌ها به پروتوکورم تبدیل شدند. یافته‌های ارائه شده در این گزارش می‌تواند درک جدیدی برای تولید گیاهان ارکیده و حفاظت از این گونه دارویی ارائه نماید.

کلمات کلیدی: ارکیده، پروتوکورم، فاکتورهای جوانه‌زنی، تنظیم‌کننده رشد.

ویراستار علمی
دکتر سیدکمال کاظمی‌تبار،
دانشگاه علوم کشاورزی و منابع طبیعی ساری، ایران

تاریخ
دریافت: ۳۱ خرداد ۱۴۰۲
پذیرش: ۲۱ مهر ۱۴۰۲
چاپ: ۱۱ دی ۱۴۰۲

نویسنده مسئول
زینب مسعودی جوزچال
Zeinab.Masoodi3271@gmail.com

ارجاع به این مقاله
Masoudi Jozchal, Z., Bagheri, N., Babaeian Jelodar, N., Ranjbar, Gh. and Farmani, J. (2023). *In vitro* asymbiotic germination of mature seed of medicinal orchid (*Orchis simia* Lam.). *J Plant Mol Breed* 10 (2): 19-30.
doi:10.22058/JPMB.2023.2005284.1276

JPMB | Journal of Plant Molecular Breeding
Published by Genetics and Agricultural Biotechnology Institute of Tabarestan
2022 | Volume 10 | Issue 2

Identification of drought stress-responsive long non-coding RNAs (lncRNAs) in root tip region of rice (*Oryza sativa*)

Sara Esmaeili Tazangi [1], Ali Niazi [1*], Mohammad Reza Ghaffari [2], Abbas Alemzadeh [3], Ahmad Tahmasebi [1]

[1.] Institute of Biotechnology, Shiraz University, Shiraz, Iran.
[2.] Department of Systems Biology, Agricultural Biotechnology Research Institute of Iran (ABRII), Karaj, Iran.
[3.] Department of Plant Production and Genetics, School of Agriculture, Shiraz University, Shiraz, Iran

Original paper

Abstract: Drought severely affects global rice production. Recent evidence highlights the critical role of long non-coding RNAs (lncRNAs) in the response to abiotic stress. Our research identified drought stress-induced lncRNAs in the root tip region of rice using transcriptome sequencing analysis on drought-stressed and control conditions in the sensitive rice genotype (IR64). We identified 358 differentially expressed lncRNAs (DElncRNA), with over 60% located in intergenic regions. Our results demonstrated that DElncRNAs can directly or indirectly regulate 710 and 7535 mRNAs in cis and trans, respectively. Additionally, the target genes of DElncRNAs were involved in drought resistance, lateral root growth, and auxin transport. We also identified 24 conserved sequence motifs in the upstream regions of DElncRNAs and differentially expressed mRNAs (DEmRNAs) motifs. Functional analysis revealed their involvement in the regulation of transcription, translation, and the transmembrane receptor protein tyrosine kinase signaling pathway. Finally, we constructed a network of DElncRNAs and DEmRNAs. Our functional analysis of the top 10 hub lncRNAs in the network demonstrated their involvement in growth processes, cellular responses to stimuli, and signaling pathways. These results offer a comprehensive perspective on potentially functional lncRNAs and provide insight into the molecular mechanisms underlying drought resistance in rice root tip.

Keywords: drought stress, rice, transcriptome, root tip, lncRNAs.

OPEN ACCESS

Edited by
Dr. S Hamidreza Hashemipetroudi, Genetics and Agricultural Biotechnology Institute of Tabarestan (GABIT), Sari Agricultural Sciences and Natural Resources University (SANRU), Iran

Date
Received: 25 July 2023
Accepted: 19 November 2023
Published: 6 January 2024

Correspondence
Dr. Ali Niazi
niazi@shirazu.ac.ir

Citation
Esmaeili Tazangi, S., Niazi, A., Ghaffari, M.R., Alemzadeh A. and Tahmasebi, A. (2022). Identification of drought stress-responsive long non-coding RNAs (lncRNAs) in root tip region of rice (*Oryza sativa*). *J Plant Mol Breed 10*(2): 31-45. doi:10.22058/JPMB.2023.2007831.1280

Introduction

Rice (*Oryza sativa* L.) is one of the most important crops in the world and the main source of food for billions of people (Sun et al., 2013). Asian cultivated rice (*Oryza sativa* L.) is one of the most important cultivated species that provides almost 20% of the calories consumed by humans (Smith, 1995). Unpredictable climate changes have caused aggravation of all types of stress, including drought stress, and this, in turn, leads to a decrease in the yield of cultivated rice (Lafitte et al., 2004). Leaves and roots are organs that coordinate the defense mechanism to respond to abiotic stresses (Kaashyap et al., 2018; Nadarajah and Kumar, 2019). It has been shown that the root system can change under stress leading to an increase in yield (Lynch et al., 2014). Due to its spreading and dense root system, rice is very sensitive to drought stress. Therefore, root length density and root diameter determine the development rate of the rice root system (Yoshida and Hasegawa, 1982). Drought tolerance is a complex trait that involves the regulation of several physiological and biochemical processes, including stomatal compaction (Ishimaru et al., 2001), leaf rolling (Yue et al., 2006), osmotic regulation (Peleg et al., 2009), and root system development (Barbez et al., 2017) at different developmental stages. Different mechanisms and a wide range of genes are also involved in response to drought stress. lncRNAs, eukaryotic RNAs with a length of more than 200 nucleotides, are part of the plant's defense mechanism, which, in addition to responding to abiotic stresses, play a vital role in various processes such as growth and development, seed yield, male sterility, and seed and leaf morphology (Caixia et al., 2020). In recent years, studies have identified a number of stress-related lncRNAs in plants. The identification of lncRNAs involved in drought stress can provide important help in identifying regulatory gene networks and improving drought stress tolerance in drought-sensitive rice cultivars. It has been reported that lncRNAs derived from transposon elements are responsible for the response to abiotic stresses in rice (Brunkard and Baker, 2018). Also, some lncRNAs have been discovered in rice in response to heat stress, cold stress, heavy metals, nitrogen and phosphorus treatments, and abscisic acid (Chen et al., 2018; Tang et al., 2019). On the other hand, the types of lncRNAs involved in the response to drought stress have been identified in different rice varieties, which play a vital role in the mechanism of improving tolerance against that stress (Xu et al., 2016; Li et al., 2019). In addition, research has shown that lncRNAs can act as traps for miRNAs targeting mRNAs involved in the response to drought stress and thereby protect mRNA translation. Also, as precursors of miRNA or siRNA, they can play a role in tolerance to biotic and abiotic stresses in rice (Nejat and Mantri, 2018). In the present study, we performed a transcriptome analysis to identify lncRNAs that participate in response to drought stress in the root tip region.

Materials and Methods

Plant materials and experimental design

IR64 genotype seeds were obtained from the International Rice Research Institute (IRRI). The seeds were surface disinfected using 5.25% sodium hypochlorite for 30 minutes followed by 70% ethanol for one minute. Then, the sterilized seeds were placed on moist filter paper for germination. The seven-day-old seedlings were transferred to a container containing Yoshida's liquid culture medium (Yoshida, 1976) for two weeks at a temperature of 27-25 degrees Celsius and a humidity of 60-70%. They were in light for a duration of 8 hours and 16 hours in dark with a light intensity of 500. They were placed up to 1000 par. After that, the seedlings were transferred to 3 × 25 × 40 cm boxes containing a mixture of clay, cocopeat, and sand in a ratio of 1:1:2, and each box contained two seedlings.

The seedlings were kept in the growth conditions mentioned above until stress was applied. Applying water stress (interruption of irrigation) was done on one hundred 35-day-old plants as a treatment, which reached 25-35% field capacity in 14 days. After the stress, sampling was done from the root tips of the stressed and control seedlings. The samples were collected and quickly frozen in liquid nitrogen. The roots tip from forty stressed seedlings were individually collected as the samples for whole transcriptome sequencing, with two biological repetitions.

RNA extraction and preparation

Total RNA was extracted from a pool of root tip samples from each condition using Invitrogen TRIZol reagent (Thermo Fisher Scientific, Waltham, MA, USA) (Xiao et al., 2011). RNA quantity and quality were determined using Nanodrop (NP80 NanoPhotometer, IMPLEN, Munich, Germany) and 1% agarose gel, respectively.

Sequence data analysis

RNA sequencing was performed based on Illumina HiSeq 2500 technique at the Beijing Genomics Institute (BGI, China). FastQC tool (version 0.11.9) was used to evaluate the quality of raw data reads. After pre-processing (remove adapter sequences and low-quality reads) clean reads were mapped to the *Oryza sativa Japonica* (IRGSP- 1.0) reference genome using hiSAT2 software. StringTie (version 2.1.5) under default settings was used to assemble the mapped reads.

lncRNA identification

To identify lncRNAs, transcripts of less than 200 nucleotides and transcripts with significant homology to known rice genes were removed. In addition, remaining transcripts were BlastX Pfam and UniProt databases, and transcripts with known protein domains were excluded. Finally, the coding potential of the transcripts was evaluated using CPC2 (Coding Potential Calculator) and CNCI (Coding-Noncoding Index) software and transcripts with a score less than zero were considered as potential lncRNA. According to the location of lncRNAs on the chromosome, they were divided into 4 overlapping, antisense, intergenic and intronic groups. The DESeq2 R package was used to identify differentially expressed long non-coding RNA (DElncRNA) between normal and stress conditions with a $|\text{fold change}| \geq 1$ and an adjusted p-value < 0.01.

Prediction of target genes of lncRNAs

Potential target genes of lncRNAs were divided into cis and trans based on their location. The genes located within 10 kb upstream and downstream of lncRNAs were predicted as the cis-targets. In addition, RIblast Fukunaga and Fukunaga and Hamada (2017) was used to predict the trans-targets mRNAs based on a cutoff of hybridization energy < −30 kcal/mol.

Enrichment analysis

Gene ontology enrichment analysis of target genes of lncRNAs was performed using agriGo version 2.0 (http://systembiology.cau.edu.cn/agriGOv2/). GO terms with the FDR value ≤ 0.01 were considered as the statistical significance. In addition, the DAVID tool was employed to perform pathway analysis. Pathways with an adjusted p-value < 0.05 were only considered as enriched.

Cis-elements analysis

The 1 kbp upstream flanking regions of DElncRNA and DEmRNA were extracted from Ensembl Plants (http://plants.ensembl.org). MEME (meme.nbcr.net/meme/intro.html) (Bailey et al., 2009) was used to discover conserved motifs on the sequences with its default parameters and threshold E-value of <1e-4. We used Tomtom v 5.0.1 tool (http://meme-suite.org/tools/tomtom) (Gupta et al., 2007) to eliminate redundant motifs and define known CRE based on plant JASPAR database (Khan et al., 2018) with a threshold E-value cut-off of 0.05. Subsequently, GoMo tool (http://meme-suite.org/tools/gomo) was applied to identify possible links of motifs with gene ontology terms (Buske et al., 2010).

Identification of lncRNAs as a potential target of miRNAs

The known miRNA sequences of *Oryza sativa* were downloaded from the miRBase database. The psRNATarget was utilized for the identification of the interaction relationship between lncRNAs and miRNAs with the default parameters and maximum expectation = 2.

lncRNA-mRNA network

Co-expression regulatory network was constructed based on calculation of correlation between DElncRNA and DEmRNA. Pearson correlations were determined by Hmisc R package and were filtered with $r > |0.7|$ and $P < 0.01$ thresholds. The network was visualized by Cytoscape (version 3.9.1.).

Results

Identification of differentially expressed lncRNAs

Total RNA from root tip in IR64 genotype under control and drought stress conditions were sequenced using the Illumina technique. By

removing reads containing adapter, reads containing ploy-N and low-quality reads from raw data, clean reads were eventually obtained (Supplementary Table S1). All assembled transcripts with a length of more than 200 nucleotides that do not have any indication of coding potential, including open reading frames (ORF) length of fewer than 300 nucleotides, were kept and CNC2 and CNCI packages and the Pfam database were used to further evaluate the remaining transcripts.

Finally, 1815 lncRNAs were identified, of which 358 were DElncRNAs with |FC|>1 and adjusted p-value<0.05 obtained from the IR64-Z1 sample (Supplementary Table S2). Figure 1 shows the distribution and frequency of DElncRNAs on rice chromosomes, where DElncRNAs are located on all 12 rice chromosomes. Among them, chromosome 1 had the highest number of lncRNAs (53) and chromosome 12 had the lowest number (only 18) (Figure 1A). Examining the expression levels of DElncRNAs involved in the response to drought stress by different types in rice showed that in general 204 and 154 DElncRNAs had increased and decreased expression, respectively. According to the relative position of lncRNAs compared to protein-coding genes, lncRNAs were divided into four groups: intergenic lncRNAs (long intergenic noncoding RNAs), intronic lncRNAs (derived from the Intron regions of protein-coding genes), overlapping lncRNAs, and antisense lncRNAs (overlapping with protein-coding genes on the opposite strand) (Lee, 2012). Examining the expression levels of DElncRNAs involved in the response to drought stress by different types in rice shown in Figure 1B. Overall, within this study, the Long intergenic non-coding RNAs (lincRNA) group accounted for the highest proportion, representing 69.6% of the total.

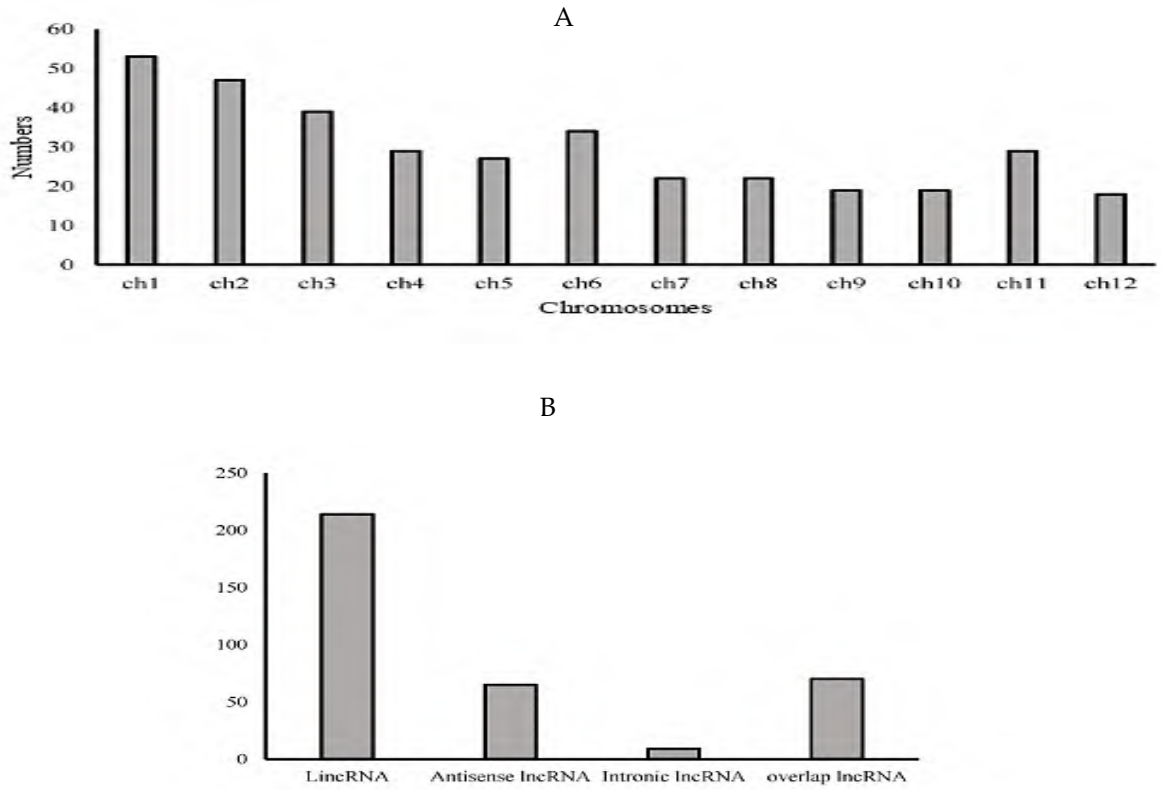

Figure 1. (A) Distribution of DElncRNAs on rice chromosomes. lncRNAs were distributed on all 12 rice chromosomes, with the highest number on chromosome 1 (53) and the lowest number on chromosome 12 (18). (B) Classification of rice lncRNAs based on genomic location. lncRNAs were divided into four categories according to their relative position compared to protein coding genes (LincRNA, Antisense RNA, Intronic RNA, Overlap lncRNA).

Target genes of DElncRNAs

In the current investigation, we examined the regulatory connections between lncRNAs and mRNAs within the root tip region of the IR64 variety. Specifically, we identified a total of 338 differentially expressed lncRNAs (DElncRNAs) that regulate 710 differentially expressed mRNAs (DEmRNAs) in a cis-regulatory manner, as indicated by their co-location within 10 kb upstream and downstream regions. Additionally, we found that 351 DElncRNAs are associated with 7535 DEmRNAs in a trans-regulatory state, established based on a minimum free energy of base pairing ($\Delta G < -30$ kcals mol-1) (Figure 2).

Functional annotation of the DElnRNAs

Gene ontology (GO) enrichment analysis of the predicted target genes of the lncRNAs showed that a total of 43 biological processes, 17 molecular functions and 38 cell components were significantly altered in response to salt treatment (Supplementary Table S3). The findings indicated that within the biological process group, the translation term featured 126 genes. In the molecular function category, the term structural molecule activity showcased an impressive 101 enriched genes. Meanwhile, within the cellular component category, the term intrinsic to membrane exhibited enrichment with 136 genes, and the ribonucleoprotein complex term featured 108 genes, demonstrating the highest rich factors. (Figure 3). Moreover, terms such as response to abiotic stimuli (GO:0009628), signal transduction (GO:0007165) and secondary metabolic process (GO:0006720) are significant in biological process (BP) and terms such as ribosome (GO:0005840) and plasma membrane (GO:0005886) are significant in cellular components (CC). Finally, in molecular functions (MF), the receptor activity term (GO:0004872) was significant (S6).

Cis-regulatory element analysis

To discover the conserved motifs and consensus cis-regulatory elements (CREs) in the promoters of DEmRNAs and DElncRNAs, we applied the MEME tool and identified 24 motifs with lengths ranging from 20 to 50 aa (Table 1). We also compared the identified motifs with known motifs in the JASPAR CORE 2022 plants database. We found that sixteen of the motifs were matched to the known motifs related to various TFs, including AP2/EREBP, CH3, C2H2 zinc finger factors, BBR/BPC, basic helix-loop-helix factors (bHLH), and other C4 zinc finger-type factors (Supplementary Table S4). GO term analysis for motifs revealed that motifs are involved in the regulation of transcription (GO:0006355), translation (GO:0006412), transmembrane receptor protein tyrosine kinase signaling pathway (GO:0007169) (Table 1, Supplementary Table S4, S5).

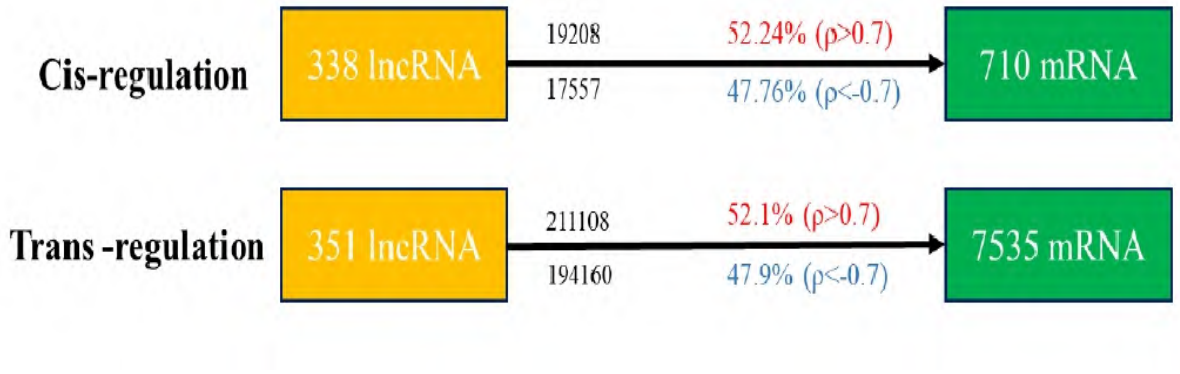

Figure 2. Summary of regulatory relationships between lncRNAs and mRNAs. The number of different combinations between lncRNAs and their target genes is marked in black. The red and blue values indicate the percentage of lncRNAs that show a positive and negative correlation with their target mRNAs, respectively. ρ is Pearson's correlation coefficient.

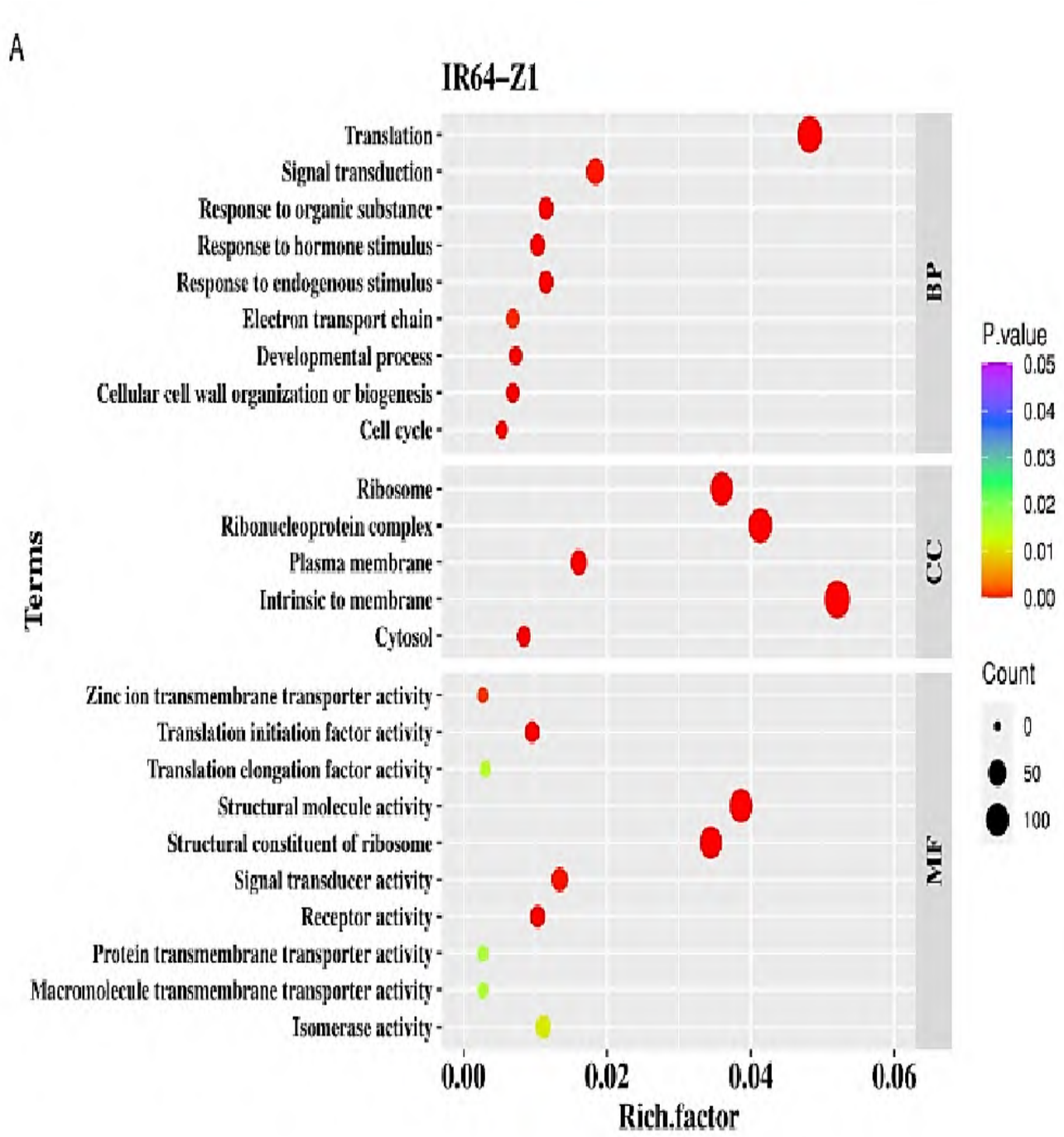

Figure 3. GO enrichment analysis of target mRNAs of DElncRNAs including biological process (BP), cellular components (CC) and molecular function (MF) categories.

Table 1. The conserved motifs found in promoter of DEmRNAs by the MEME analysis.

logo	E-value	Width	Best match in JASPAR	Significant GO term identified by GOMO
	6.1e-426	29	MA1257.1 (ERF9)	
	7.1e-249	21	MA2022.1 (LOB)	BP regulation of transcription, DNA-dependent
	6.6e-150	21	MA1404.1 (BPC1)	BP regulation of transcription
	1.4e-118	21	MA1818.1 (Zm00001d052229)	BP translation
	1.3e-134	29	MA1267.1 (DOF5.8)	
	4.1e-058	50	MA1812.1 (ASR1)	BP translation
	1.6e-055	29	MA1267.1 (DOF5.8)	
	1.3e-050	20	MA1240.1 (ERF10)	
	5.0e-033	21	MA1416.1 (RAMOSA1)	BP regulation of transcription
	9.7e-032	21	MA1063.1 (TCP19)	BP translation

Identification of lncRNAs as potential targets of miRNAs

In this study, a total of 32 miRNAs were found, all of which belonged to 14 conserved families (Supplementary Table S6). Among the detected miRNAs, the osa-miR439, osa-miR818 and osa-miR821families comprised the highest frequency with 9, 5, and 3 members, respectively. In this study, miRNAs from miR393 and miR439 and etc. families were identified.

Construction of lncRNA-mRNA network

The edge between nodes represents the interaction between these biomolecules (Shannon et al., 2003). The lncRNA-mRNA regulatory pairs were further integrated based on the common mRNA of lncRNA-mRNA co-expression interaction pairs, followed by visualization of the lncRNA-mRNA regulatory network using Cytoscape, an open-source bioinformatics software. As shown in Figure 4, the lncRNA-mRNA regulatory network is contained. We have recognized 10 pivotal lncRNAs (Os01g0768200, Os02g0686400, Os07g0203300, Os02g0229800, Os02g0216300, Os06g0692050, Os05g0138300, Os06g0308300, Os08g0553450, Os04g0474300) as central hub genes within the lncRNA-mRNA network. The target genes of these top 10 lncRNAs were analyzed ontologically in order to understand the potential function of lnRNAs during drought stress. The functional analysis revealed that they were involved in developmental process (GO:0032502), cellular response to stimulus (GO:0051716), and signaling pathway (GO:0023033).

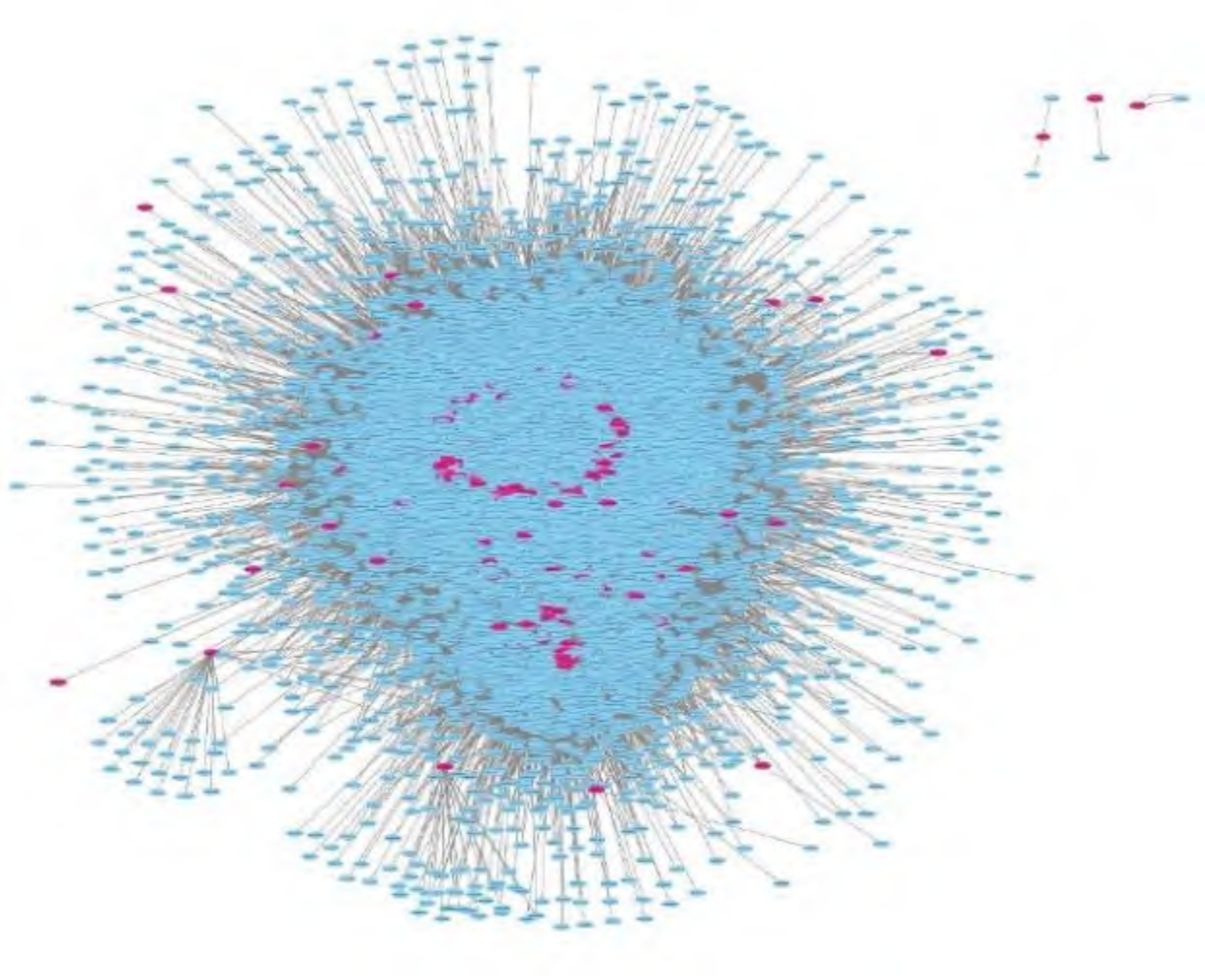

Figure 4. lncRNA-mRNA regulator network. Pink and blue circles indicate lncRNAs and mRNAs, respectively.

Discussion

Rice constitutes a crucial crop with regards to food security. However, the crop's susceptibility to yield loss due to drought stress is a notable concern. In 1985, the cultivar (lowland-*indica*) IR64 was developed by IRRI and released in the Philippines. In addition to high yield, early maturity and high disease resistance, it has excellent baking quality that matches the best available varieties. These concessions have led to its rapid expansion and cultivation in more than 10 million people in the two decades since its publication. Because of its success as a variety, it has been extensively studiedf for scientific use and is well characterized genetically. Continued basic studies on IR64 and related varieties should contribute to understanding the complex genetic control of yield and other traits of interest to rice farmers and consumers (Mackill and Khush, 2018). A dearth of knowledge exists regarding drought-responsive lncRNAs in rice. lncRNAs are a recently discovered class of molecules that serve important functions in a wide range of biological processes, including growth regulation and stress response. However, the precise mechanisms involved in these processes remain largely unknown. In the case of plants, recent evidence from various species inIicates that lncRNAs are expressed in response to multiple stresses, such as salI in *Gossypium hirsutum* (Deng et al., 2018) and *Medicago truncatula* (Wang et al., 2015), as well as heat and drought in *Brassica juncea* (Bhatia

et al., 2020). To further investigate the role of lncRNAs in response to drought stress, we conducted a study involving the IR64 cultivar, which has a shallow rooting system. The meristem region was sampled in order to gain a better understanding of the function of lncRNAs in response to drought. Since the tip includes the meristem and elongated regions where cells divide, grow and elongate and is one of the most important root factors in determining traits and adaptive strategies to water stress (Bizet et al., 2015). We selected the root tip region for further studies on root lncRNA strategy as a result of water deficit. The current study aimed to identify drought stress-responsive lncRNAs present in the root system architecture (RSA) as vital growth trait that performs a pivotal role in plant adaptation and productivity in environments constrained by water availability.

Here, a total of 1815 lncRNAs were detected the majority of them were lincRNAs. Previous studies have shown that, among lncRNAs, lincRNAs accounted for the largest number, which were observed in rice (76%) and maize (93%), respectively (Li et al., 2014; Zhang et al., 2014). Espinosa (2017) showed that lincRNAs can act as local enhancers to activate the transcription of their chromosomal neighboring genes, which emphasizes the possible important functions of lncRNAs in or nearby. In the results of research conducted on IR64 and Pokkali cultivars under salt stress, it has been shown that lncRNAs are distributed on all 12 chromosomes, and the lncRNAs that respond to salinity among the 12 chromosomes are unequal in both genetics. They have not followed a specific process similar to this research (Tiwari et al., 2023). The finding in this study further substantiate this conclusion. It is interesting that in this study, chromosomes 1, 2, and 3 have the number of lncRNA respectively. In a research conducted on the identification and functional analysis of lncRNAs on seed senescence, most lncRNAs were distributed on chromosomes 1, 2, and 3, and mRNAs and lncRNAs had a similar distribution in these chromosomes (Zhang et al., 2022). A total of 358 lncRNA genes were identified that showed differential expression in the stress response in the root tip which suggests that these lncRNAs may have a key role in the response to stress rice.

lncRNAs act by influencing gene expression and affect protein-coding genes through cis-regulation of neighboring genes and trans-regulation of distant genes (Rossetto et al., 2013). The functional enrichment analysis revealed that the potential target genes influenced by the differentially expressed lncRNAs (DElncRNAs) were primarily associated with responses to abiotic stimuli, reactions to chemical stimuli, and reactions to hormonal stimuli (Supplementary S6). Additionally, there was an enrichment of terms related to secondary metabolic processes and the transduction of hormonal signals. Moreover, an increased quantity of secondary metabolites, such as phenylpropanoids, is often observed in response to challenging environmental conditions. In many plants, endogenous phenolic compounds play a pivotal role in regulating drought tolerance mechanisms (Akula and Ravishankar, 2011). Drought stress triggers downstream pathways involving phytohormone regulation and their associated signaling pathways, consequently initiating the synthesis of diverse protective secondary metabolites. These secondary metabolites are instrumental in conferring tolerance to a wide range of stressors, including both abiotic and biotic stresses (Yadav et al., 2021).

We identified potential sequence motifs and TFs binding sites in DElncRNAs and DEmRNAs promoters. We detected 16 motifs related to the TF families such as AP2/EREBP, CH3, C2H2 zinc finger factors, BBR/BPC, basic helix-loop-helix factors (bHLH), and other C4 zinc finger-type factors. Multiple reports have indicated that all these transcription factors play a significant role in response to stress. The AP2/EREBP genes hold varied responsibilities in both developmental processes and stress-related responses in plants (Sakuma et al., 2002). In times of drought, the AP2/EREBP transcription factor regulates a multitude of target genes by binding to the cis-element (A/GCCGAC) located in the promoter region of the candidate genes (Sharoni et al., 2012). C2H2 zinc finger proteins are part of a relatively large family of transcriptional regulators in plants. Recent research has shown that C2H2 zinc finger proteins serve as crucial transcriptional regulators

in the plant's response to a broad spectrum of stress conditions such as extreme temperatures, salinity, drought, oxidative stress, excessive light, and silique shattering(Wang et al., 2019). Furthermore, these proteins can enhance drought resistance in rice plants by regulating the levels of ROS-scavenging activities, proline, H_2O_2, and other cellular components (Wang et al., 2019). The bHLH proteins are among the many transcription factors present in all eukaryotic organisms, involved in a wide range of regulatory processes (Jin et al., 2014). Overexpression of the bHLH12 gene endows plants with drought, salt, and osmotic stress resistance, whereas the bhlh122 mutant plants showed heightened sensitivity to these stressors when compared to the wild type plants. Additionally, bHLH122 regulates the expression of stress-related genes directly (Liu et al., 2014).

The lncRNAs act as target mimics of miRNAs that can affect regulation of gene expression. We identified the targets of lncRNAs on miRNAs using psRNATarget server. A total of 32 miRNAs were identified, with the majority of them belonging to the osa-miR439, osa-miR818, and osa-miR821 families. Studies have demonstrated that osa-miR821 is up-regulated in the roots of plants subjected to salt stress(Sanan-Mishra et al., 2009), while miR439 has been associated with H_2O_2 accumulation (Junhua et al., 2021). Furthermore, research has indicated that miRNA393 is involved in the heat stress response in wheat (Ragupathy et al., 2016).

We constructed a co-expression lncRNA-mRNA network to assess regulatory mechanism of lncRNAs in root tip region. Based on results, 10 hub genes, including Os01g0768200, Os02g0686400, Os07g0203300, Os02g0229800, Os02g0216300, Os06g0692050, Os05g0138300, Os06g0308300, Os08g0553450, and Os04g0474300 were identified. The function of these genes was significantly associated with developmental process, cellular response to stimulus and signaling pathway. One of the hub genes, Os02g0686400, demonstrated the maximum expression increase under drought conditions compared to control conditions. These hub genes have important targets, including the OsPIN9 gene (Os01g0802700), which has been reported to respond significantly to abiotic stress in the roots of rice seedlings (Xu et al., 2022). OsPIN9 potentially regulates abiotic stress and hormone signaling to balance plant growth and various exogenous stimuli by directing auxin flux. Another target gene is IAA13 (Os03g0742900), a candidate gene for salinity resistance. Auxin/IAA proteins are short-lived and regulate cell division and elongation to direct plant growth and development (Jung et al., 2015; Singh and Jain, 2015).

Conclusion

In the current investigation, the transcriptome analysis of the IR64 genotype with shallow roots led to the identification of a number of DE-lncRNAs, which are presumed to participate in the drought stress response of rice. The functional analysis of these lncRNAs exhibited a specific enrichment for signal transduction pathways and hormonal stimuli responses. Additionally, our findings revealed the relationship of DE-lncRNAs with several transcription factor families, including AP2/EREBP and bHLH, as well as with miRNAs such as osa-miR439, osa-miR818, and osa-miR821. Specifically, our results highlight the crucial roles played by lncRNAs, including Os01g0768200 and Os02g0686400, in the regulatory networks involved in the drought response of the root tip region. This study provides novel insights into the involvement of lncRNAs in the response to drought stress and enhances our understanding of their functions in the root tip region of rice.

Supplementary Materials

The Supplementary Material for this article can be found online at: https://www.jpmb-gabit.ir/article_709081.html

Supplementary Table S1. Transcriptome sequencing statistics.

Supplementary Table S2. List of DElncRNAs identified associated with drought stress response in IR64-Z1.

Supplementary Table S3. GO term enriched.

Supplementary Table S4. List of known motifs by Tomtom search against the JASPAR database.

Supplementary Table S5. Significant GO term enriched by GOMO analysis.

Supplementary Table S6. List of lncRNAs as potential target of miRNAs.

Author Contributions

Conceptualization, A.N. and S.E.T.; Methodology, S.E.T. and A.T.; software, S.E.T.; formal analysis, S.E.T. and A.T.; Investigation, A.N., S.E.T., A.A. and M.R.G.; Data curation, S.E.T.; Writing – original draft, S.E.T. and A.T.; Visualization, S.E.T.; Writing – review & editing, A.N., A.T., A.A. and M.R.G. All authors have read and agreed to the published version of the manuscript.

Funding

This research did not receive any external funding.

Acknowledgments

The authors thank the Agricultural Biotechnology Research Institute of Iran (ABRII) for providing funding for this work.

Conflicts of Interest

The authors declare no conflict of interest.

References

Akula, R., and Ravishankar, G.A. (2011). Influence of abiotic stress signals on secondary metabolites in plants. *Plant Signal Behav* 6(11): 1720-1731.

Bailey, T.L., Boden, M., Buske, F.A., Frith, M., Grant, C.E., Clementi, L., Ren, J., Li, W.W., and Noble, W.S. (2009). MEME SUITE: tools for motif discovery and searching. *Nucleic Acids Res* 37(Web Server issue): W202-208. doi: 10.1093/nar/gkp335.

Barbez, E., Dunser, K., Gaidora, A., Lendl, T., and Busch, W. (2017). Auxin steers root cell expansion via apoplastic pH regulation in *Arabidopsis thaliana*. *Proc Natl Acad Sci USA* 114(24): E4884-E4893. doi: 10.1073/pnas.1613499114.

Bhatia, G., Singh, A., Verma, D., Sharma, S., and Singh, K. (2020). Genome-wide investigation of regulatory roles of lncRNAs in response to heat and drought stress in *Brassica juncea* (Indian mustard). *Environ Exp Bot* 171: 103922.

Bizet, F., Hummel, I., and Bogeat-Triboulot, M.B. (2015). Length and activity of the root apical meristem revealed in vivo by infrared imaging. *J Exp Bot* 66(5): 1387-1395. doi: 10.1093/jxb/eru488.

Brunkard, J.O., and Baker, B. (2018). A two-headed monster to avert disaster: HBS1/SKI7 is alternatively spliced to build eukaryotic RNA surveillance complexes. *Front Plant Sci* 9: 1333.

Buske, F.A., Boden, M., Bauer, D.C., and Bailey, T.L. (2010). Assigning roles to DNA regulatory motifs using comparative genomics. *Bioinformatics* 26(7): 860-866. doi: 10.1093/bioinformatics/btq049.

Caixia, G., Xiuwen, Z., Hubo, L., Mlekwa, U.A., Yu, G., and Jie, X. (2020). Roles of lncRNAs in rice: advances and challenges. *Rice Sci* 27(5): 384-395.

Chen, L., Shi, S., Jiang, N., Khanzada, H., Wassan, G.M., Zhu, C., Peng, X., Xu, J., Chen, Y., and Yu, Q. (2018). Genome-wide analysis of long non-coding RNAs affecting roots development at an early stage in the rice response to cadmium stress. *BMC Genomics* 19: 1-10.

Deng, F., Zhang, X., Wang, W., Yuan, R., and Shen, F. (2018). Identification of *Gossypium hirsutum* long non-coding RNAs (lncRNAs) under salt stress. *BMC Plant Biol* 18(1): 23. doi: 10.1186/s12870-018-1238-0.

Espinosa, J.M. (2017). On the origin of lncRNAs: missing link found. *Trends Genet* 33(10): 660-662.

Fukunaga, T., and Hamada, M. (2017). RIblast: an ultrafast RNA-RNA interaction prediction system based on a seed-and-extension approach. *Bioinformatics* 33(17): 2666-2674. doi: 10.1093/bioinformatics/btx287.

Gupta, S., Stamatoyannopoulos, J.A., Bailey, T.L., and Noble, W.S. (2007). Quantifying similarity between motifs. *Genome Biol* 8(2): 1-9.

Ishimaru, K., Shirota, K., Higa, M., and Kawamitsu, Y. (2001). Identification of quantitative trait loci for adaxial and abaxial stomatal frequencies in *Oryza sativa*. *Int J Plant Physiol Biochem* 39(2): 173-177.

Jin, J., Zhang, H., Kong, L., Gao, G., and Luo, J. (2014). PlantTFDB 3.0: a portal for the functional and evolutionary study of plant transcription factors. *Nucleic Acids Res* 42(Database issue): D1182-1187. doi: 10.1093/nar/gkt1016.

Jung, H., Lee, D.-K., Do Choi, Y., and Kim, J.-K. (2015). *OsIAA6*, a member of the rice Aux/IAA gene family, is involved in drought tolerance and tiller outgrowth. *Plant Sci* 236: 304-312.

Junhua, L., Xuemei, Y., Jinfeng, C., Tingting, L., Zijin, H., Ying, X., Jinlu, L., Jiqun, Z., Mei, P., and Hui, F. (2021). Osa-miR439 negatively regulates rice immunity against *Magnaporthe oryzae*. *Rice Sci* 28(2): 156-165.

Kaashyap, M., Ford, R., Kudapa, H., Jain, M., Edwards, D., Varshney, R., and Mantri, N. (2018). Differential regulation of genes involved in root morphogenesis and cell wall modification is associated with salinity tolerance in chickpea. *Scientific Rep* 8(1): 4855.

Khan, A., Fornes, O., Stigliani, A., Gheorghe, M., Castro-Mondragon, J.A., Van Der Lee, R., Bessy, A., Cheneby, J., Kulkarni, S.R., and Tan, G. (2018). JASPAR 2018: update of the open-access database of transcription factor binding profiles and its web framework. *Nucleic Acids Res* 46(D1): D260-D266.

Lafitte, H., Ismail, A., and Bennett, J. (2004). "Abiotic stress tolerance in rice for Asia: progress and the future", in: *New directions for a diverse planet: Proceedings of the 4 th International Crop Science Congress,* Edited by *Fischer, T., Turner, N., Angus, J., McIntyre, L., Robertson, M., Borrell, A. and Lloyd, D. Brisbane, Australia.* (International Rice Research Institute: Citeseer).

Lee, J.T. (2012). Epigenetic regulation by long noncoding RNAs. *Science* 338(6113): 1435-1439. doi: 10.1126/science.1231776.

Li, L., Eichten, S.R., Shimizu, R., Petsch, K., Yeh, C.T., Wu, W., Chettoor, A.M., Givan, S.A., Cole, R.A., Fowler, J.E., Evans, M.M., Scanlon, M.J., Yu, J., Schnable, P.S., Timmermans, M.C., Springer, N.M., and Muehlbauer, G.J. (2014). Genome-wide discovery and characterization of maize long non-coding RNAs. *Genome Biol* 15(2): R40. doi: 10.1186/gb-2014-15-2-r40.

Li, P., Yang, H., Wang, L., Liu, H., Huo, H., Zhang, C., Liu, A., Zhu, A., Hu, J., Lin, Y., and Liu, L. (2019). Physiological and transcriptome analyses reveal short-term responses and formation of memory under drought stress in rice. *Front Genet* 10: 55. doi: 10.3389/fgene.2019.00055.

Liu, W., Tai, H., Li, S., Gao, W., Zhao, M., Xie, C., and Li, W.X. (2014). b HLH 122 is important for drought and osmotic stress resistance in *Arabidopsis* and in the repression of ABA catabolism. *New Phytol* 201(4): 1192-1204.

Lynch, J.P., Chimungu, J.G., and Brown, K.M. (2014). Root anatomical phenes associated with water acquisition from drying soil: targets for crop improvement. *J Exp Bot* 65(21): 6155-6166. doi: 10.1093/jxb/eru162.

Mackill, D.J., and Khush, G.S. (2018). IR64: a high-quality and high-yielding mega variety. *Rice (N Y)* 11(1): 18. doi: 10.1186/s12284-018-0208-3.

Nadarajah, K., and Kumar, I.S. (2019). Drought response in rice: the mirna story. *Int J Mol Sci* 20(15): 3766. doi: 10.3390/ijms20153766.

Nejat, N., and Mantri, N. (2018). Emerging roles of long non-coding RNAs in plant response to biotic and abiotic stresses. *Crit Rev Biotechnol* 38(1): 93-105. doi: 10.1080/07388551.2017.1312270.

Peleg, Z., Fahima, T., Krugman, T., Abbo, S., Yakir, D., Korol, A.B., and Saranga, Y. (2009). Genomic dissection of drought resistance in durum wheat x wild emmer wheat recombinant inbreed line population. *Plant Cell Environ* 32(7): 758-779. doi: 10.1111/j.1365-3040.2009.01956.x.

Ragupathy, R., Ravichandran, S., Mahdi, M.S., Huang, D., Reimer, E., Domaratzki, M., and Cloutier, S. (2016). Deep sequencing of wheat sRNA transcriptome reveals distinct temporal expression pattern of miRNAs in response to heat, light and UV. *Sci Rep* 6(1): 39373. doi: 10.1038/srep39373.

Rossetto, C.C., Tarrant-Elorza, M., and Pari, G.S. (2013). Cis and trans acting factors involved in human cytomegalovirus experimental and natural latent infection of CD14 (+) monocytes and CD34 (+) cells. *PLoS Pathog* 9(5): e1003366. doi: 10.1371/journal.ppat.1003366.

Sakuma, Y., Liu, Q., Dubouzet, J.G., Abe, H., Shinozaki, K., and Yamaguchi-Shinozaki, K. (2002). DNA-binding specificity of the ERF/AP2 domain of Arabidopsis DREBs, transcription factors involved in

dehydration- and cold-inducible gene expression. *Biochem Biophys Res Commun* 290(3): 998-1009. doi: 10.1006/bbrc.2001.6299.

Sanan-Mishra, N., Kumar, V., Sopory, S.K., and Mukherjee, S.K. (2009). Cloning and validation of novel miRNA from basmati rice indicates cross talk between abiotic and biotic stresses. *Mol Genet Genom* 282: 463-474.

Shannon, P., Markiel, A., Ozier, O., Baliga, N.S., Wang, J.T., Ramage, D., Amin, N., Schwikowski, B., and Ideker, T. (2003). Cytoscape: a software environment for integrated models of biomolecular interaction networks. *Genome Res* 13(11): 2498-2504. doi: 10.1101/gr.1239303.

Sharoni, A.M., Nuruzzaman, M., Satoh, K., Moumeni, A., Attia, K., Venuprasad, R., Serraj, R., Kumar, A., Leung, H., Islam, A.K., and Kikuchi, S. (2012). Comparative transcriptome analysis of AP2/EREBP gene family under normal and hormone treatments, and under two drought stresses in NILs setup by Aday Selection and IR64. *Mol Genet Genomics* 287(1): 1-19. doi: 10.1007/s00438-011-0659-3.

Singh, V.K., and Jain, M. (2015). Genome-wide survey and comprehensive expression profiling of Aux/IAA gene family in chickpea and soybean. *Front Plant Sci* 6: 918. doi: 10.3389/fpls.2015.00918.

Smith, B.D. (1995). *The emergence of agriculture.* United States: W H Freeman & Co.

Sun, Q., Csorba, T., Skourti-Stathaki, K., Proudfoot, N.J., and Dean, C. (2013). R-loop stabilization represses antisense transcription at the *Arabidopsis* FLC locus. *Science* 340(6132): 619-621.

Tang, Z., Xu, M., Ito, H., Cai, J., Ma, X., Qin, J., Yu, D., and Meng, Y. (2019). Deciphering the non-coding RNA-level response to arsenic stress in rice (*Oryza sativa*). *Plant Signal Behav* 14(9): 1629268. doi: 10.1080/15592324.2019.1629268.

Tiwari, S., Jain, M., Singla-Pareek, S.L., Bhalla, P.L., Singh, M.B., and Pareek, A. (2023). Pokkali: A naturally evolved salt-tolerant rice shows a distinguished set of lncrnas possibly contributing to the tolerant phenotype. *Int J Mol Sci* 24(14): 11677.

Wang, K., Ding, Y., Cai, C., Chen, Z., and Zhu, C. (2019). The role of C2H2 zinc finger proteins in plant responses to abiotic stresses. *Physiol Plant* 165(4): 690-700. doi: 10.1111/ppl.12728.

Wang, T.Z., Liu, M., Zhao, M.G., Chen, R., and Zhang, W.H. (2015). Identification and characterization of long non-coding RNAs involved in osmotic and salt stress in *Medicago truncatula* using genome-wide high-throughput sequencing. *BMC Plant Biol* 15(1): 131. doi: 10.1186/s12870-015-0530-5.

Xiao, X., Wu, Z.-C., and Chou, K.-C. (2011). A multi-label classifier for predicting the subcellular localization of gram-negative bacterial proteins with both single and multiple sites. *PLoS One* 6(6): e20592.

Xu, H., Zhang, Y., Yang, X., Wang, H., and Hou, D. (2022). Tissue specificity and responses to abiotic stresses and hormones of PIN genes in rice. *Biologia* 77(5): 1459-1470.

Xu, X.W., Zhou, X.H., Wang, R.R., Peng, W.L., An, Y., and Chen, L.L. (2016). Functional analysis of long intergenic non-coding RNAs in phosphate-starved rice using competing endogenous RNA network. *Sci Rep* 6(1): 20715. doi: 10.1038/srep20715.

Yadav, B., Jogawat, A., Rahman, M.S., and Narayan, O.P. (2021). Secondary metabolites in the drought stress tolerance of crop plants: A review. *Gene Rep* 23: 101040.

Yoshida, S. (1976). Routine procedures for growing rice plants in culture solution. *Laboratory manual for physiological studies of rice*: 61-66.

Yoshida, S., and Hasegawa, S. (1982). The rice root system: its development and function. *Drought resistance in crops with emphasis on rice* 10: 97-134.

Yue, B., Xue, W., Xiong, L., Yu, X., Luo, L., Cui, K., Jin, D., Xing, Y., and Zhang, Q. (2006). Genetic basis of drought resistance at reproductive stage in rice: separation of drought tolerance from drought avoidance. *Genetics* 172(2): 1213-1228.

Zhang, Y., Fan, F., Zhang, Q., Luo, Y., Liu, Q., Gao, J., Liu, J., Chen, G., and Zhang, H. (2022). Identification and functional analysis of long non-coding RNA (lncRNA) in response to seed aging in rice. *Plants (Basel)* 11(23): 3223. doi: 10.3390/plants11233223.

Zhang, Y.C., Liao, J.Y., Li, Z.Y., Yu, Y., Zhang, J.P., Li, Q.F., Qu, L.H., Shu, W.S., and Chen, Y.Q. (2014). Genome-wide screening and functional analysis identify a large number of long noncoding RNAs involved in the sexual reproduction of rice. *Genome Biol* 15(12): 512. doi: 10.1186/s13059-014-0512-1.

JPMB
Journal of Plant Molecular Breeding
Published by Genetics and Agricultural Biotechnology Institute of Tabarestan
2022 | Volume 10 | Issue 2

مقاله پژوهشی

شناسایی RNAهای طولانی غیر کدکننده (lncRNAs) پاسخگو به تنش خشکی در ناحیه نوک ریشه برنج

سارا اسماعیلی‌تازنگی[۱]، علی نیازی[۱]*، محمدرضا غفاری[۲]، عباس عالم‌زاده[۳]، احمد طهماسبی[۱]

[۱] پژوهشکده بیوتکنولوژی، دانشگاه شیراز، شیراز، ایران
[۲] گروه بیولوژی سیستم‌ها، پژوهشکده بیوتکنولوژی کشاورزی ایران، کرج، ایران
[۳] گروه تولیدات گیاهی و اصلاح‌نباتات، دانشکده کشاورزی، دانشگاه شیراز، شیراز، ایران

چکیده: خشکسالی تولید جهانی برنج را به شدت تحت تاثیر قرار می دهد. شواهد اخیر، نقش کلیدی که RNAهای طولانی غیرکدکننده (lncRNAs) در پاسخ به استرس غیرزیستی ایفا می‌کنند، را نشان می‌دهند. در این مطالعه، با استفاده از آنالیز توالی‌یابی رونوشت‌های lncRNAهای ناشی از تنش خشکی در ناحیه نوک ریشه برنج روی نهال‌های ژنوتیپ حساس برنج (IR64) تحت شرایط خشکی و کنترل شناسایی شد. در مجموع ۳۵۸ lncRNA با بیان متفاوت (DElncRNA) شناسایی شد که بیش از ۶۰ درصد آنها در مناطق بین ژنی بودند. نتایج نشان داد که DElncRNAها می‌توانند به طور مستقیم یا غیرمستقیم ۷۱۰ و ۷۵۳۵ mRNA تنظیم کنند. علاوه بر این، DElncRNA بر روی ژن‌های هدف مرتبط با ژن‌های مقاومت به خشکی، رشد ریشه جانبی و ژن‌های مؤثر بر انتقال اکسین اثر داشته‌اند. همچنین ۲۴ موتیف حفاظت‌شده در نواحی بالادست DElncRNAها و mRNAها با بیان متفاوت (DEmRNA) شناسایی گردید. تجزیه و تحلیل عملکردی این موتیف‌ها نشان دهنده دخالت آن‌ها در تنظیم رونویسی، ترجمه و مسیر سیگنالینگ پروتئین گیرنده غشایی تیروزین کیناز بود. با استفاده از آنالیز شبکه DElncRNA و DEmRNA، ۱۰ lncRNA به عنوان ژن‌های مرکزی شناسایی شدند. تجزیه و تحلیل عملکردی نشان داد که این ژن‌ها در فرآیندهای رشد، پاسخ‌های سلولی به محرک‌ها و مسیرهای سیگنال‌دهی دخالت دارند. این نتایج دیدگاه جامعی را در مورد lncRNAهای بالقوه کاربردی و بینشی در مورد مکانیسم‌های مولکولی نهفته در مقاومت به خشکی در ناحیه نوک ریشه برنج ارائه می‌دهد.

کلمات کلیدی: تنش خشکی، برنج، رونوشت، نوک ریشه، lncRNAs.

ویراستار علمی
دکتر سیدحمیدرضا هاشمی‌پطرودی،
پژوهشکده ژنتیک و زیست‌فناوری کشاورزی طبرستان،
دانشگاه علوم کشاورزی و منابع طبیعی ساری

تاریخ
دریافت: ۴ مرداد ۱۴۰۲
پذیرش: ۲۸ آبان ۱۴۰۲
چاپ: ۱۶ دی ۱۴۰۲

نویسنده مسئول
دکتر علی نیازی
niazi@shirazu.ac.ir

ارجاع به این مقاله
Esmaeili Tazangi, S., Niazi, A., Ghaffari, M.R., Alemzadeh A. and Tahmasebi, A. (2022). Identification of drought stress-responsive long non-coding RNAs (lncRNAs) in root tip region of rice (*Oryza sativa*). *J Plant Mol Breed 10*(2): 31-45.
doi:10.22058/ JPMB .2023.2007831.1280.

JPMB | Journal of Plant Molecular Breeding
Published by Genetics and Agricultural Biotechnology Institute of Tabarestan
2022 | Volume 10 | Issue 2

Marker-trait association of Russian wheat aphid (*Diuraphis noxia*) resistance in a globally diverse set of wild barley

Original paper

Zahra Tahmasebi *[1], Sara Safari [1], Ali Arminian [1], Foad Fatehi [2]

[1] Department of Agronomy and Plant Breeding, Faculty of Agriculture, Ilam University, Ilam, Iran
[2] Department of Agriculture, Payame Noor University (PNU), Tehran, Iran

Abstract: The Russian wheat aphid (RWA, *Diuraphis noxia*), prevalent pest affecting barley globally, can severely damage barley yield and grain quality. The present study aimed to identify simple sequence repeat (SSR) markers associated with RWA resistance in wild barley (*Hordeum vulgare* subsp. *spontaneum*). Thirty wild barley accessions were selected from the ICARDA GeneBank and Iran to represent 10 Asia countries scattered along the natural geographic distribution of the species for RWA resistance. Five traits, including leaf chlorosis, leaf rolling, chlorophyll a, b, and total chlorophyll concentration, were evaluated. Fourteen SSR markers were used to assess genetic diversity. The association between 52 polymorphic SSR markers and RWA resistance traits was examined using both general linear model (GLM) and mixed linear model (MLM) approaches. The population structure analysis revealed seven subpopulations in the entire collection (K=7). Eleven marker-trait associations (MTA) were identified on chromosomes 1H, 2H, 3H, 4H, and 7H, with significant associations found for markers Bmag007, Bmag6, Bmac0399, Bmag0125, and EBmac0701 with RWA resistance traits in both GLM and MLM. This study identified novel genomic regions putatively linked with RWA resistance traits, offering insights into the genetic architecture of RWA resistance in barley. These findings may guide the utilization of RWA resistant accessions of *H. spontaneum* as parents for barley breeding programs.

Keywords: association analysis, seedling resistance, SSR marker, subpopulations.

OPEN ACCESS

Edited by
Prof. Ahmad Arzani,
Isfahan University of Technology, Iran

Date
Received: 6 June 2023
Accepted: 8 October 2023
Published: 6 January 2024

Correspondence
Dr. Zahra Tahmasebi
z.tahmasebi@ilam.ac.ir

Citation
Tahmasebi, Z., Safari, S., Arminian, A. and Fatehi, F. (2022). Marker-trait association of Russian wheat aphid (*Diuraphis noxia*) resistance in a globally diverse set of wild barley. *J Plant Mol Breed* 10(2): 46-60. doi:10.10.22058/JPMB.2023.2004093.1275.

Introduction

The Russian wheat aphid, *Diuraphis noxia* (Kurdjumov) (*Hemiptera aphididae*), is a significant pest affecting two important cereal crops: wheat (*Triticum aestivum* L.) and barley (*Hordeum vulgare* L.). Russian wheat aphids (RWA) cause a significant loss in grain yield and quality in barley. As a phloem-feeding aphid, it causes symptoms such as leaf rolling and streaking, head trapping, and the eventual death death of the infested plants (Nieto Lopez and Blake, 1994). RWA infestation decreases plant height, shoot weight, and number of spikes (Gharaghanipor et al., 2022).

Hordeum vulgare ssp. *spontaneum* is the direct progenitor of domesticated barley, the only wild species in the barley primary gene pool and hence readily crossable species (Zhang et al., 2017). Genetic diversity of *H. spontaneum* has been estimated to be twice that of cultivated barley (Able et al., 2007). Many resistance attributes to diseases and pests have been lost during domestication process in the wild relatives of cultivated crops (Moreira et al., 2018). Screening crop wild relatives for (partial) resistance to aphids supports a fine chance for identifying potentially beneficial traits (Zohary and Hopf, 2000) and introducing them into agricultural cultivars (Webster et al., 1991; Arora et al., 2019).

Exploring new sources of resistance and understanding of complex genetic components involved in pest resistance is necessary to develop pest resistant cultivars. Marker assistant selection (MAS) may be employed efficiently with DNA markers strongly related to target loci and highly polymorphic, allowing for low-cost recognition of RWA resistant plants (Pritchard et al., 2000; Collard and Mackill, 2008; Joukhadar et al., 2013). Scanty research has focused on association mapping of RWA resistance (Heng-Moss et al., 2003; Dahleen et al., 2012; Joukhadar et al., 2013; Tolmay et al., 2013; Dahleen et al., 2015; Zhang et al., 2017). Resistance to RWA in barley was associated with loci on chromosomes 1H, 2H, 3H, 5H, and 7H (Dahleen et al., 2012). A total of 605 high-quality bin-mapped SNPs were positioned in seven linkage groups with a total map length of 1208.9 cM and average marker distance of 2.02 cM. Composite interval mapping identified five different quantitative trait loci (QTLs) on chromosomes 1H, 3H, 5H and 6H associated with aphid resistance and related traits (Rohlf, 1988). The novel chromosomal regions that could contribute to RWA resistance in wheat were found, and the intricate genetics that could control RWA resistance were uncovered (Kisten et al., 2020). Macaulay et al. (2020) proved an aphid resistance site on the distal fragment of the 2HS chromosome, with resistance inherited from the previously identified *H. v.* ssp. *spontaneum* (Ahman and Bengtsson, 2019).

Association genetics or association mapping (AM) is one of the approaches that is currently being used because of its multiple applications to many crops. Association genetics is useful as a novel strategy for discovery of new markers to use in marker-assisted selection (MAS) and breeding or for confirmation of quantitative trait loci (QTL) (Alvarez et al., 2014). Because of its ability to use the natural diversity and to search for functional variants in a broader germplasm, association mapping is becoming popular among researchers (Kisten et al., 2020).

The present study was conducted to evaluate a diverse set of *H. spontaneum* accessions for RWA resistance and identification of SSR markers associated with RWA resistance by association analysis.

Materials and Methods

Plant materials

Thirty natural accessions of wild barley (*H. spontaneum*), 27 accessions provided from International Center for Agricultural Research in Dry Areas (ICARDA) GeneBank representing nine countries scattered along the natural geographic distribution of the species and three genotypes collected from the west and north-west of Iran, were evaluated (Table 1).

Phenotyping

Plant growth**:** The plant seeds were sterilized in 2% (v/v) hypochlorite and rinsed with distilled H_2O. Afterwards, they were incubated at 4°C for 14 days. Then they were kept at room temperature for 48 h. The pots were filled with a mixture of soil, sand, gravel, peat moss and perlite in a ratio of 1: 1: 1: 1: 3, respectively. The germinated seedlings were grown in controlled greenhouse conditions with a

temperature of 20° C during the day, 15° C at night, 16 hours of light per day and 8 hours at night. The germinated seedlings were grown in controlled greenhouse conditions with a temperature of 20° C during the day, 15 ° C at night, 16 hours of light per day and 8 hours at night. Aphid tests**:** *D. noxia* was collected from wheat fields near Ilam (Iran).

Table 1. Origin of wild barley accessions used in this study.

No.	Accession number	Collection location		Latitude	Longitude
		Province	Country		
1	IG 120790	Krasnvvdsk	Turkmenistan	N38 25 55	E056 16 44
2	IG 38654	Faryab	Afghanistan	N35 44	E063 59
3	IG 38669	Samangan	Afghanistan	N36 16	E068 01
4	IG 40155	Kashkadrya	Uzbekistan	N38 57	E66 50
5	IG 117888	Aydlyb	Syria	N36 12 30	E36 46 38
6	IG 40154	Kashkadrya	Uzbekistan	N38 48	E66 28
7	IG 39919	Svydya	Syria	N32 36 00	E36 44 30
8	IG 120794	Ashgabat	Turkmenistan	N38 35	E57 07
9	IG 39565	West Bank	Palestine	N31 46 20	E35 15 37
10	IG 140189	Kulyab	Tajikistan	37.82496	70.18093
11	IG 144170	Alsalt	Jordan	N32.10835	E35.74527
12	IG 137596	Arart	Armenia	N39 47	E45 22
13	IG 120793	Ashgabat	Turkmenistan	N38 30	E56 50
14	IG 129152	Nineveh	Iraq	N36 21	E43 08
15	IG 38936	West Bank	Palestine	N32 24	E35 06
16	IG 142356	Svghad	Tajikistan	N39 48 04	E68 53 35
17	IG 119447	Aydlyb	Syria	N35 32 45	E37 01 20
18	IG 38657	Kandahar	Afghanistan	N31 40	E65 29
19	IG 121853	Svydya	Syria	N32 37 30	E36 46 25
20	IG 139141	Alkrak	Jordan	N31 19.786	E35 43.341
21	IG 142486	Svghad	Tajikistan	N40 07 30	E69 13 57
22	IG 119438	Hvms	Syria	N35 00 48	E36 42 09
23	IG 40152	Svrkhandarya	Uzbekistan	N37 48	E67 00
24	IG 140352	Kulyab	Tajikistan	38.25927	69.83140
25	IG 39489		Syria	N35 00	E038 00
26	IG 140073	Dushanbe	Tajikistan	38.37815	68.70809
27	IG 140302	Kulyab	Tajikistan	38.09862	69.79325
28	IG1	Kurdistan	Iran	N35 0 55	E46 57 52
29	IG2	Kermanshah	Iran	N24 32 08	E48 01 39
30	IG3	Kermanshah	Iran	N24 25 01	E47 02 44

Experiments were conducted in a greenhouse on susceptible 'Sardari' barley plants at Ilam University. The identity of *D. noxia* biotype 2 was confirmed in diagnostic barley differential

greenhouse assays. At the stage of two to four leaves, five aphids were used to infest each plant. The aphid needed for infestation was collected from the wheat fields in Ilam province and transferred to the incubator with the conditions of temperature 25±1, humidity 85%, 14 hours of light and 10 hours of darkness (Girma et al., 1993). In order to achieve the required number of aphids to infest plants and create a pure population, aphids were propagated on the sensitive barley variety (Sarroud). The infestation of the population was conducted using five aphid nymphs aged 4-5 were released on each seedling. Twenty eight days after infestion, reaction to RWA infestation of *H. spontaneum* accessions was recorded by six replicates with five seedlings tested per accession within each replicate (Tocho et al., 2012).

All Plants were visually scored for leaf chlorosis and leaf rolling. Chlorosis was recorded on a scale of 0–9 (Tolmay et al., 2020), where 0 is immune, 1 represents healthy appearing plant, 2 denotes prominent isolated chlorotic spots, and 9 represents dead or damaged beyond recovery. Leaf rolling was recorded using a 1–3 scale (Tolmay et al., 2020) where 1 showed unfolded, 2 indicates one or more folded leaves, and 3 indicates one or more ring-shaped folded leaves.

Chlorophyll concentration

To measure the amount of chlorophyll a, b and total chlorophyll, about 0.5g of control and aphid-infested plant leaves were ground with liquid nitrogen. Five ml of the 80% acetone was added up to extract photosynthetic pigments (chlorophyll a, b, and total). Approximately 1.5 ml of the blend was aspirated and then centrifuged at 3000 rpm for 15 min to remove unsolvable plant tissues. In order to guarantee the absorbance readings at 663 nm below 1.5, the resultant supernatant was diluted with 80 % acetone. Next, pigment extract absorbance was calculated at 646 nm and 663 nm wave lengths, respectively in a spectrophotometer (Cary-50 model made by Varian Company, Australia). Three types of pigment concentrations were determined according to equation bellow 6:

$$C_a \text{ (mg gr}^{-1}) = 12.21\ A_{663} - 2.81\ A_{646}$$
$$C_b \text{ (mg gr}^{-1}) = 20.13\ A_{646} - 5.03\ A_{663}$$
$$Ct \text{ (mg gr}^{-1}) = Ca + Cb$$

In these equations, Ca, Cb, and Ct represent the chlorophyll a, b, and total concentrations, respectively. A_x represents the x nm absorbance.

Genotyping

DNA extraction was done at the plant stage of three to five leaves 34. PCR mixture was comprised of 40-50 ng/µl genomic DNA, 1 mM deoxyribonucleotide triphosphates (dNTPs), 2 mM $MgCl_2$, 19 PCR buffer, 1.5 U *Taq* DNA polymerase (Sina clone Company, Karaj, Iran), and 0.7 µM of forward and reverse primers reported by Raman and Read (2000) (Table 2) in a total volume of 20 µl. The PCR reaction was performed using the protocol of Cakir et al. (2009). The amplified products were resolved on a non-denatured polyacrylamide gel at a concentration of 6%. The electrophoresed gels were visualized under UV light.

Statistical analysis

The analysis of variance was was conducted using a completely randomized design, and genotypic means were compared using Duncan's multiple range post-hoc tests in SAS version 9.2.

Polymorphic information content (PIC) indicates the genetic diversity of primers. The PIC for each primer was determined by the following equation (Moreira et al., 2018):

$$PIC = 1 - \Sigma (P_{ij})^2$$

In this equation, P_{ij} is the frequency of j^{th} allele in i^{th} primer.

In order to calculate genetic relationships among the wild barley accessions NTSYSpc 2.02e software was used for computing Jaccard's similarity coefficients. Furthermore, cluster analysis was conducted utilizing an unweighted pair-group (UPGMA) approach to develop dendrograms 39 using th above software. Genome-wide association analyses were carried out using the general linear model (GLM) and mixed linear model (MLM) approaches in TASSEL 4.0 and the association between each RWA resistance related traits and the SSR markers was tested (Bradbury et al., 2007). The relevant Q values were used as covariates in GLM and MLM analyses. Manhattan plots showed the relationship between a phenotypic trait and a SSR marker ($P \leq 0.05$). The population structure of the wild barley accessions was determined by the Bayesian clustering method using STRUCTURE version 2.3.4 (Oliver et al., 2010).

Table 2. Detailed information on SSR markers used in the present study.

GenBank	Primer location	Melting temperature (°C)	Product size (bp)	Primer sequence (5'–3')
Bmac0399	1H	60	145	R:CGATGCTTTACTATGAGAGGT F:GGGTCTGAAGCCTGAAC
Bmac0032	1H	60	215	R:CCATCAAAGTCCGGCTAG F: GTCGGGCCTCATACTGAC
Bmac0134	2H	55	148	R:CCAACTGAGTCGATCTCG F: CTTCGTTGCTTCTCTACCTT
Bmag0125	2H	55	134	R:AATTAGCGAGAACAAAATCAC F:AGATAACGATGCACCACC
Bmac0067	3H	55	171	R:AACGTACGAGCTCTTTTTCTA F:ATGCCAACTGCTTGTTTAG
Bmag0006	3H	58	174	R:TTAAACCCCCCCCCTCTAG F:TGCAGTTACTATCGCTGATTTAGC
EBmac0701	4H	55	149	R:ATGATGAGAACTCTTCACCC F: TGGCACTAAAGCAAAAGAC
Bmac0310	4H	55	176	R:CTACCTCTGAGATATCATGCC F:ATCTAGTGTGTGTTGCTTCCT
Bmag0223	5H	58	127	R:TTAGTCACCCTCAACGGT F: CCCCTAACTGCTGTGATG
GBM1483	5H	55	150	R:CAGTGATATGGACTACGGCG F:CTTGTTCTCCACCTCGAAGC
EBmac602	6H	58	205	R:GATTGGAGCTTCGGATCAC F:CCGTCTAGGGAGAGGTTCTC
Bmag0173	6H	58	150	R:CATTTTTGTTGGTGACGG F:ATAATGGCGGGAGAGACA
Bmag0007	7H	58	185	R:TGAAGGAAGAATAAACAACCAACA F:TCCCCTATTATAGTGACGGTGTG
Bmag0135	7H	58	161	R:ACGAAAGAGTTACAACGGATA F: GTTTACCACAGATCTACAGGTG

Results

Phenotypic evaluation

The reaction of 30 wild barley genotypes to RWA feeding was evaluated. The results of the analysis of variation showed highly significant genotypic effects for rolling ($F = 160.41$, $df_t = 29$, $df_e = 720$, $P < 0.0001$) and chlorosis ($F = 22.12$, $df_t = 29$, $df_e = 720$, $P < 0.0001$).

A wide range of resistance to susceptibility was observed for leaf chlorosis with the average of 1.06 to 9. Mean reactions ranged from 1.03 to 3 for leaf rolling. Regarding chlorosis, IG140073 and IG120794 genotypes had the scores of 1.06 and 1.37, respectively, which categorize as resistant. IG129152 and IG117888 were susceptible with the scores 9 and 8.82, respectively (Table 3). IG2 (1.03) and IG120794 (1.04) had the least leaf rolling and were the most resistant genotypes. On the other hand, IG3 (3.00) was a moderately susceptible (Table 3).

Chlorophyll concentration

Chlorophyll a ($F = 3.2$, $df_t = 29$, $df_e = 60$, $P < 0.001$), b ($F = 3.54$, $df_t = 29$, $df_e = 720$, $P < 0.001$), and total

chlorophyll (F = 3.45, df_t =29, df_e = 720, P <0.001) concentrations were significantly different among the RWA-infested *H. spontaneum* populations. Chlorophyll a, b, and total chlorophyll concentrations were decreased significantly (0.88, 0.62 and 1.49 mg/g, respectively) on RWA-infested *H. spontaneum* populations when compared with those of the uninfested plants (1.08, 0.80 and 1.61 mg/g). In the RWA-infested condition, IG40154 genotype had the highest chlorophyll a (1.56 mg/g), b (1.159 mg/g), and total (2.72 mg/g). Additionally, IG129152 genotype exhibited the lowest levels of chlorophyll a (0 mg/g), chlorophyll b (0 mg/g), and total chlorophyll concentration (0 mg/g) (Table 4).

Table 3. Mean comparison of leaf chlorosis and leaf rolling in wild barley accessions under infestation with Russian wheat aphid at seedling stage.

Accessions	Plant chlorosis	Leaf rolling
IG129152	9.00 a	1.58 j
IG117888	8.82 a	2.89 cd
IG144170	7.93 b	2.89 d
IG38657	6.54 c	2.51 g
IG121853	5.95 d	2.54 g
IG119447	5.25 e	1.80 j
IG39919	5.17 e	2.82 d
IG38654	5.16 e	2.80 de
IG137596	4.35 f	2.93bc
IG139141	3.75 g	2.00 h
IG120790	3.69 gh	2.95 b
IG120793	3.44 ghi	2.03 g
IG1	3.40 ghi	1.85 i
IG142486	3.38 ghi	1.83 i
IG39489	3.29 hi	2.02 h
IG119438	3.21 i	2.6 ef
IG38936	3.14 i	2.54 ef
IG140352	2.72 j	2.02 h
IG140302	2.68 j	2.58 fg
IG2	2.45 jk	1.03 k
IG140189	2.44 jk	1.89 i
IG39565	2.31 jk	1.54 g
IG40155	2.16 k	1.41 j
IG38669	2.15 k	1.57 i
IG3	2.10 k	3.00 a
IG40152	2.06 k	1.49 j
IG142356	1.60 l	1.08 k
IG40154	1.46 l	1.44 j
IG120794	1.37 lm	1.04 k
IG140073	1.06 m	1.07k

*In each column, the means with at least one similar letter do not differ significantly at the 5% probability level.

Screening of SSR marker and assessment of genetic diversity

The system of SSR markers was used for analyzing the genetic diversity of 30 wild barley genotypes. Out of 14 microsatellite primers used, 10 primers (71%) showed acceptable polymorphism. Four pairs of primers (Bmag0135, Bmac0032, GBM1483 and Bmag0173) were excluded from further analysis due to the production of non-specific bands (Table 5). A total of 52 alleles were detected. Number of observed alleles ranged 4 to 8 with an average number of 5.2 alleles per locus. Bmag007 marker had eight alleles while Bmac0399, Bmag0125, Bmag0223, and EBmac602 had 4 alleles (Table 5). Moreover, at the DNA level, 100 percent of the amplification products showed polymorphism, indicating substantial diversity among *H. spontaneum* accessions (Table 5).

Table 4. Mean comparison of Chlorophyll a, b and total Chlorophyll in barley accessions under infestation with Russian wheat aphid at seedling stage.

Accession	Chlorophyll b	Chlorophyll a	Total chlorophyll
IG40154	1.159a	1.56 a	2.72a
IG140073	0.96ab	1.39ab	2.35ab
IG2	0.957 ab	1.28a-d	2.23a-c
IG1	0.883a-c	1.34 a-c	2.23a-c
IG120790	0.819a-d	1.17a-d	1.986a-d
IG38936	0.816 a-d	1.14a-e	1.947a-d
IG38669	0.782b-d	1.13a-e	1.914a-d
IG140189	0.741b-d	1.09a-e	1.833b-d
IG40152	0.739b-d	1.081a-f	1.819b-d
IG3	0.725b-e	1.073a-f	1.798b-e
IG139141	0.706b-e	1.012b-f	1.72 b-e
IG39919	0.698b-e	1.015b-f	1.71 b-e
IG120794	0.696b-e	0.978b-f	1.67 b-e
IG142356	0.686b-e	0.988b-f	1.68 b-e
IG120793	0.679b-f	0.928 b-f	1.61 b-e
IG40155	0.617b-f	0.877b-g	1.49 b-f
IG38654	0.615b-f	0.897b-g	1.52 b-f
IG39489	0.599b-f	0.847c-g	1.45c-f
IG119438	0.571 c-g	0.802c-h	1.37c-g
IG140352	0.570 c-g	0.802c-h	1.37 c-g
IG140302	0.565c-g	0.760d-h	1.32 c-g
IG137596	0.519c-h	0.785d-h	1.305d-g
IG142486	0.496d-h	0.675 e-i	1.17d-h
IG39565	0.476d-h	0.658e-i	1.13d-h
IG119447	0.442 d-h	0.653e-i	1.09d-h
IG121853	0.353e-h	0.550f-i	0.903e-h
IG38657	0.309f-i	0.391 g-j	0.701 f-i
IG117888	0.228g-i	0.285h-j	0.514g-i
IG144170	0.165hi	0.191ij	0.356hi
IG129152	0.000l	0.000j	0.000l

*In each column, the means with at least one similar letter do not differ significantly from each other at the 5% level.

The highest and lowest PIC was for primer Bmag007 (0.812) and Bmac0399 (0.374), respectively. As a result, primer Bmag007 is an efficient and helpful marker for detecting genetic variations amongst *H. spontaneum* accessions (Table 5). According to the cluster analysis, the thirty accessions were divided into seven groups (Figure 1).

Table 5. Allele number (Na), number of effective alleles, marker index, Shannon index and polymorphism information content recorded in 30 wild barley accessions using 10 SSR markers.

Primer name	Number of observed alleles	Polymorphism information content (PIC)	Number of effective alleles	Marker index	Shannon index
Bmac0399	4	0.374	1.60	1.50	0.72
Bmac134	5	0.746	3.93	3.73	1.48
Bmag0125	4	0.470	1.88	1.88	0.76
Bmac0067	5	0.601hg	2.50	3.01	1.20
Bmag6	7	0.608	2.55	4.26	1.35
EBmac0701	6	0.765	4.26	4.59	1.60
Bmac310	5	0.713	3.48	3.57	1.37
Bmag0223	4	0.643	2.80	2.57	1.10
EBmac602	4	0.557	2.26	2.23	1.02
Bmag007	8	0.812	5.31	6.49	1.84

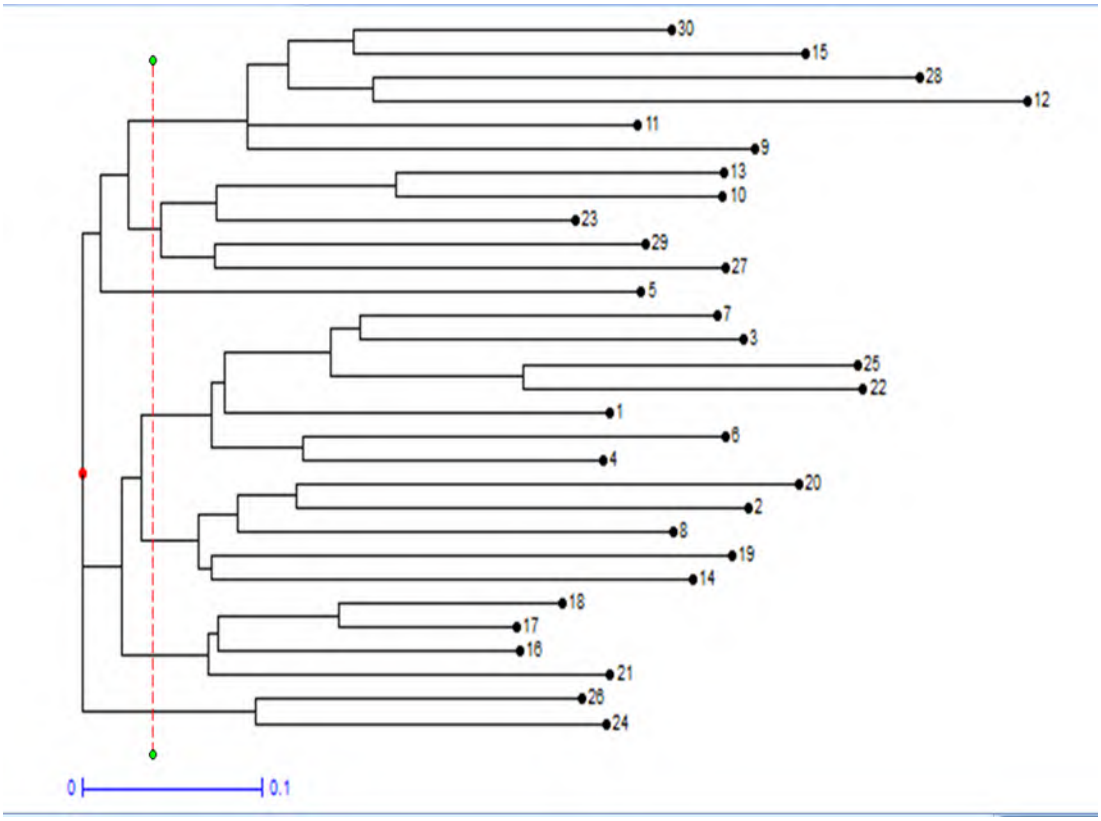

Figure 1. A dendrogram based on SSR markers of the 30 *H. spontaneum* populations by UPGMA method.

The first cluster consisted of six genotypes of Iranian accession (Kermanshah NO. 30), Iranian accession (Kurdistan), IG38936 (Palestine), IG137596 (Armenia), IG144170 (Jordan), and IG39565 (Palestine). The second cluster included five accessions such as IG 120793 (Turkmenistan), IG 140189 (Tajikistan), IG40152 (Uzbekistan), Iranian accession (Kermanshah NO. 29), and IG140302 (Tajikistan). The third cluster had only one accession, IG117888 (Syria). The fourth cluster comprised seven accessions, IG 39919 (Syria), IG38669 (Afghanistan), IG 39489 (Syria), IG119438 (Syria), IG120790 (Turkmenistan), IG120794 (Turkmenistan), and IG40155 (Uzbekistan). The fifth cluster included five accessions, IG139141 (Jordan), IG38654 (Afghanistan), IG120794 (Turkmenistan), IG121853 (Syria), and IG129152 (Iraq). The sixth cluster had four accessions, including IG38657 (Afghanistan), IG119447 (Syria), IG142356 (Tajikistan), and IG142486 (Tajikistan). The seventh cluster included two accessions, (IG 140073 (Tajikistan) and IG140352 (Tajikistan).

Population structure

K and ΔK statistics were extracted by determining the population structure using the MCMC algorithm. The maximum value was K=7 (Figure 2). Thus, the 30 *H. spontaneum* accessions were divided into seven subpopulations (Figure 2). All subpopulations had the same proportion of membership (0.143). Therefore, the same number of accessions was observed in each subpopulation. The highest genetic differentiation belonged to the fourth subpopulation (0.0743). The seventh subpopulation had the lowest genetic differentiation (0.0002) (Table 6).

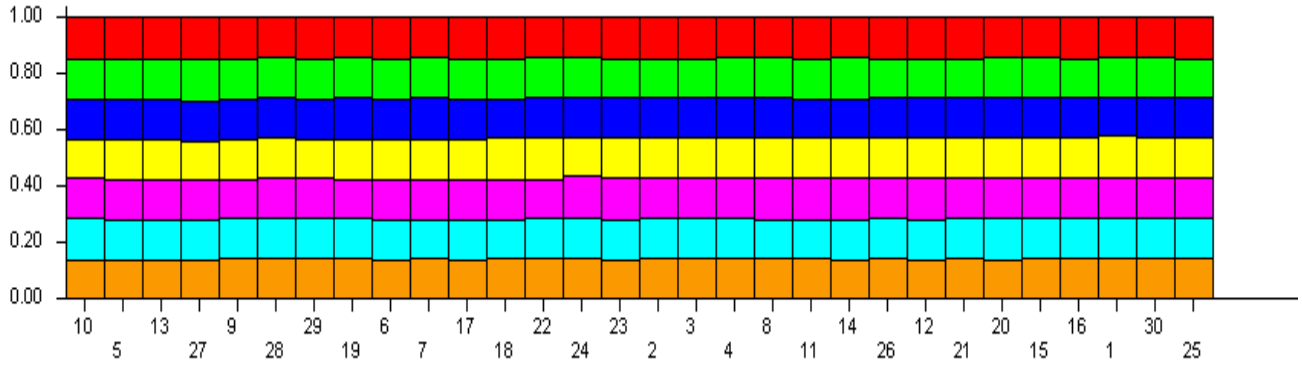

Figure 2. Genetic relatedness of 30 *H. spontaneum* populations with 10 SSR primer combinations as analyzed by the STRUCTURE program.

Table 6. Percentage of accessions, differentiation index and genetic distance of the extracted subpopulations.

Subpopulation	Proportion of membership	differentiation index (fst)	Genetic distance						
			1	2	3	4	5	6	7
1	0.143	0.0363	-	0.0000	0.0000	0.0000	0.0000	0.0000	0.0000
2	0.143	0.0050	0.0000	-	0.0000	0.0001	0.0000	0.0000	0.0000
3	0.143	0.0386	0.0000	0.0000	-	0.0000	0.0000	0.0000	0.0000
4	0.143	0.0743	0.0000	0.0001		-	0.0000	0.0001	0.0001
5	0.143	0.0007	0.0000	0.0000	0.0000	0.0001	-	0.0000	0.0000
6	0.143	0.0183	0.0000	0.0000	0.0000	0.0001		-	0.0000
7	0.143	0.0002	0.0000	0.0000	0.0000	0.0001	0.0000		-

Association analysis

Association analysis was conducted with only 11 marker loci, as they exhibited a minor allele frequency (i.e., below 5%) (Table 7). Bmag007 (on 7H), Bmag6 (on the 3H), and Bmac0399 (on the 1H) were significantly associated with leaf rolling in two loci. Bmag0125 (on the 2H) was significantly associated with Chlorophyll a, Total Chlorophyll, and Chlorophyll b. Furthermore, there were significant associations between the marker EBmac0701 (on the 4H) and Total Chlorophyll, Chlorophyll b, Chlorophyll a, and chlorosis. Further, EBmac0701 (on the 4H) was significantly associated with leaf chlorosis (Table 7).

Discussion

This study contributes new insights into the genetic diversity among *H. spontaneum* populations for RWA-resistance, offering valuable information for integration into the breeding programs aimed at improving RWA resistance in barley cultivars. IG120794 collected from Turkmenistan showed the least leaf chlorosis and rolling, which reveal its potential for using in a barley-breeding program in future. High resistance in recent study could be considered as a valuable *D. noxia* resistance source that could be exploited by development of resistant *H. vulgare* germplasms through a backcross program. Although they lacked the 2HS resistance QTL, DH lines with a moderate resistance impact were reported to introgress aphid resistance from the wild barley source *H. spont* (Ahman and Bengtsson, 2019). Leybourne et al. (Kulwal and Singh, 2021) showed that *H. spont*. possesses partial resistance involved elevated basal expression of thionin and phytohormone signaling genes as well as a reduction in phloem quality.

The effect of feeding by this aphid species can be assessed by both chlorophyll and carotenoid concentrations. IG129152 genotype had the lowest chlorophyll a, chlorophyll b, and total chlorophyll concentration, and was the most susceptible population. Chlorosis is the loss of chlorophylls (i.e., chlorophylls a and b) caused by *D. noxia* feeding. Prior studies have thoroughly investigated *D. noxia*-induced chlorophyll reductions and their implications on plant photosynthetic efficiency (Fouche et al., 1984; Burd and Elliott, 1996; Gupta et al., 2005; Macaulay et al., 2020). Likewise Burd and Elliott (1996) compared the chlorophyll content kinetics in susceptible and resistant plants and found that *D. noxia* feeding reduced chlorophyll a, b, and total content in susceptible wheat (Tavon' and 'TAM W-IOl') and barley ('Wintermalt') but not in resistant plants. Resistant plants seem to counteract the deleterious effects of aphid herbivory on leaves through up-regulation of detoxication mechanisms and faster regeneration of photosynthetic active centers and RuBP.

Table 7. Marker-trait associations using MLM and GLM models.

Traits	Marker name	No. of associations	P. value		R^2(%)
			MLM	GLM	
Leaf rolling	Bmag007	2	0.0056	0.0056	0.2455
Chlorophyll a	Bmag0125	3	0.0107	0.0093	0.1975
Total Chlorophyll	Bmag0125	3	0.0112	0.0096	0.1919
Chlorophyll b	Bmag0125	3	0.0127	0.0109	0.1841
Leaf rolling	Bmag007	2	0.0149	0.0149	0.1976
Total Chlorophyll	EBmac0701	3	0.0289	0.0289	0.1428
Chlorophyll b	EBmac0701	3	0.0296	0.0296	0.1399
Chlorophyll a	EBmac0701	3	0.0306	0.0306	0.1433
Leaf rolling	Bmac0399	1	0.0342	0.0342	0.1545
Leaf chlorosis	EBmac0701	4	0.0344	0.0344	0.1369
Leaf rolling	Bmag6	1	0.045	0.045	0.1400

In contrast, leaves of susceptible plants are unable to sustain these processes and become senescent (Franzen et al., 2014).

Gray et al. (1990) determined the association between marker alleles and phenotypes in the homogeneous subpopulations by focusing on the fundamental idea of a population-based mixed population into several unstructured subpopulations. At K = 7, the 30 *H. spontaneum* populations applied for association analysis were divided into seven subpopulations in this study. Subpopulations within a population may exist owing to differences in genotype, geographical origin, natural or human selection, or genetic drift 8). Bayesian clustering in STRUCTURE, PCoA and AMOVA analyses revealed that the population might be differentiated mainly due to the different breeding program origins and by ear row type and divided into five subpopulations (Capo-Chichi et al., 2022). Several reports show that both geographical origin and ear-row type are factors influencing barley population structure (Bengtsson et al., 2017; Capo-Chichi et al., 2022). The geographical separation of the barley genotypes observed in this study could also be justified by local adaptation associating with alterations in geographical attributes in the regions of origin. Genetic diversity, manifested through allelic variants of the involved genes, is a critical factor in selecting the candidate parents to improve a desired agronomic trait.

Association mapping enabled a much larger pool of germplasm to be analyzed for regions related to RWA resistance than the method used in the alternative approaches which depend on biparental mapping populations. SSR markers Bmag007, Bmag6, Bmac0399, Bmag0125, and EBmac0701 exhibited significant associations with RWA resistance traits. As expected, the considerably expanded pool of *H. spontaneum* populations shed light on the genetics of RWA resistance and identified new regions associated with resistance including loci on 1H, 2H, 3H, 4H, and 7H chromosomes. Previous studies identified loci on lH and (Nei, 1973; Macedo, 2003; Mittal et al., 2008; Radchenko et al., 2022). Resistance to RWA in barley, analyzed through QTL analysis and genome-wide association mapping, showed multiple relevant genes, including sites on chromosomes 2H and 3H (Nei, 1973; Dahleen et al., 2012; Leybourne et al., 2019; Singh et al., 2023).

Conclusion

the genetic diversity within wild barley accessions presents a valuable resource for enhancing the genetic foundation of barley and developing superior cultivars. Employing association analysis with a diverse array of wild barley accessions proves effective in pinpointing Marker-Trait Associations (MTAs) for traits such as RWA resistance. The significant markers identified in this study, once validated, can be integrated into marker-assisted breeding programs. Moreover, the preliminary association analysis results for RWA resistance provide a foundation for screening genotypes with aphid tolerance. Future exploration of the putatively linked genomic regions holds promise for uncovering crucial insights into RWA resistance mechanisms in barley.

Supplementary Materials

No supplementary material is available for this article.

Author Contributions

Supervision of the study, Z.T.; Collection of experimental data and writing the manuscript, S.S.; molecular and statistical analysis, A.A.; review of the manuscript, F.F.

Funding

This research project received funding from Deputy Research and Technology of Ilam University.Acknowledgments:

We thank Ilam University for funding this research.

Conflicts of Interest

The authors declare that they have no conflict of interest.

References

Able, J.A., Langridge, P., and Milligan, A.S. (2007). Capturing diversity in the cereals: many options but little promiscuity. *Trends Plant Sci* 12(2): 71-79. doi: 10.1016/j.tplants.2006.12.002.

Ahman, I., and Bengtsson, T. (2019). Introgression of resistance to *Rhopalosiphum padi* L. from wild barley into cultivated barley facilitated by doubled haploid and molecular marker techniques. *Theor Appl Genet* 132: 1397-1408.

Alvarez, M.F., Mosquera, T., and Blair, M.W. (2014). The use of association genetics approaches in plant breeding. *Plant Breed Rev* 38: 17-68.

Arora, S., Steuernagel, B., Gaurav, K., Chandramohan, S., Long, Y., Matny, O., Johnson, R., Enk, J., Periyannan, S., Singh, N., Asyraf Md Hatta, M., Athiyannan, N., Cheema, J., Yu, G., Kangara, N., Ghosh, S., Szabo, L.J., Poland, J., Bariana, H., et al. (2019). Resistance gene cloning from a wild crop relative by sequence capture and association genetics. *Nat Biotechnol* 37(2): 139-143. doi: 10.1038/s41587-018-0007-9.

Bengtsson, T., Manninen, O., Jahoor, A., and Orabi, J. (2017). Genetic diversity, population structure and linkage disequilibrium in Nordic spring barley (*Hordeum vulgare* L. subsp. vulgare). *Genet Resour Crop Evol* 64: 2021-2033.

Bradbury, P.J., Zhang, Z., Kroon, D.E., Casstevens, T.M., Ramdoss, Y., and Buckler, E.S. (2007). TASSEL: software for association mapping of complex traits in diverse samples. *Bioinformatics* 23(19): 2633-2635. doi: 10.1093/bioinformatics/btm308.

Burd, J.D., and Elliott, N.C. (1996). Changes in chlorophyll a fluorescence induction kinetics in cereals infested with Russian wheat aphid (*Homopetra: Aphididea*). *J Econ Entomol* 89(5): 1332-1337.

Cakir, M., Vitou, J., Kollehn, D., Lawson, W., Ilbi, H., Haley, S., Peairs, F., Mornhinweg, D., Bohssini, M., and Ogbonnaya, F. (2009). "A global effort in breeding for resistance to Russian wheat aphid in wheat and barley", in: *19th International Triticeae Mapping Initiative - 3rd COST Tritigen.* (Clermont-Ferrand, France).

Capo-Chichi, L.J.A., Elakhdar, A., Kubo, T., Nyachiro, J., Juskiw, P., Capettini, F., Slaski, J.J., Ramirez, G.H., and Beattie, A.D. (2022). Genetic diversity and population structure assessment of Western Canadian barley cooperative trials. *Front Plant Sci* 13: 1006719. doi: 10.3389/fpls.2022.1006719.

Collard, B.C., and Mackill, D.J. (2008). Marker-assisted selection: an approach for precision plant breeding in the twenty-first century. *Philos Trans R Soc Lond B Biol Sci* 363(1491): 557-572. doi: 10.1098/rstb.2007.2170.

Dahleen, L.S., Bregitzer, P., Mornhinweg, D., and Jackson, E.W. (2012). Association mapping of Russian wheat aphid resistance in barley as a method to identify diversity in the national small grains collection. *Crop Sci* 52(4): 1651-1662.

Dahleen, L.S., Bregitzer, P., Mornhinweg, D., and Klos, K.E. (2015). Genetic diversity for Russian wheat aphid resistance as determined by genome‐wide association mapping and inheritance in progeny. *Crop Sci* 55(5): 1925-1933.

Fouche, A., Verhoeven, R., Hewitt, P., Walters, M., Friel, C., and De Jager, J. (1984). Russian aphid (*Diuraphis noxia*) feeding damage on wheat, related cereals and a *Bromus* grass species. *Tech commun - Repub S Afr Dep Agric*: 22–33.

Franzen, L.D., Gutsche, A.R., Heng-Moss, T.M., Higley, L.G., Sarath, G., and Burd, J.D. (2014). Physiological and biochemical responses of resistant and susceptible wheat to injury by Russian wheat aphid. *J Econ Entomol* 100(5): 1692-1703.

Gharaghanipor, N., Arzani, A., Rahimmalek, M., and Ravash, R. (2022). Physiological and transcriptome indicators of salt tolerance in wild and cultivated barley. *Front Plant Sci* 13: 819282. doi: 10.3389/fpls.2022.819282.

Girma, M., Wilde, G.E., and Harvey, T. (1993). Russian wheat aphid (*Homoptera*: *Aphididae*) affects yield and quality of wheat. *J Econ Entomol* 86(2): 594-601.

Gray, S.N., Robinson, P., Wilding, N., and Markham, P. (1990). Effect of oleic acid on vegetative growth of the aphid-pathogenic fungus *Erynia neoaphidis*. *FEMS Microbiol Ecol* 68(1-2): 131-136.

Gupta, P.K., Rustgi, S., and Kulwal, P.L. (2005). Linkage disequilibrium and association studies in higher plants: present status and future prospects. *Plant Mol Biol* 57(4): 461-485. doi: 10.1007/s11103-005-0257-z.

Heng-Moss, T., Ni, X., Macedo, T., Markwell, J.P., Baxendale, F.P., Quisenberry, S., and Tolmay, V. (2003). Comparison of chlorophyll and carotenoid concentrations among Russian wheat aphid (*Homoptera*: *Aphididae*)-infested wheat isolines. *J Econ Entomol* 96(2): 475-481.

Joukhadar, R., El-Bouhssini, M., Jighly, A., and Ogbonnaya, F. (2013). Genome-wide association mapping for five major pest resistances in wheat. *Mol Breed* 32: 943-960.

Kisten, L., Tolmay, V.L., Mathew, I., Sydenham, S.L., and Venter, E. (2020). Genome-wide association analysis of Russian wheat aphid (*Diuraphis noxia*) resistance in Dn4 derived wheat lines evaluated in South Africa. *PLoS One* 15(12): e0244455. doi: 10.1371/journal.pone.0244455.

Kulwal, P.L., and Singh, R. (2021). Association mapping in plants. *Methods Mol Biol* 2264: 105-117. doi: 10.1007/978-1-0716-1201-9_8.

Leybourne, D.J., Valentine, T.A., Robertson, J.A.H., Perez-Fernandez, E., Main, A.M., Karley, A.J., and Bos, J.I.B. (2019). Defence gene expression and phloem quality contribute to mesophyll and phloem resistance to aphids in wild barley. *J Exp Bot* 70(15): 4011-4026. doi: 10.1093/jxb/erz163.

Macaulay, M., Ramsay, L., and Åhman, I. (2020). Quantitative trait locus for resistance to the aphid *Rhopalosiphum padi* L. in barley (*Hordeum vulgare* L.) is not linked with a genomic region for gramine concentration. *Arthropod-Plant Int* 14: 57-65.

Macedo, T.B. (2003). *Physiological responses of plants to piercing-sucking arthropods.* Doctora of Philosophy, The University of Nebraska-Lincoln.

Mittal, S., Dahleen, L.S., and Mornhinweg, D. (2008). Locations of quantitative trait loci conferring Russian wheat aphid resistance in barley germplasm STARS - 9301B. *Crop Sci* 48(4): 1452-1458.

Moreira, X., Abdala-Roberts, L., Gols, R., and Francisco, M. (2018). Plant domestication decreases both constitutive and induced chemical defences by direct selection against defensive traits. *Sci Rep* 8(1): 12678.

Nei, M. (1973). Analysis of gene diversity in subdivided populations. *Proc Natl Acad Sci U S A* 70(12): 3321-3323. doi: 10.1073/pnas.70.12.3321.

Nieto Lopez, R.M., and Blake, T.K. (1994). Russian wheat aphid resistance in barley: inheritance and linked molecular markers. *Crop Sci* 34(3): 655-659.

Oliver, R.E., Obert, D.E., Hu, G., Bonman, J.M., O'Leary-Jepsen, E., and Jackson, E.W. (2010). Development of oat-based markers from barley and wheat microsatellites. *Genome* 53(6): 458-471. doi: 10.1139/g10-021.

Pritchard, J.K., Stephens, M., and Donnelly, P. (2000). Inference of population structure using multilocus genotype data. *Genetics* 155(2): 945-959. doi: 10.1093/genetics/155.2.945.

Radchenko, E.E., Abdullaev, R.A., and Anisimova, I.N. (2022). Genetic resources of cereal crops for Aphid resistance. *Plants* 11(11): 1490. doi: 10.3390/plants11111490.

Raman, H., and Read, B.J. (2000). Molecular breeding for resistance against Russian wheat aphid in Australian barley. *J Agric Genome* 5: 1-7.

Rohlf, F.J. (1988). *NTSYS-pc: numerical taxonomy and multivariate analysis system.* Exeter Publishing.

Singh, B., Bhatia, D., Narang, D., Kaur, R., and Chhuneja, P. (2023). High-resolution genetic mapping of QTL governing resistance to corn leaf aphid, *Rhopalosiphum maidis* (Fitch) in barley. *Cereal Res Commun* 51(2): 379-389.

Tocho, E., Ricci, M., Tacaliti, M., Giménez, D., Acevedo, A., Lohwasser, U., Börner, A., and Castro, A. (2012). Mapping resistance genes conferring tolerance to RWA (*Diuraphis noxia*) in barley (*Hordeum vulgare*). *Euphytica* 188: 239-251.

Tolmay, V., Jankielsohn, A., and Sydenham, S. (2013). Resistance evaluation of wheat germplasm containing *Dn4* or *Dny* against R ussian wheat aphid biotype RWASA 3. *J Appl Entomol* 137(6): 476-480.

Tolmay, V.L., Sydenham, S.L., Sikhakhane, T.N., Nhlapho, B.N., and Tsilo, T.J. (2020). Elusive diagnostic markers for Russian wheat aphid resistance in bread wheat: deliberating and reviewing the status quo. *Int J Mol Sci* 21(21): 8271. doi: 10.3390/ijms21218271.

Webster, J., Baker, C., and Porter, D. (1991). Detection and mechanisms of Russian wheat aphid (*Homoptera*: *Aphididae*) resistance in barley. *J Econ Entomol* 84(2): 669-673.

Zhang, H., Mittal, N., Leamy, L.J., Barazani, O., and Song, B.H. (2017). Back into the wild—Apply untapped genetic diversity of wild relatives for crop improvement. *Evol Appl* 10(1): 5-24.

Zohary, D., and Hopf, M. (2000). *Domestication of plants in the Old World: The origin and spread of cultivated plants in West Asia, Europe and the Nile Valley*. Oxford University Press.

JPMB
Journal of Plant Molecular Breeding
Published by Genetics and Agricultural Biotechnology Institute of Tabarestan
2022 | Volume 10 | Issue 2

مقاله پژوهشی

ارتباط نشانگر صفت مقاومت شته گندم روسی (*Diuraphis noxia*) در مجموعه متنوع جهانی جو وحشی

زهرا طهماسبی*[۱]، سارا صفری[۱]، علی ارمینیان[۱] فواد فاتحی[۲]

[۱].گروه زراعت و اصلاح نباتات، دانشکده کشاورزی، دانشگاه ایلام، ایلام، ایران
[۲].گروه کشاورزی، دانشگاه پیام نور، تهران، ایران

چکیده: شته روسی گندم (*Diuraphis noxia* Kurdjumov ،RWA) به عملکرد و کیفیت دانه جو به شدت آسیب می‌رساند. مطالعه حاضر با هدف شناسایی نشانگرهای ردیف‌های تکراری ساده (SSR) مرتبط با مقاومت به RWA در جو وحشی (*Hordeum vulgare* subsp. *spontaneum*) انجام شد. جمعیتی متشکل از ۳۰ نمونه جو وحشی، از بانک ژن ایکاردا و ایران که از ۱۰ کشور آسیایی در امتداد پراکندگی جغرافیایی طبیعی گونه بودند، انتخاب شد. برای مطالعه تنوع ژنتیکی از ۱۴ نشانگر SSR استفاده شد. ارتباط ۵۲ نشانگر SSR چندشکلی با صفات مقاومت RWA مرتبط با استفاده از روش‌های مدل خطی عمومی (GLM) و مدل خطی مختلط (MLM) مورد آزمایش قرار گرفت. تجزیه و تحلیل ساختار جمعیت هفت زیرجمعیت را در کل مجموعه نشان داد (K=7). یازده نشانگر مرتبط با صفت روی کروموزوم‌های ۱H، ۲H، ۳H، ۴H و ۷H شناسایی شد. نشانگرهای Bmag007، Bmag6، Bmac0399، Bmag0125 و EBmac0701 ارتباط معنی‌داری با صفات مقاومت به RWA نشان دادند. هر پنج نشانگر در هر دو روش GLM و MLM با صفات مرتبط بودند. این مطالعه مناطق ژنومی جدیدی را شناسایی نمود که با صفات مقاومت به RWA مرتبط هستند، که می‌تواند برای درک معماری ژنتیکی مقاومت به RWA در جو مورد مطالعه قرار گیرد.

کلمات کلیدی: تجزیه ارتباطی، زیرجمعیت، مقاومت گیاهچه‌ای، نشانگر SSR .

ویراستار علمی
دکتر احمد ارزانی
دانشگاه صنعتی اصفهان، ایران

تاریخ
دریافت: ۱۶ خرداد ۱۴۰۲
پذیرش: ۱۵ مهر ۱۴۰۲
چاپ: ۱۶ دی ۱۴۰۲

نویسنده مسئول
دکتر زهرا طهماسبی
z.tahmasebi@ilam.ac.ir

ارجاع به این مقاله
Tahmasebi, Z., Safari, S., Arminian, A. and Fatehi, F. (2022). Marker-trait association of Russian wheat aphid (*Diuraphis noxia*) resistance in a globally diverse set of wild barley. *J Plant Mol Breed* 10(2): 46-60. doi:10.10.22058/JPMB.2023.2004093.1275.

JPMB | Journal of Plant Molecular Breeding
Published by Genetics and Agricultural Biotechnology Institute of Tabarestan
2022 | Volume 10 | Issue 2

Co-expression network analysis for identification of key long non-coding RNA and mRNA modules associated with alkaloid biosynthesis in *Catharanthus roseus*

Original paper

Farzaneh Aram [1,2], Seyed Hassan Marashi *[1], Ahmad Tahmasebi [2], Alireza Seifi [1], Behzad Shahin-kaleybar [3]

1. Department of Biotechnology and Plant Breeding, Faculty of Agriculture, Ferdowsi University of Mashhad, Mashhad, Iran.
2. Institute of Biotechnology, Shiraz University, Shiraz, Iran.
3. Genetics and Agricultural Biotechnology Institute of Tabrestan, Sari Agricultural Sciences &Natural Resources University, Sari, Iran.

Abstract: *Catharanthus roseus*, produces a diverse array of specialized metabolites known as monoterpene indole alkaloids (MIAs) through an extensive and intricately branched metabolic pathway. It is imperative to unravel the intricate regulatory networks and relationships between the genes involved in the production of these metabolites. Long non-coding RNAs (lncRNAs) are emerging as significant regulatory factors in various biological processes. In this study, 4303 out of 86726 transcripts were identified as potential lncRNAs in *C. roseus*. Subsequently, we identified coding genes that exhibited a high correlation with CrlncRNA, designating them as potential target genes for collectively modulating the MIA pathway using Weighted Gene Co-Expression Network Analysis (WGCNA), leading to the identification of crucial gene clusters associated with the biosynthesis of MIAs. Based on the findings, three modules (dark turquoise, magenta, and orange) and hub genes were pinpointed as being linked to MIAs. Additionally, the most prominent known coding genes were 10-hydroxygeraniol oxidoreductase, GATA-like transcription factor (*GATA1*), 7-deoxyloganetic acid UDP-glucosyltransferase (*7DLGT*), desacetoxyvindoline 4-hydroxylase (*DH4*), *MYC2*, and *MPK6*. The unknown target genes were related to stress response and the intricate process of hormone transduction. *ORCA*, *MYC2*, and *GATA1* are crucial in regulating the MIA pathway, likely requiring cooperation with CrlncRNAs.

Keywords: lncRNAs, specialized metabolites, transcription factors (TFs), medicinal plants, gene modules.

OPEN ACCESS

Edited by
Dr. Mohammad Mojarrad
Karlsruhe Institute of Technology, Germany

Date
Received: 9 August 2023
Accepted: 4 September 2023
Published: 6 January 2023

Correspondence
Dr. Seyed Hassan Marashi
marashi@um.ac.ir

Citation
Aram, F., Marashi , S.H.,Tahmasebi, A., Seifi, A. and Shahin-kaleybar, B. (2022). Co-expression network analysis for identification of key long non-coding RNA and mRNA modules associated with alkaloid biosynthesis in *Catharanthus roseus*. *J Plant Mol Breed 10* (2): 61-75.
doi:10.22058/JPMB.2023.2008918.1282.

Introduction

Isoprenoids, also known as terpenoids, are a diverse group of about 30,000 unique compounds found in plants. They perform a range of functions in plants, including acting as essential components of primary metabolism, such as photosynthetic pigments, hormones, and redox cofactors. They also include specialized metabolites that play a role in attracting pollinators and defending plants against pathogens and herbivores (Bouvier et al., 2005; Gershenzon and Dudareva, 2007). Monoterpene indole alkaloids are plant secondary metabolites, also known as specialized metabolites, mainly found in the Gentianales, consisting of more than 3,000 MIAs derived from their central precursor strictosidine, which exhibits a remarkable structural diversity and pharmacological activities (O'Connor and Maresh, 2006; Brown et al., 2015).

Plants of the Apocynaceae, Nyssaceae, Loganiaceae and Rubiaceae families are known to synthesize MIAs as part of their defense mechanisms (O'Connor and Maresh, 2006; De Luca et al., 2014).

The medicinal plant *Catharanthus roseus* (L.) G. Don produces dimeric (bis-indole) MIAs, serving aseither anticancer agents (vinblastine and vincristine) (Martino et al., 2018) or precursors (anhydrovinblastine) for the synthesis of natural and semi-synthetic anticancer alkaloids (e.g. vinorelbine) (Ngo et al., 2009). Vincristine and vinblastine have been listed by the US Food and Drug Administration as anticancer drugs with shortages in 2019-2020 (Fox and Unguru, 2020). *C. roseus* synthesizes MIAs through an extensive and intricately branched 31-step metabolic pathway. Over the past few decades, 38 MIA pathway genes including structural genes and several transcription factors involved in the MIA biosynthesis pathway have been discovered using co-expression analysis of tissue-derived omics datasets and biochemical knowledge of the reactions (Figure 1) (Li et al., 2022).

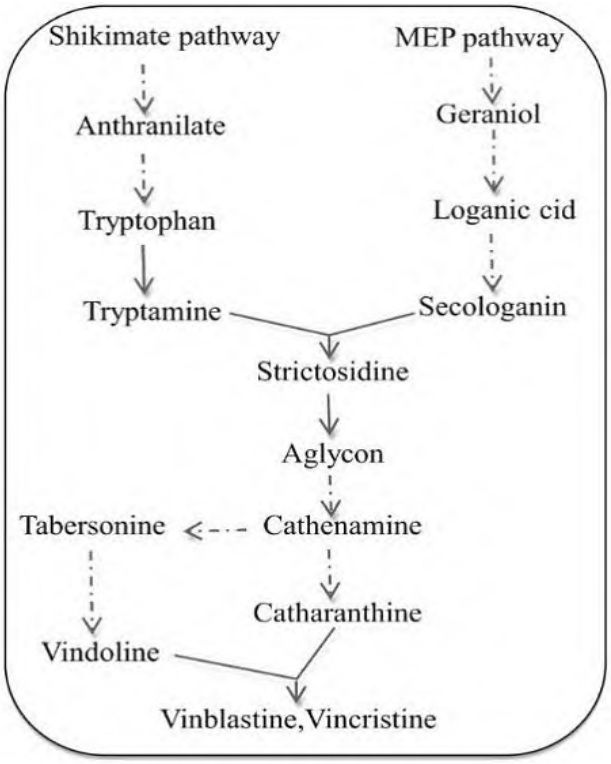

Figure 1. Schematic of the MIA pathway in *C. roseus*. The biosynthesis of MIA starts with the coupling of secologanin (terpenoid moiety) and tryptamine (indole moiety). The terpenoid moiety originates from geraniol, which produced by the mevalonate-independent pathway (MEP). The indole part is derived via anthranilate from the shikimate pathway.

The first transcription factors identified in *C. roseus* belonged to the AP2-ERF ORCA (octadecanoid derivative- responsive catharanthus apetala 2-domain) family. These transcription factor gene clusters, including *ORCA2*, *ORCA3*, *ORCA4*, *ORCA5* and *ORCA6*, are able to upregulate the transcription of key enzyme-encoding genes in the downstream biosynthetic pathway of MIA, such as *STR*, *TDC*, *IS* and *G10H*, and consequently MIAs accumulation (Menke et al., 1999; Van der Fits and Memelink, 2000; Paul et al., 2017; Yang et al., 2023). The basic helix-loop-helix (bHLH) transcription factor CrMYC2 regulates the *TDC* gene, a key gene for tryptamine biosynthesis, and STR and MIA accumulation. Upon perception of jasmonic acid (JA) (Zhang et al., 2011), the MAP kinase cascade, consisting of CrMAPK3/6, CrMAPKKK1, CrMAPKK1 and phosphorylates CrMYC2 and subsequently the CrMYC2 activates the *ORCA* gene cluster and the *TIA* pathway genes (Paul et al., 2017; Singh et al., 2020).

Other transcription factors involved in the regulation of different parts of the pathway including bHLH iridoid synthesis (BIS), such as *BIS1*, *BIS2* and *BIS3* genes, regulate the expression of genes involved in the secoiridoid pathway (Van Moerkercke et al., 2015). CrWRKY1 regulates the serpentine branch of MIA biosynthesis pathway by activating TDC and repressing *ORCA* genes (Suttipanta et al., 2011). CrGATA1 has been identified and confirmed to be involved in vindoline production in response to light (Liu et al., 2019).

In *C. roseus*, transcription repressors have also been identified, suggesting their involvement in the modulation of MIA biosynthesis. Two G-box binding factor (GBF) proteins, CrGBF1 and CrGBF2, may act as transcriptional repressors of MIA biosynthesis (Sibéril et al., 2001). They act as antagonists of CrMYC2 and modulate gene expression in MIA biosynthesis (Sui et al., 2018). Zinc finger proteins such as ZCT1, ZCT2 and ZCT3 act as transcriptional repressors of TDC and STR promoters (Pauw et al., 2004; Rizvi et al., 2016; Paul et al., 2017). RMT1 binding to the ORCA3 promoter, a target of MYC2, suggesting that RMT1 represses the *ORCA3* gene by competing with CrMYC2 for binding to the same cis-element (Patra et al., 2018). Furthermore, the involvement of microRNAs (miRNAs) in regulating MIA pathway has been investigated in *C. roseus* (Prakash et al., 2015; Shen et al., 2017). Conversely, no study has reported the involvement of long non-coding RNAs in the regulation of MIA biosynthesis, especially in *C. roseus*.

RNA transcripts longer than 200 nt with no or minimal coding potential or lacking an ORF encoding >100 amino acids are classified as lncRNAs (Yu et al., 2019). They can affect all elements of genes, including exons, introns, promoters, untranslated regions and terminators, and control gene expression at multiple levels, including modification of chromatin accessibility, translation, transcription and splicing. The integrity of the genome is protected by certain lncRNAs, while others react to environmental cues such as drought, temperature, nutrients and pathogens. The majority of lncRNAs are investigated in the context of protein coding gene regulation and may, therefore, have a functional relationship with mRNA expression (Wierzbicki et al., 2021). The expression of most reported plant lncRNAs is regulated by environmental conditions. They respond to developmental or environmental cues (Yu et al., 2019). Over the last decade, several lncRNAs have been identified along with their potential targets and mechanisms of action that contribute to the growth, development and stress response in plants. In the case of prolonged cold exposure, a process known as vernalization COLDAIR, COLDWRAP and COOLAIR lncRNAs are required to effectively silence FLC transcription which accelerates flowering (Swiezewski et al., 2009; Heo and Sung, 2011; Csorba et al., 2014; Kim and Sung, 2017). APOLO regulates the expression of *PID* gene and auxin signal transduction (Ariel et al., 2020). IPS1 controls the expression of the target gene *PHO2* under Pi starvation, facilitating its uptake phosphate homeostasis (Franco-Zorrilla et al., 2007). The key role of ASCO in regulating alternative splicing (Rigo et al., 2020), SUF in female identity (Hisanaga et al., 2019), 1GOD in seed dormancy (Fedak et al., 2016), ELENA1 in enhancing immunity to *Pseudomonas syringae* PV. (Seo et al., 2019), SVALKA in freezing response (Kindgren et al., 2018), slylnc0195 and slylnc1077 lncRNAs in TYLCV infection response (Wang et al., 2015), DRIR in enhanced drought tolerance (Borah

et al., 2018), ENOD40 in root nodulation (Sousa et al., 2001; Campalans et al., 2004; Rohrig et al., 2004) has been demonstrated.

In this research, we aimed to identify the regulatory function of lncRNAs in collaboration with key coding genes associated with the MIA biosynthesis pathway in *C. roseus*.

Materials and Methods

Data collection

Transcriptomics and metabolomics data of *C. roseus* were obtained from two different databases. The transcriptomics data were retrieved from the Medicinal Plant Genomics Resource (MPGR) database (http://mpgr.uga.edu) (Gongora-Castillo et al., 2012; Kellner et al., 2015). Additionally, the metabolomics data were obtained from the plant/eukaryotic and microbial systems resource database (https://metnetweb.gdcb.iastate.edu/PMR/).

Prediction of candidate lncRNAs

The assembled transcripts of *C. roseus* were acquired from MPGR. To distinguish lncRNAs from all the assembled transcripts, transcripts with a length less than 200 nt and an open reading frame (ORF) longer than 100 amino acids were excluded (Yu et al., 2019). The remaining transcripts underwent a BLASTX search (E-value cutoff of 1E-5) against Pfam, TAIR, Uniprot, and NCBI databases to remove those with probable coding proteins. Further evaluation of coding potential was performed using the coding potential calculator (CPC) and coding-non-coding index (CNCI). Transcripts with a CPC score less than −1 and a CNCI score less than 0 were retained. The transcripts that passed the above-mentioned stringent filtering pipeline were considered as candidate lncRNAs and were considered for the next step of the analysis.

Co-expression network construction

WGCNA package of the R software analysis was applied to construct the *C. roseus* mRNA-lncRNA co-expression network and to identify clusters of transcripts exhibiting similar expression patterns (Langfelder and Horvath, 2008). A similarity matrix was generated by calculating Pearson correlations between each pair of transcripts. The resulting matrix was transformed into an adjacency matrix using a power function (β=12). Subsequently, the topological overlap matrix (TOM) was calculated for hierarchical clustering analysis. The dynamic tree cut algorithm was then utilized to detect distinct modules within the network. These WGCNA modules were subsequently correlated with metabolites to uncover relevant networks. Modules displaying significant gene-metabolite correlations (Pearson's correlation coefficient) were singled out for further investigation. Hub genes were identified by evaluating intramolecular connectivity. Finally, the visualization of module's network was accomplished using Cytoscape software version 3.6.1.

Target gene prediction and enrichment analysis

The identified protein-coding transcripts were annotated using BLASTX against the TAIR database. In addition, genes that co-occurred with lncRNAs in the same module were considered potential targets of those lncRNAs. To gain a deeper insight into the functions of these coding transcripts, GO enrichment analysis and Kyoto Encyclopedia of Genes and Genomes (KEGG) pathway analysis were performed using the gProfiler tool.

Results

Identification of key lncRNAs

To identify lncRNAs in the *C. roseus*, we conducted an analysis of assembled transcripts obtained from the MPGR database. Our filtering criteria excluded transcripts with a length of less than 200 base pairs and an open reading frame (ORF) length exceeding 100 amino acids. Additionally, we checked for sequence similarity to known protein sequences by blastx against various databases. The remaining transcripts were subjected to further assessment using CPC and CNCI programs to determine their protein-coding potential. Following stringent filtration, a total of 4303 transcripts were identified as potential lncRNAs (Supplementary Table S4).

Construction of co -expression modules

LncRNAs and coding genes correlated to MIAs were screened out by WGCNA package implemented in R (Langfelder and Horvath, 2008). By utilizing the WGCNA algorithm the coding and non-coding contigs with similar co-expression

patterns and correlation to metabolites are classified into a set of modules.

A total of 22 modules were constructed, each distinguished by different colors (Figure 2). The number of genes within each module varied, ranging from 32 genes (module palevioletred3) to 3513 genes (dark turquoise). Three modules were found to be highly correlated with the biosynthesis of alkaloids. The results indicated that the dark turquoise and orange modules were correlated with catharanthine, serpentine, and secologanin. Additionally, the orange module showed a correlation with vindoline, the magenta module was associated with catharanthine and vindoline. Furthermore, the number of coding and non-coding genes in each module differed. The orange module comprised 2644 coding genes and 671 lncRNAs, the dark turquoise module had 3097 coding genes and 416 lncRNAs finally, the magenta module contained 633 coding genes and 43 lncRNAs.

Functional annotation

The Gene Ontology (GO) analysis showed significant enrichment on genes of the three selected modules. Specifically, the orange module was enriched with 112 biological processes (BPs), 37 molecular functions (MFs), and 49 cell components (CCs) (Supplementary Table S1). The dark turquoise module showed enrichment in 128 BPs, 43 MFs, and 47 CCs (Supplementary Table S3).

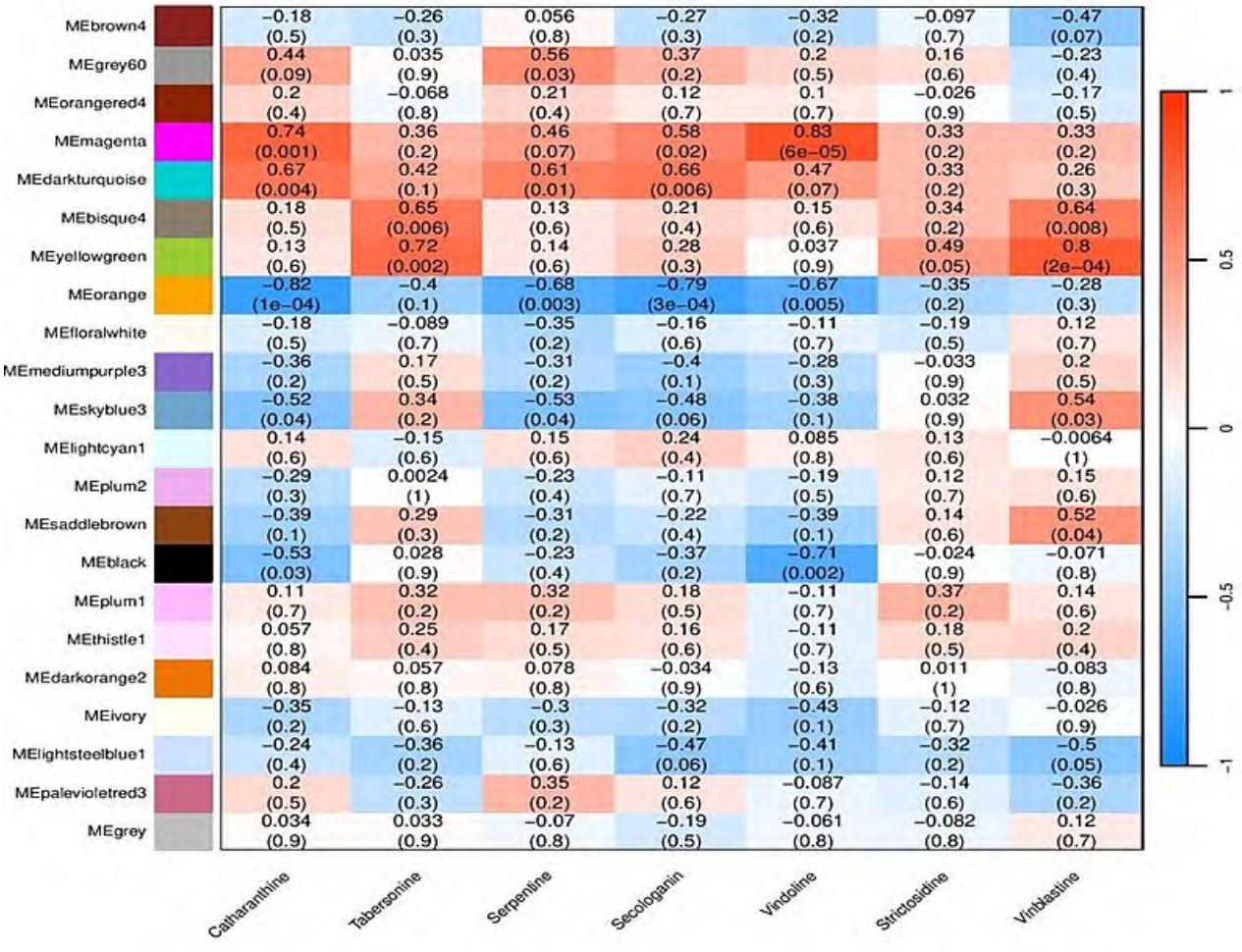

Figure 2. Correlation analysis between eigengene modules and MIAs. Each row shows a module eigengene, each column shows a secondary metabolite. The number in each box represents the correlation value with the numbers in brackets representing correlation *p-values.* Each module contained both coding and non-coding elements (lncRNAs) that correlated with MIAs.

Table 1. Prediction of the function of the top twenty hub genes by BLASTX search against TAIR .

Hub genes	Type	Function
cra_locus_2149	Protein coding	RIBOSOMAL RNA PROCESSING 4
cra_locus_5284	Protein coding	ELKS/Rab6-interacting/CAST family protein, chromosome condensation
cra_locus_8209	Protein coding	MACPF protein which promotes pathogen resistance by activating SA signaling
cra_locus_3069	Protein coding	Hypothetical protein, RNA metabolic process, regulation of gene expression
cra_locus_134	Protein coding	Acyl acid amido synthetases catalysing the conjugation of IAA to amino acids.
cra_locus_10800	Protein coding	Not available
cra_locus_8643	Protein coding	Not available
cra_locus_3578	Protein coding	Structural polyprotein
cra_locus_9321	Protein coding	MAIN-LIKE 1, Encodes aminotransferase like protein containing a plant mobile domain
cra_locus_9332	Protein coding	Protein phosphatase 2C family protein
cra_locus_5559	Protein coding	HEXOKINASE-LIKE 3, response to various abiotic stresses including UV, drought, osmotic, heat and cold.
cra_locus_10506	Protein coding	Encodes a subunit of RNA polymerase I
cra_locus_7967	Protein coding	Eukaryotic translation initiation factor 2B complex
cra_locus_4093	Protein coding	Not available
cra_locus_2086	Protein coding	Endoplasmic reticulum vesicle transporter protein
cra_locus_7687	Protein coding	Zinc finger protein, regulation of gibberellic acid mediated signaling pathway
cra_locus_123151	LncRNA	-
cra_locus_29870	LncRNA	-
cra_locus_123996	LncRNA	-
cra_locus_47564	LncRNA	-

Finally, the magenta module displayed enrichment in 100 BPs, 21 MFs, and 59 CCs (Supplementary Table S2). In the orange module, there was a significant enrichment of genes associated with organic substance metabolic process, cellular process and metabolic process processes. While, the dark turquoise module primarily consisted of genes enriched in cellular process and establishment of localization and response to chemicals. Meanwhile, the genes in the magenta module were associated with the photosynthesis-related functions (Figure 3 and Supplementary Tables S1-3).

The selected modules 'pathway enrichment analysis demonstrated that the 'metabolic pathways' primary metabolism, 'nitrogen compound metabolic process' and ' biosynthesis of secondary metabolites' were the top significantly enriched pathways (Supplementary Tables S1-3).

Identification of hub genes of interested modules

To discover the central and key genes associated with the MIAs, we determined genes with high connectivity within each module, and the top 20 candidate hub genes were selected based on their connectivity levels. Intramodular connectivity of orange modules are visualized in Figure 4.

Of the twenty first hub genes, 4 were lncRNAs and 16 were coding genes. The transcript sequences of

the coding genes were searched against the Arabidopsis genome database (TAIR). The results identified the transcripts as MACPF protein which involved in pathogen resistance enhancing, HEXOKINASE-LIKE 3 involved in various abiotic responses, MACPF protein promotes pathogen resistance by activating SA signaling, Indole-3-Acetic Acid–Amido synthetase that maintains auxin homeostasis, zinc finger transcription factor responsible for gibberellic acid homeostasis and ribosomal RNA processing proteins (Table 1).

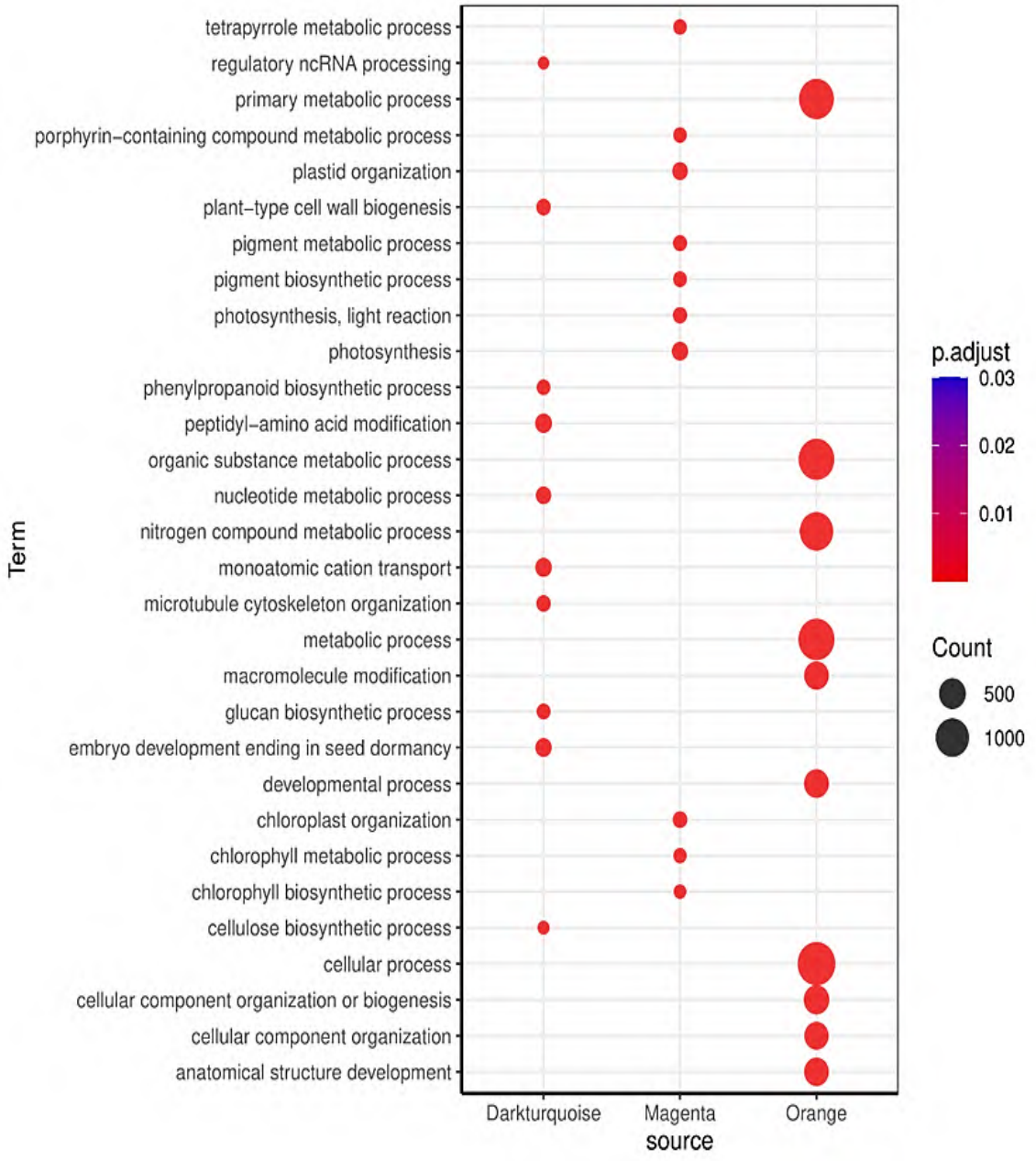

Figure 3. Gene ontology (GO) enrichment analysis of the genes of selected modules. Top GO terms were selected based on the adjusted $p < 0.05$ for categories of biological process. The genes of three selected modules were significantly enriched in terms including primary metabolic process, metabolic process, nitrogen metabolic compound, organic substance metabolic process and cellular process.

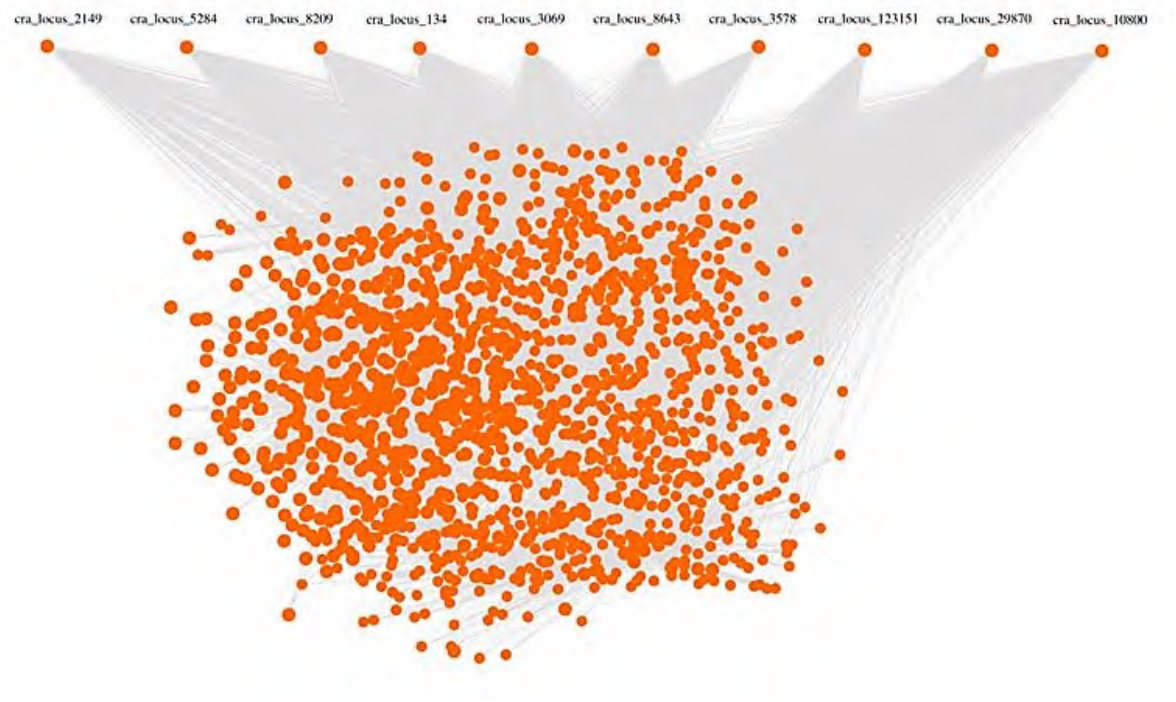

Figure 4. The gene-gene interaction network in orange module.

Among hub genes, we identified known MIA biosynthetic genes including 10-hydroxygeraniol oxidoreductase (*10HGO*), GATA-like transcription factor (*GATA1*), 7-deoxyloganetic acid UDP-glucosyltransferase (*7-DLGT*), desacetoxyvindoline 4-hydroxylase (*CrDH4*), MYC2 and MPK6.

Discussion

C. roseus produces a wide range of specialized metabolites of the MIA class via a complex, long and highly branched metabolic pathway. Reconstitution of the natural product pathway in plants is a unique challenge due to the number of enzymatic steps, the complex tissue and subcellular localization of the intermediates, and the intricate regulatory networks, as exemplified by the vinblastine biosynthesis pathway (Yamamoto et al., 2019). Tissue metabolome and transcriptome datasets in plants are necessary for metabolic pathway gene discovery, where the genes correlated with the molecule of interest or phenotype, together with extensive knowledge of enzymatic biochemical reactions, are important for gene discovery (Li et al., 2022).

In recent years, significant progress has been made in the isolation and characterization of genes encoding key biosynthetic enzymes, transporters and transcription factors in the MIA pathway (Colinas et al., 2020; Singh et al., 2020; Li et al., 2022) however, the potential regulatory role of lncRNAs has not been investigated. In the present study, the key roles of coding and non-coding (lncRNAs) genes associated with MIA pathway biosynthesis were investigated. The coding genes that correlate with lncRNAs can be considered as their targets where they exert their regulatory role by altering the transcriptional and post-transcriptional situation of their coding target genes (Wang et al., 2019; Yu et al., 2019; Zhang et al., 2019) and possibly the accumulation of MIAs.

In the present study, we focused on identifying lncRNAs in *C. roseus*. This endeavour was achieved through the implementation of a bioinformatics pipeline, resulting in the successful detection of a total of 4303 lncRNAs. In addition, our investigation extended to the use of co-expression network analysis, a tool that enabled us to pinpoint both the relevant coding genes and the lncRNAs involved in the intricate process of alkaloid biosynthesis.

This analytical approach unveiled the presence of three distinct modules: orange, dark turquoise, and magenta. Remarkably, these modules exhibited a robust correlation with the alkaloid biosynthesis pathway. Notably, the orange module displayed an enrichment of C2H2, C3H, Homeobox, bHLH and AP2-EREBP TF families. Turning our attention to the dark turquoise module, our examination uncovered a range of TFs such as C3H, bHLH, C2H2, bZIP and Homeobox. Among the TFs found to correlate with MIAs in this study, the regulatory function of the bHLH-CrMYC2 and AP2-ERF ORCA TFs has been demonstrated in previous studies (Van der Fits and Memelink, 2000; Zhang et al., 2011; Pan et al., 2012; Sui et al., 2018; Singh et al., 2020; Yang et al., 2023). CrMYC2 acts upstream of ORCA3, directly regulating it by binding to its promoter and indirectly controlling ORCA4 and ORCA5. CrMYC2, activates ORCA3, which in turn induces the expression of several MIA biosynthetic genes (Zhang et al., 2011) in the tryptamine or vindoline branches, including cytochrome p450 reductase (*CPR*), anthranilate synthase (*AS*), D-1-deoxyxylulose 5 -phosphate synthase (*DXS*), tryptophan decarboxylase (*TDC*), STR and desacetoxyvindoline 4-hydroxylase (*D4H*) but not those in the seco-iridoid branch, such as iridoid synthase (*IS*) and geraniol 10-hydroxylase (*G10H)* (Van der Fits and Memelink, 2000; Van Moerkercke et al., 2015). The top five TF families detected in magenta module were bHLH, C2H2, MYB, bZIP, C2C2-Gata. Interestingly the GATA TF was detected at a high frequency in the magenta module, which this module showed a high correlation with vindoline (0.83, p-value 0.00006). The GATA TF regulates light-induced vindoline biosynthesis in *C. roseus*. Expression of 5 out of 7 genes in the vindoline pathway is significantly induced by GATA TF in response to light (Liu et al., 2019).

Based on the pathway analysis conducted on the hub genes contained within the selected modules, our observations revealed substantial enrichment in pathways denoted as metabolic pathways, porphyrin metabolism, photosynthesis and biosynthesis of secondary metabolites. Furthermore, we conducted a screening process to identify hub genes, revealing that the orange module's most prominent hub genes were *G10H*, GATA-like TF (*GATA1*), 7-deoxyloganetic acid UDP-glucosyltransferase (*7-DLGT*), *D4H* and *MYC2* TFs. Similarly, the dark turquoise module showed MPK6 as its central hub gene, while the magenta module's key hub gene was UDP-glucosyltransferase. The catalytic or regulatory role of the identified hub genes in the MIA pathway will be described. A previous study demonstrated that the CrMAPK6, as a member of the CrMAPKK1-MAPK3/6 cascade, acts upstream of the *ORCA* gene cluster and CrMYC2 TFs to modulate MIA pathway gene expression and MIA accumulation (Paul et al., 2017).

The iridoid pathway begins with the enzyme G10H, a cytochrome P450 monooxygenase that hydroxylates geraniol to 10-hydroxygeraniol. Production of several MIAs enhanced by overexpression of G10H in hairy roots (Wang et al., 2010; Peebles et al., 2011). G10H is regulated by BIS1 transcription factor (Van Moerkercke et al., 2015). Overexpression of *ORCA3* and a structural gene *G10H* results in increased accumulation of strictosidine, vindoline, catharanthine and ajmalicine in *C. roseus* plants. (Pan et al., 2012). *7-DLGT* catalyses the glucosylation of 7-deoxyloganetic acid to 7-deoxyloganic acid in the secoiridoid pathway. The endpoint of the iridoid or secoiridoid branch is secologanin, which couples with tryptamine to form strictosidine, the universal and important MIA precursor in plants. (Miettinen et al., 2014). D4H is involved in the conversion of tebersonine to vindoline. Vinblastine, the end product of the MIA biosynthetic pathway, is derived from the coupling of vindoline and catharanthine (Liu et al., 2019).

Furthermore, hub genes that play crucial roles in stress response and the intricate process of hormone transduction were identified. These genes were highly correlated with hub CrlncRNAs such as *Crlnc808*, *Crlnc758*, *Crlnc316* and *Crlnc1046*. Because of the mutual molecular mechanisms between stress responses and the specialized metabolites biosynthesis these coding sequences can be considered as the targets of CrlncRNAs that possibly involved in regulating MIA biosynthesis.

A collaboration model, involving BPL3-nalcFL7-FL7 to coordinate plant immunity, exists as a result of interaction among lncRNA and code genes. In this cascade, the lncRNA (nalncFL7) negatively

regulates resistance to *Phytophthora capsica* by suppressing the accumulation of FL7 (FORKED-LIKE7) transcripts, which positively regulate plant immunity to *P. capsica* (Ai et al., 2022). In another example, lncRNA and transcription factors working together to regulate the stress response, it has been shown that lncRNA33732, activated by WRKY1, induces RBOH expression to increase H_2O_2 accumulation in the induced defense in tomato plants against *P. infestans* and enhances tomato resistance to *P. infestans* (Cui et al., 2019).

Highly correlated CrlncRNAs with known MIA-associated genes, including catalytic enzymes and transcription factors, as well as MIAs, suggest that CrlncRNAs represent a new layer of regulatory elements of the MIA pathway. In addition, we introduce the correlated genes with CrlncRNAs as their possible coding target genes, which CrlncRNAs can regulate MIAs accumulation by modulating their targets.

Conclusion

C. roseus produces an extensive variety of specialized metabolites belonging to the MIA class through a highly complex and branched pathway. This implies a complex regulation by specific transcription factors, of which several families have been discovered in the last few decades. Conversely, no study has reported the involvement of lncRNAs in the regulation of MIA biosynthesis. In the current study, WGCNA was used to directly integrate transcriptome and metabolome data to construct gene networks that reflect the relationships between lncRNAs and metabolites. The next step was to identify coding genes that correlated with candidate CrlncRNAs and MIAs. Among the known MIA pathway genes, *10HGO*, *GATA1*, *7-DLGT*, *D4H*, *MYC2*, and *MPK6* were tightly correlated with candidate lncRNAs and MIAs. Therefore they can be proposed as coding targets of lncRNAs that modulate MIAs production in a cooperative manner. In addition, these findings further highlight the regulatory role of the MPK6-MYC2-ORCA cascade in the MIA pathway.

Supplementary Materials

The Supplementary Material for this article can be found online at: https://www.jpmb-gabit.ir/article_709096.html.

Supplementary Table S1. The GO enrichment results of orange module.

Supplementary Table S1. The GO enrichment results of magenta module.

Supplementary Table S3. The GO enrichment results of darkturquoise module.

Supplementary Table S3. Identified lncRNAs associated with MIAs in *C. roseus*.

Author Contributions

Conceptualization, H.M. and A.T.; methodology, F.A., A.T.; software, A.T., F.A. and A.S.; formal analysis, F.A., B.S.K.; investigation, H.M.; data curation, F.A., A.T.; writing—original draft preparation, F.A.; writing—review and editing, A.S. and A.T.; visualization, F.A. and B.S.K.; supervision, H.M.; All authors have read and agreed to the published version of the manuscript.

Funding

This research received no external funding.

Acknowledgments

Conflicts of Interest

The authors declare no conflict of interest.

References

Ai, G., Li, T., Zhu, H., Dong, X., Fu, X., Xia, C., Pan, W., Jing, M., Shen, D., and Xia, A. (2022). BPL3 binds the long non-coding RNA *nalncFL7* to suppress *FORKED-LIKE7* and modulate HAI1-mediated MPK3/6 dephosphorylation in plant immunity. *Plant Cell* 35(1): 598-616. doi: https://doi.org/10.1093/plcell/koac311.

Ariel, F., Lucero, L., Christ, A., Mammarella, M.F., Jegu, T., Veluchamy, A., Mariappan, K., Latrasse, D., Blein, T., Liu, C., Benhamed, M., and Crespi, M. (2020). R-Loop mediated trans action of the APOLO long noncoding RNA. *Mol Cell* 77(5): 1055-1065 e1054. doi: 10.1016/j.molcel.2019.12.015.

Borah, P., Das, A., Milner, M.J., Ali, A., Bentley, A.R., and Pandey, R. (2018). Long non-coding RNAs as endogenous target mimics and exploration of their role in low nutrient stress tolerance in plants. *Genes* 9(9): 459.

Bouvier, F., Rahier, A., and Camara, B. (2005). Biogenesis, molecular regulation and function of plant isoprenoids. *Prog Lipid Res* 44(6): 357-429. doi: 10.1016/j.plipres.2005.09.003.

Brown, S., Clastre, M., Courdavault, V., and O'Connor, S.E. (2015). De novo production of the plant-derived alkaloid strictosidine in yeast. *Proc Natl Acad Sci USA* 112(11): 3205-3210. doi: 10.1073/pnas.1423555112.

Campalans, A., Kondorosi, A., and Crespi, M. (2004). *Enod40*, a short open reading frame-containing mRNA, induces cytoplasmic localization of a nuclear RNA binding protein in *Medicago truncatula*. *Plant Cell* 16(4): 1047-1059. doi: 10.1105/tpc.019406.

Colinas, M., Pollier, J., Vaneechoutte, D., Malat, D., Schweizer, F., De Clercq, R., Guedes, J., Martínez-Cortés, T., Molina Hidalgo, F., and Sottomayor, M. (2020). A modular system regulates specialized metabolite pathway branch choice in the medicinal plant Catharanthus roseus. *BioRxiv*. doi: https://doi.org/10.1101/2020.05.04.075671.

Csorba, T., Questa, J.I., Sun, Q., and Dean, C. (2014). Antisense COOLAIR mediates the coordinated switching of chromatin states at FLC during vernalization. *Proc Natl Acad Sci* 111(45): 16160-16165.

Cui, J., Jiang, N., Meng, J., Yang, G., Liu, W., Zhou, X., Ma, N., Hou, X., and Luan, Y. (2019). LncRNA33732 - respiratory burst oxidase module associated with WRKY1 in tomato - *Phytophthora* infestans interactions. *Plant J* 97(5): 933-946.

De Luca, V., Salim, V., Thamm, A., Masada, S.A., and Yu, F. (2014). Making iridoids/secoiridoids and monoterpenoid indole alkaloids: progress on pathway elucidation. *Curr Opin Plant Biol* 19: 35-42. doi: 10.1016/j.pbi.2014.03.006.

Fedak, H., Palusinska, M., Krzyczmonik, K., Brzezniak, L., Yatusevich, R., Pietras, Z., Kaczanowski, S., and Swiezewski, S. (2016). Control of seed dormancy in *Arabidopsis* by a cis-acting noncoding antisense transcript. *Proc Natl Acad Sci U S A* 113(48): E7846-E7855. doi: 10.1073/pnas.1608827113.

Fox, E.R., and Unguru, Y. (2020). Oncology drug shortages in the USA—business as usual. *Nat Rev Clin Oncol* 17(3): 128-129.

Franco-Zorrilla, J.M., Valli, A., Todesco, M., Mateos, I., Puga, M.I., Rubio-Somoza, I., Leyva, A., Weigel, D., Garcia, J.A., and Paz-Ares, J. (2007). Target mimicry provides a new mechanism for regulation of microRNA activity. *Nat Genet* 39(8): 1033-1037. doi: 10.1038/ng2079.

Gershenzon, J., and Dudareva, N. (2007). The function of terpene natural products in the natural world. *Nat Chem Biol* 3(7): 408-414. doi: 10.1038/nchembio.2007.5.

Gongora-Castillo, E., Childs, K.L., Fedewa, G., Hamilton, J.P., Liscombe, D.K., Magallanes-Lundback, M., Mandadi, K.K., Nims, E., Runguphan, W., Vaillancourt, B., Varbanova-Herde, M., Dellapenna, D., McKnight, T.D., O'Connor, S., and Buell, C.R. (2012). Development of transcriptomic resources for interrogating the biosynthesis of monoterpene indole alkaloids in medicinal plant species. *PLoS One* 7(12): e52506. doi: 10.1371/journal.pone.0052506.

Heo, J.B., and Sung, S. (2011). Vernalization-mediated epigenetic silencing by a long intronic noncoding RNA. *Science* 331(6013): 76-79. doi: 10.1126/science.1197349.

Hisanaga, T., Okahashi, K., Yamaoka, S., Kajiwara, T., Nishihama, R., Shimamura, M., Yamato, K.T., Bowman, J.L., Kohchi, T., and Nakajima, K. (2019). A cis-acting bidirectional transcription switch controls sexual dimorphism in the liverwort. *EMBO J* 38(6): e100240. doi: 10.15252/embj.2018100240.

Kellner, F., Kim, J., Clavijo, B.J., Hamilton, J.P., Childs, K.L., Vaillancourt, B., Cepela, J., Habermann, M., Steuernagel, B., Clissold, L., McLay, K., Buell, C.R., and O'Connor, S.E. (2015). Genome-guided investigation of plant natural product biosynthesis. *Plant J* 82(4): 680-692. doi: 10.1111/tpj.12827.

Kim, D.H., and Sung, S. (2017). Vernalization-triggered intragenic chromatin loop formation by long noncoding RNAs. *Dev Cell* 40(3): 302-312 e304. doi: 10.1016/j.devcel.2016.12.021.

Kindgren, P., Ard, R., Ivanov, M., and Marquardt, S. (2018). Transcriptional read-through of the long non-coding RNA *SVALKA* governs plant cold acclimation. *Nat Commun* 9(1): 4561. doi: 10.1038/s41467-018-07010-6.

Langfelder, P., and Horvath, S. (2008). WGCNA: an R package for weighted correlation network analysis. *BMC Bioinform* 9(1): 559. doi: 10.1186/1471-2105-9-559.

Li, C., Wood, J.C., Vu, A.H., Hamilton, J.P., Rodriguez Lopez, C.E., Payne, R.M., Serna Guerrero, D.A., Yamamoto, K., Vaillancourt, B., and Caputi, L. (2022). Single-cell multi-omics enabled discovery of alkaloid biosynthetic pathway genes in the medical plant *Catharanthus roseus*. *BioRxiv*: 2022.2007. 2004.498697.

Liu, Y., Patra, B., Pattanaik, S., Wang, Y., and Yuan, L. (2019). GATA and phytochrome interacting factor transcription factors regulate light-induced vindoline biosynthesis in *Catharanthus roseus*. *Plant Physiol* 180(3): 1336-1350. doi: 10.1104/pp.19.00489.

Martino, E., Casamassima, G., Castiglione, S., Cellupica, E., Pantalone, S., Papagni, F., Rui, M., Siciliano, A.M., and Collina, S. (2018). Vinca alkaloids and analogues as anti-cancer agents: Looking back, peering ahead. *Bioorganic Med Chem Lett* 28(17): 2816-2826.

Menke, F.L., Champion, A., Kijne, J.W., and Memelink, J. (1999). A novel jasmonate- and elicitor-responsive element in the periwinkle secondary metabolite biosynthetic gene *Str* interacts with a jasmonate- and elicitor-inducible AP2-domain transcription factor, ORCA2. *EMBO J* 18(16): 4455-4463. doi: 10.1093/emboj/18.16.4455.

Miettinen, K., Dong, L., Navrot, N., Schneider, T., Burlat, V., Pollier, J., Woittiez, L., van der Krol, S., Lugan, R., Ilc, T., Verpoorte, R., Oksman-Caldentey, K.M., Martinoia, E., Bouwmeester, H., Goossens, A., Memelink, J., and Werck-Reichhart, D. (2014). The seco-iridoid pathway from *Catharanthus roseus*. *Nat Commun* 5(1): 3606. doi: 10.1038/ncomms4606.

Ngo, Q.A., Roussi, F., Cormier, A., Thoret, S., Knossow, M., Guenard, D., and Gueritte, F. (2009). Synthesis and biological evaluation of vinca alkaloids and phomopsin hybrids. *J Med Chem* 52(1): 134-142. doi: 10.1021/jm801064y.

O'Connor, S.E., and Maresh, J.J. (2006). Chemistry and biology of monoterpene indole alkaloid biosynthesis. *Nat Prod Rep* 23(4): 532-547. doi: 10.1039/b512615k.

Pan, Q., Wang, Q., Yuan, F., Xing, S., Zhao, J., Choi, Y.H., Verpoorte, R., Tian, Y., Wang, G., and Tang, K. (2012). Overexpression of ORCA3 and G10H in *Catharanthus roseus* plants regulated alkaloid biosynthesis and metabolism revealed by NMR-metabolomics. *PLoS One* 7(8): e43038. doi: 10.1371/journal.pone.0043038.

Patra, B., Pattanaik, S., Schluttenhofer, C., and Yuan, L. (2018). A network of jasmonate-responsive bHLH factors modulate monoterpenoid indole alkaloid biosynthesis in *Catharanthus roseus*. *New Phytol* 217(4): 1566-1581. doi: 10.1111/nph.14910.

Paul, P., Singh, S.K., Patra, B., Sui, X., Pattanaik, S., and Yuan, L. (2017). A differentially regulated AP 2/ERF transcription factor gene cluster acts downstream of a MAP kinase cascade to modulate terpenoid indole alkaloid biosynthesis in *Catharanthus roseus*. *New Phytol* 213(3): 1107-1123.

Pauw, B., Hilliou, F.A., Martin, V.S., Chatel, G., de Wolf, C.J., Champion, A., Pré, M., van Duijn, B., Kijne, J.W., and van der Fits, L. (2004). Zinc finger proteins act as transcriptional repressors of alkaloid biosynthesis genes in *Catharanthus roseus*. *J Biol Chem* 279(51): 52940-52948.

Peebles, C.A., Sander, G.W., Hughes, E.H., Peacock, R., Shanks, J.V., and San, K.Y. (2011). The expression of 1-deoxy-D-xylulose synthase and geraniol-10-hydroxylase or anthranilate synthase increases terpenoid indole alkaloid accumulation in *Catharanthus roseus* hairy roots. *Metab Eng* 13(2): 234-240. doi: 10.1016/j.ymben.2010.11.005.

Prakash, P., Ghosliya, D., and Gupta, V. (2015). Identification of conserved and novel microRNAs in *Catharanthus roseus* by deep sequencing and computational prediction of their potential targets. *Gene* 554(2): 181-195.

Rigo, R., Bazin, J., Romero - Barrios, N., Moison, M., Lucero, L., Christ, A., Benhamed, M., Blein, T., Huguet, S., and Charon, C. (2020). The *Arabidopsis* lnc RNA ASCO modulates the transcriptome through interaction with splicing factors. *EMBO Rep* 21(5): e48977.

Rizvi, N.F., Weaver, J.D., Cram, E.J., and Lee-Parsons, C.W. (2016). Silencing the transcriptional repressor, ZCT1, illustrates the tight regulation of terpenoid indole alkaloid biosynthesis in *Catharanthus roseus* hairy roots. *PLoS One* 11(7): e0159712. doi: 10.1371/journal.pone.0159712.

Rohrig, H., John, M., and Schmidt, J. (2004). Modification of soybean sucrose synthase by S-thiolation with ENOD40 peptide A. *Biochem Biophys Res Commun* 325(3): 864-870. doi: 10.1016/j.bbrc.2004.10.100.

Seo, J.S., Diloknawarit, P., Park, B.S., and Chua, N.H. (2019). ELF18-Induced long noncoding RNA 1 evicts fibrillarin from mediator subunit to enhance pathogenesis-releated gene 1 (PR1) expression. *New Phytol* 221(4): 2067-2079. doi: 10.1111/nph.15530.

Shen, E.M., Singh, S.K., Ghosh, J.S., Patra, B., Paul, P., Yuan, L., and Pattanaik, S. (2017). The miRNAome of *Catharanthus roseus*: identification, expression analysis, and potential roles of microRNAs in regulation of terpenoid indole alkaloid biosynthesis. *Sci Rep* 7: 43027. doi: 10.1038/srep43027.

Sibéril, Y., Benhamron, S., Memelink, J., Giglioli-Guivarc'h, N., Thiersault, M., Boisson, B., Doireau, P., and Gantet, P. (2001). *Catharanthus roseus* G-box binding factors 1 and 2 act as repressors of strictosidine synthase gene expression in cell cultures. *Plant Mol Biol* 45: 477-488.

Singh, S.K., Patra, B., Paul, P., Liu, Y., Pattanaik, S., and Yuan, L. (2020). Revisiting the ORCA gene cluster that regulates terpenoid indole alkaloid biosynthesis in *Catharanthus roseus*. *Plant Sci* 293: 110408.

Sousa, C., Johansson, C., Charon, C., Manyani, H., Sautter, C., Kondorosi, A., and Crespi, M. (2001). Translational and structural requirements of the early nodulin gene enod40, a short-open reading frame-containing RNA, for elicitation of a cell-specific growth response in the alfalfa root cortex. *Mol Cell Biol* 21(1): 354-366. doi: 10.1128/MCB.21.1.354-366.2001.

Sui, X., Singh, S.K., Patra, B., Schluttenhofer, C., Guo, W., Pattanaik, S., and Yuan, L. (2018). Cross-family transcription factor interaction between MYC2 and GBFs modulates terpenoid indole alkaloid biosynthesis. *J Exp Bot* 69(18): 4267-4281.

Suttipanta, N., Pattanaik, S., Kulshrestha, M., Patra, B., Singh, S.K., and Yuan, L. (2011). The transcription factor CrWRKY1 positively regulates the terpenoid indole alkaloid biosynthesis in *Catharanthus roseus*. *Plant Physiol* 157(4): 2081-2093. doi: 10.1104/pp.111.181834.

Swiezewski, S., Liu, F., Magusin, A., and Dean, C. (2009). Cold-induced silencing by long antisense transcripts of an *Arabidopsis Polycomb* target. *Nature* 462(7274): 799-802. doi: 10.1038/nature08618.

Van der Fits, L., and Memelink, J. (2000). ORCA3, a jasmonate-responsive transcriptional regulator of plant primary and secondary metabolism. *Science* 289(5477): 295-297. doi: 10.1126/science.289.5477.295.

Van Moerkercke, A., Steensma, P., Schweizer, F., Pollier, J., Gariboldi, I., Payne, R., Vanden Bossche, R., Miettinen, K., Espoz, J., Purnama, P.C., Kellner, F., Seppanen-Laakso, T., O'Connor, S.E., Rischer, H., Memelink, J., and Goossens, A. (2015). The bHLH transcription factor BIS1 controls the iridoid branch of the monoterpenoid indole alkaloid pathway in *Catharanthus roseus*. *Proc Natl Acad Sci U S A* 112(26): 8130-8135. doi: 10.1073/pnas.1504951112.

Wang, J., Yu, W., Yang, Y., Li, X., Chen, T., Liu, T., Ma, N., Yang, X., Liu, R., and Zhang, B. (2015). Genome-wide analysis of tomato long non-coding RNAs and identification as endogenous target mimic for microRNA in response to TYLCV infection. *Sci Rep* 5(1): 1-16.

Wang, P., Dai, L., Ai, J., Wang, Y., and Ren, F. (2019). Identification and functional prediction of cold-related long non-coding RNA (lncRNA) in grapevine. *Sci Rep* 9(1): 6638. doi: 10.1038/s41598-019-43269-5.

Wang, Q., Yuan, F., Pan, Q., Li, M., Wang, G., Zhao, J., and Tang, K. (2010). Isolation and functional analysis of the *Catharanthus roseus* deacetylvindoline-4-O-acetyltransferase gene promoter. *Plant Cell Rep* 29(2): 185-192. doi: 10.1007/s00299-009-0811-2.

Wierzbicki, A.T., Blevins, T., and Swiezewski, S. (2021). Long noncoding RNAs in plants. *Annu Rev Plant Biol* 72: 245-271. doi: 10.1146/annurev-arplant-093020-035446.

Yamamoto, K., Takahashi, K., Caputi, L., Mizuno, H., Rodriguez-Lopez, C.E., Iwasaki, T., Ishizaki, K., Fukaki, H., Ohnishi, M., Yamazaki, M., Masujima, T., O'Connor, S.E., and Mimura, T. (2019). The complexity of intercellular localisation of alkaloids revealed by single-cell metabolomics. *New Phytol* 224(2): 848-859. doi: 10.1111/nph.16138.

Yang, Y., Ding, L., Zhou, Y., Guo, Z., Yu, R., and Zhu, J. (2023). Establishment of recombinant *Catharanthus roseus* stem cells stably overexpressing ORCA4 for terpenoid indole alkaloids biosynthesis. *Plant Physiol Biochem* 196: 783-792. doi: 10.1016/j.plaphy.2023.02.039.

Yu, Y., Zhang, Y., Chen, X., and Chen, Y. (2019). Plant noncoding RNAs: Hidden players in development and stress responses. *Annu Rev Cell Dev Biol* 35: 407-431. doi: 10.1146/annurev-cellbio-100818-125218.

Zhang, H., Hedhili, S., Montiel, G., Zhang, Y., Chatel, G., Pré, M., Gantet, P., and Memelink, J. (2011). The basic helix‐loop‐helix transcription factor CrMYC2 controls the jasmonate‐responsive expression of the ORCA genes that regulate alkaloid biosynthesis in *Catharanthus roseus*. *Plant J* 67(1): 61-71.

Zhang, X., Dong, J., Deng, F., Wang, W., Cheng, Y., Song, L., Hu, M., Shen, J., Xu, Q., and Shen, F. (2019). The long non-coding RNA lncRNA973 is involved in cotton response to salt stress. *BMC Plant Biol* 19: 1-16.

JPMB
Journal of Plant Molecular Breeding
Published by Genetics and Agricultural Biotechnology Institute of Tabarestan
2022 | Volume 10 | Issue 2

مقاله پژوهشی

آنالیز شبکه هم‌بیانی جهت شناسایی ماژول‌های mRNA و long non-coding RNA کلیدی مرتبط با بیوسنتز آلکالوئیدها در گیاه *Catharanthus roseus*

فرزانه آرام[۲،۱]، سیدحسن مرعشی[*۱]، احمد طهماسبی[۲]، علیرضا صیفی[۱]، بهزاد شاهین کلیبر[۳]

۱. گروه بیوتکنولوژی و اصلاح نباتات، دانشکده کشاورزی، دانشگاه فردوسی مشهد، مشهد، ایران
۲. مؤسسه بیوتکنولوژی، دانشگاه شیراز، شیراز، ایران
۳. مؤسسه ژنتیک و بیوتکنولوژی کشاورزی طبرستان، دانشگاه علوم کشاورزی و منابع طبیعی ساری، ساری، ایران

چکیده: گیاه *Catharanthus roseus*، طیف متنوعی از متابولیت‌های تخصصی به نام مونوترپن ایندول آلکالوئیدها (MIAs) را از طریق یک مسیر متابولیکی گسترده و پیچیده تولید می‌کند. بنابراین شناسایی شبکه‌های تنظیمی پیچیده و روابط بین ژن‌های دخیل در تولید این متابولیت‌ها ضروری بنظر می‌رسد. RNAهای طولانی غیر کدکننده (lncRNAs) اخیرا به عنوان عوامل تنظیم‌کننده مهم در فرآیندهای زیستی متنوع ظهور پیدا کرده‌اند. در این مطالعه، ۴۳۰۳ از ۸۶۷۲۶ رونوشت به عنوان lncRNA بالقوه در گیاه *C. roseus* شناسایی شدند. متعاقباً، ژن‌های کدکننده بسیار همبسته با CrlncRNA شناسایی شدند و آن‌ها به‌عنوان ژن‌های هدف بالقوه دخیل در تنظیم مسیر MIA با استفاده از تجزیه و تحلیل شبکه هم‌بیانی ژن وزنی (WGCNA) تعیین شدند که منجر به شناسایی خوشه‌های ژنی مهم مرتبط با بیوسنتز MIA شد. بر اساس یافته‌ها، سه ماژول (dark turquoise ، magenta و orange) و همچنین ژن‌های هاب مرتبط با MIA مشخص شدند. به‌علاوه، مهمترین ژن‌های کدکننده شناخته‌شده مسیر شامل 10-hydroxygeraniol oxidoreductase، فاکتور رونویسی *GATA1*، 7-deoxyloganetic acid UDP-glucosyltransferase (*7-DLGT*)، desacetoxyvindoline 4-hydroxylase (DH4)، *MYC2* و *MPK6* با lncRNAs و متابولیت‌های MIA همبستگی داشتند. ژن‌های هدف ناشناخته، با فرآیندهایی مانند پاسخ به استرس و انتقال هورمون مرتبط بودند. نتایج بدست آمده نشان دهنده اهمیت ژن‌های *ORCA* ، *MYC2* و *GATA1* در تنظیم مسیر MIA است و به احتمال زیاد این ژن‌ها نقش خود را در همکاری CrlncRNAs ایفا می‌کنند.

کلمات کلیدی: LncRNAs، متابولیت‌های تخصصی، فاکتورهای رونویسی، گیاهان دارویی.

ویراستار علمی
دکتر محمد مجرد،
موسسه فناوری کارلسروهه، آلمان

تاریخ
دریافت: ۱۸ مرداد ۱۴۰۲
پذیرش: ۱۳ شهریور ۱۴۰۲
چاپ: ۱۶ دی ۱۴۰۲

نویسنده مسئول
دکتر سیدحسن مرعشی
marashi@um.ac.ir

ارجاع به این مقاله
Aram, F., Marashi , S.H.,Tahmasebi, A., Seifi, A. and Shahin-kaleybar, B. (2022). Co-expression network analysis for identification of key long non-coding RNA and mRNA modules associated with alkaloid biosynthesis in *Catharanthus roseus*. *J Plant Mol Breed 10* (2): 61-75.
doi:10.22058/JPMB.2023.2008918.1282.

JPMB | Journal of Plant Molecular Breeding
Published by Genetics and Agricultural Biotechnology Institute of Tabarestan
2022 | Volume 10 | Issue 2

Identification and comprehensive analyses of the *CBL* gene family in sweet orange (*Citrus sinensis* L.)

Seyyed Hamidreza Hashemipetroudi [1,*], Hamidreza Ghorbani [2], Firozeh Sohrevardi[1], Mozhdeh arab[1,3]

1. Genetic and Agricultural Biotechnology Institute of Tabarestan (GABIT), Sari Agricultural Sciences and Natural Resources University (SANRU), Sari, Iran
2. Crop and Horticultural Science Research Department, Mazandaran Agricultural and Natural Resources Research and Education Center, AREEO, Sari, Iran
3. National Institute of Genetic Engineering and Biotechnology (NIGEB), Tehran, Iran

Original paper

Abstract: Calcineurin B-like (CBL) proteins, as calcium sensors, serve roles in plant responses to varied abiotic stressors and in growth and development through interaction with CBL-interacting protein kinases (CIPKs). However, information on the roles and development of CBLs in sweet orange plants is limited. We surveyed the whole *Citrus sinensis* genome and found eight *CBL* genes. Domains features, position and distribution, and conserved motif revealed that the EF-hands domain was conserved across the eight CsCBLs. CsCBL proteins are classed as acidic CBL, and five myristoylation sites and six palmitoylation sites were predicted. Eight *CsCBLs* were distributed across chromosomes Chr01, Chr02, Chr04, and Chr05 and contig chrNW-006257104.1. In chromosome 05, tandem duplications likely gave rise to two *CsCBL4* and *CsCBL5* genes. The phylogeny tree of 37 CBL proteins from different plant species including *Arabidopsis thaliana*, *Oryza sativa*, *Sesamum indicum*, and *C. sinensis* showed that these CBLs are closely related. A meta-analysis of the *CsCBL* gene family's expression in different tissues/stresses revealed that *CsCBL* genes expressed differently in tissues, which could be evidence for *CsCBL* tissue/stress-specific expression. The results of this study highlight the functional properties of the *Cs*CBL gene family and provide crucial data for future research on their functional activities.

Keywords: calcineurin B-like, Calcium sensor, CBL, *Citrus sinensis*, Sweet orange, signaling, stress.

OPEN ACCESS

Edited by
Prof. Junhua Peng,
Spring Valley Agriscience Co. Ltd, China

Date
Received: 7 June 2022
Accepted: 4 January 2023
Published: 12 January 2024

Correspondence
Dr. Seyyed H. Hashemipetroudi
shr.hashemi@sanru.ac.ir;
irahamidreza@yahoo.com

Citation
Hashemipetroudi, S.H., Ghorbani, H., Sohrevardi, F. and Arab, M. (2022). Identification and comprehensive analyses of the *CBL* gene family in sweet orange (*Citrus sinensis*). *J Plant Mol Breed* 10(2): 76-91. doi:10.22058/jpmb.2023.1975801.1266.

Introduction

There are many biological systems that depend on the calcium ion to regulate basic growth and development processes and respond to diverse environmental challenges (Luan, 2009; Ma et al., 2020). Depending on the kind of cell, the concentration of Ca^{2+} might range from nM to mM (Tuteja and Mahajan, 2007; Mohanta and Sinha, 2016). Several Ca^{2+} sensors, including calcium-dependent protein kinases (CDPKs), calcium modulin, and calcineurin B-like proteins (CBLs), detect the Ca^{2+} signals, which are then sent to downstream destinations, triggering a variety of physiological reactions in the cell (Kanchiswamy et al., 2013; Sarwat et al., 2013). Each CBL contains at least three EF domains and Ca^{2+}-binding sites (Mao et al., 2016). By interacting with the CBL-interacting protein kinases (CIPKs), CBLs transfer Ca^{2+} signals (Ma et al., 2020; Tang et al., 2020). CBLs contain EF-hands and myristoylation sites, which are both conserved domains (Kolukisaoglu et al., 2004). The EF-hands are calcium sensors that may be identified by the presence of a conserved Asp (D) or Glu (E) residue (Kanchiswamy et al., 2013). Additionally, each of the themes has a helix-loop-helix structure with a total of 36 amino acid residues. Calmodulines and CBLs, in contrast to CDPKs, are small proteins that do not have an effector kinase domain.

Plant responses to environmental stressors such as drought, salinity, and lack or excess of nutrients can be controlled by CBL-CIPK (Sanyal et al., 2015; Thoday-Kennedy et al., 2015). In addition to this, it regulates the growth and development of plants, as well as the absorption and/or transport of nitrate, ammonium, and iron; the maintenance of H^+ homeostasis; and the transduction of signals involving reactive oxygen species (Li et al., 2016; Mao et al., 2016). Ten genes related to CBL proteins (CBL1-10) have been found in *Arabidopsis* with similar structural domains but minor differences in coding region length (Kolukisaoglu et al., 2004). CBL1 and CBL9 were shown to control the transmission of K^+, nitrate, and ammonium, as well as the development of stomatal opening and closing and ROS signaling (Li et al., 2006; Xu et al., 2006; Lu et al., 2017; Yin et al., 2017). Pollen germination and tube expansion are controlled by CBL2 and CBL3, which sequester Mg^{2+} (Steinhorst et al., 2015). Additionally, CBL3 is responsible for the distribution and translocation of K^+ (Liu et al., 2013). CBL10 is involved in fruit growth and quality, as well as salt tolerance, K^+ absorption, and GTPase activity modification (Kim et al., 2007; Chow et al., 2016).

CBL gene family members have been discovered at the genome-wide level in rice, maize, wheat, and other plants in recent years. CBLs are also critical regulators of plant responses to diverse abiotic stresses, as well as growth and development (Yu et al., 2014; Thoday-Kennedy et al., 2015). Cotton (*Gossypium hirsutum)* fiber elongation appears to be modulated by GhCBL2 and GhCBL3 (Gao et al., 2008). Ten *OsCBL* genes in rice have been reported to respond to diverse stress conditions [sodium chloride (NaCl), polyethylene glycol (PEG), and cold] and are expressed in several organs in the adult stage. In addition, *OsCBL8* overexpressing transgenic rice seedlings exhibited greater salt tolerance than non-transgenic seedlings (Gu et al., 2008). Cellular adaption responses to sodium carbonate stress in *S. bicolor* are assumed to be controlled by *CBL* genes, which are known to govern plant growth and development patterns (Zhang et al., 2011). Under abiotic stress, the transcripts of seven *CBL* members (PeCBL1 to PeCBL10) were found to play key roles in the response of *Populus euphratica* to certain external stimuli (Zhang et al., 2008). In their comprehensive study on the calcium sensor families in the halophyte plant *Aeluropus littoralis*, Arab et al. (2023) revealed the responses of the CBL-CIPK network to salt stress. In the current study, the CBL gene family in sweet orange was identified and characterized based on the newly released genome of *Citrus sinensis* (Wu et al., 2018). Genome-wide characterization of *CiCBL* was analyzed using the available bioinformatics tools, which included gene structure, protein domain, phylogenetic and evolutionary approaches, and gene expression profiling, to better understand the evolutionary history of *CBL* genes.

Materials and Methods

CsCBL searching and characteristics

The complete genome assembly of citrus (*C. sinensis* 'Valencia') was downloaded from the Citrus

Genome Database (www.citrusgenomedb.org; *C. sinensis* genome v2.0). Ten CBL protein sequences from *A. thaliana* (AtCBLs) were obtained from the *Arabidopsis* Information Resource (TAIR) database (www.arabidopsis.org/). Candidate citrus CBL protein sequences (CsCBLs) were selected by blasting the AtCBLs as the query sequences in proteome sequence of *C. sinensis* via local BLASTP. The default statistical parameters used in the BLASTP analysis were as follows: BLASTP-protein query of the protein database; expected threshold (E): −1, comparison matrix: BLOSUM62; no. of alignments to show: 100. Redundant proteins were manually deleted based on their E-values and identity. The identified CBLs were then checked using the Pfam database (www.pfam.xfam.org), and conserved EF-hand domains were validated for all putative CBL proteins using the NCBI CD-Search program. InterProScan (www.ebi.ac.uk/inter pro/) was used to perform the domain analysis against the protein database. ExPASy (wwww.expasy.org/compute_pi/) was used to calculate the candidate protein molecular weight (MW) and isoelectric point (pI). The MEME website (http://meme-suite.org/tools/meme) was used to find conserved motifs with the following optimized parameters: zero or one occurrence per sequence, a maximum of 10 motifs, and an optimum motif width of 6 to 50 residues. For all other parameters, default values were applied.

Phylogenetic and gene structure analysis

The 37 CBL protein sequences from *A. thaliana*, *Oryza sativa*, *Sesamum indicum* and *C. sinensis* were aligned via muscle in MEGA version 7.0, with default parameters (Tamura et al., 2013). In addition to that, a tree constructed using the neighbor-joining (NJ) algorithm was produced through bootstrapping (1000 replicates). The structure of *CsCBLs* was discovered using GFF information by matching the coding sequences to the appropriate genomic sequences. In addition, MEME program was used to create an illustration of the CsCBL protein motifs, conserved domain, gene architectures, and a phylogenetic tree. The chromosome locations of the candidate *CsCBL* genes were investigated by MCScanX (Wang et al., 2012).

Expression profiling of CsCBL genes based on RNA-seq data

To examine the function and expression of the *CsCBL* gene family, 427 RNA-seq samples from 18 bioprojects were gathered from publicly accessible RNA-seq data associated with *C. sinensis*. Transcriptome datasets were selected from various treatments or genetic backgrounds, their accession number were listed as follow: PRJNA741128, PRJNA715742, PRJNA704425, PRJNA703546, PRJNA674975, PRJNA612768, PRJNA566421, PRJNA517400, PRJNA488876, PRJNA471083, PRJNA386941, PRJNA350382, PRJNA340305, PRJNA339838, PRJNA203307. TPM (transcripts per million) had been utilized to measure transcript expression levels.

Results

Eight distinct *CsCBL* were found in *C. sinensis* (Table 1 and Supplementary Table S1). All *CsCBL* have 7 introns and 8 exons, except *SsCBL7*, which has 8 introns and 9 exons. They all code for between 213 (CsCBL3) and 259 amino acid residues (CsCBL8). For the most majority of CBLs, the theoretical isoelectric point (pI) is low and less than five, ranging from 4.67 (CsCBL3) to 5.07 (CsCBL3 and CsCBL4). Because their pI value is less than 6, plant CBL proteins are classed as acidic CBL proteins. The range of molecular weight was between 24.421 (CsCBL3) to 29.671 KDa (CsCBL8). There were five myristoylation sites and six palmitoylation sites predicted in the CsCBLs. Besides, myristoylation sites were not found on CsCBL2, CsCBL7, and CsCBL8, and palmitoylation sites were absent in CsCBL7 and CsCBL8 (Table 1). In the N-terminal region of three CsCBLs (CsCBL3, CsCBL5, and CsCBL6), conserved myristoylation and palmitoylation sites (M-G-C-) can be found. These sites play important roles in protein aggregation, stability, and trafficking.

The proteins' stability indexes are shown in Table 1. According to the evidence presented, CsCBL3 (36.71), which provides the most unstable CsCBL, and CsCBL2 (46.16), which provides the most stable CsCBLs, respectively. A peptide's gravy value is computed by multiplying the hydropathy values of each residue by the length of the sequence. The gravy of CsCBL8 (0.044) is more hydrophilic than

the other CsCBLs, according to Table 1. CsCBL1 also has a lower hydrophilicity than the other CsCBL.

Distribution of the CsCBL gene family members in the C. sinensis genome

In this study, the chromosomal distributions of the *CBL* genes were investigated in *C. sinensis* genome. In total, there were eight *CsCBLs* on five chromosomes (Chr01, Chr02, Chr04, Chr05 and chrNW-006257104.1). Cschr05 included three *CsCBLs*, while Cschr04 contained two *CsCBLs*. Cschr01, Cschr02, and CschrNW-006257104.1 each had one *CsCBL*. The positions of *CsCBL* gene family on the chromosomes of *C. sinensis* are shown in Figure 1. There were two *CBL* genes (*CsCBL4* and *CsCBL5*) identified in Cschr05 that were found to be linked together in a chromosome. Tightly linked genes are likely to have been created through tandem duplications, according to these findings. Both the duplication of genes and the divergence of their functions play an important role in the expansion of gene families and the development of new activities.

Gene structure, domains and motifs arrangement of the CsCBLs

CsCBLs were identified based on their EF-hand sites and number of EF-hand domain. All of the CBL members have been found to have EF-hand motifs, which are responsible for binding to Ca^{2+} ions and transferring calcium signals. All sequences contained four EF-hand motifs.

All CBL proteins contained EF-hand 7, and other EF-hands were located on various CBL proteins (Figure 2a). MEME motif search was used to uncover conserved motifs in 8 CsCBL proteins (Figure 2b) since CBL domains are critical for the action of CBLs. The first two and third motifs were the longest of the ten found motifs (Figure 3 and Table 2). As shown in Figure 2b, motifs 1-5 were found in all of the CsCBLs. In addition, when compared to the other CsCBLs, CBL5 and CBL8 were missing motif 9, whereas CBL1, CBL2, and CBL8 were missing motif 7. Motifs 10 and 8 were only present in CBL7 and CBL8, while motif 6 was found in CBL1 and CBL2. As shown in Figure 2b, motifs 1-5 were found in all of the CsCBLs. In addition, when compared to the other CsCBLs, CBL5 and CBL8 were missing motif 9, whereas CBL1, CBL2, and CBL8 were missing motif 7.

Motifs 10 and 8 were only present in CBL7 and CBL8, while motif 6 was found in CBL1 and CBL2.The pattern with the maximum number of motifs was found in CBL7, which did not have motif 6 (contains nine motifs), while the pattern with the lowest number of motifs was found in CBL5, which did not contain motif 6, 8, 9, or 10 (six motifs) (Figure 2b). *CsCBL* gene family had a different number of introns (between 7 and 9), and the UTR-CDS structure and the length of the coding regions were different between *CsCBLs* (Figure 2c).

Table 1. Physicochemical characteristics of *C. sinensis* CBL gene family.

Gene ID	Molecular weight (KDa)	Isoelectric point	Instability index	Aliphatic index	Gravy	N-Myristoylation	Palmitoylation
CsCBL1	26.057	4.70	39.86	90.97	-0.265	*MVQCLDGLKHFCVV	****MVQCLDGLKHF LDGLKHFCVVVVNCC FCVVVVNCCDADLYK CVVVVNCCDADLYKQ
CsCBL2	25.668	4.81	46.16	90.94	-.239	-	LFASLLQCCDTNPSR
CsCBL3	24.421	4.67	36.71	91.97	-0.114	*****MGCFQSKVA	*****MGCFQSKVAK
CsCBL4	24.495	5.07	38.70	93.41	-0.136	***MNAFGRCFCMKK	*MNAFGRCFCMKKSK NAFGRCFCMKKSKQI
CsCBL5	24.839	4.86	43.57	104.68	-0.025	******MGCVCMKQR	*****MGCVCMKQRL ***MGCVCMKQRLKS
CsCBL6	25.152	4.77	41.73	90.82	-0.187	******MGCVLTKRT	*****MGCVLTKRTK
CsCBL7	29.000	4.58	38.08	87.18	-0.101	-	-
CsCBL8	29.671	4.73	45.47	100.97	0.044	-	-

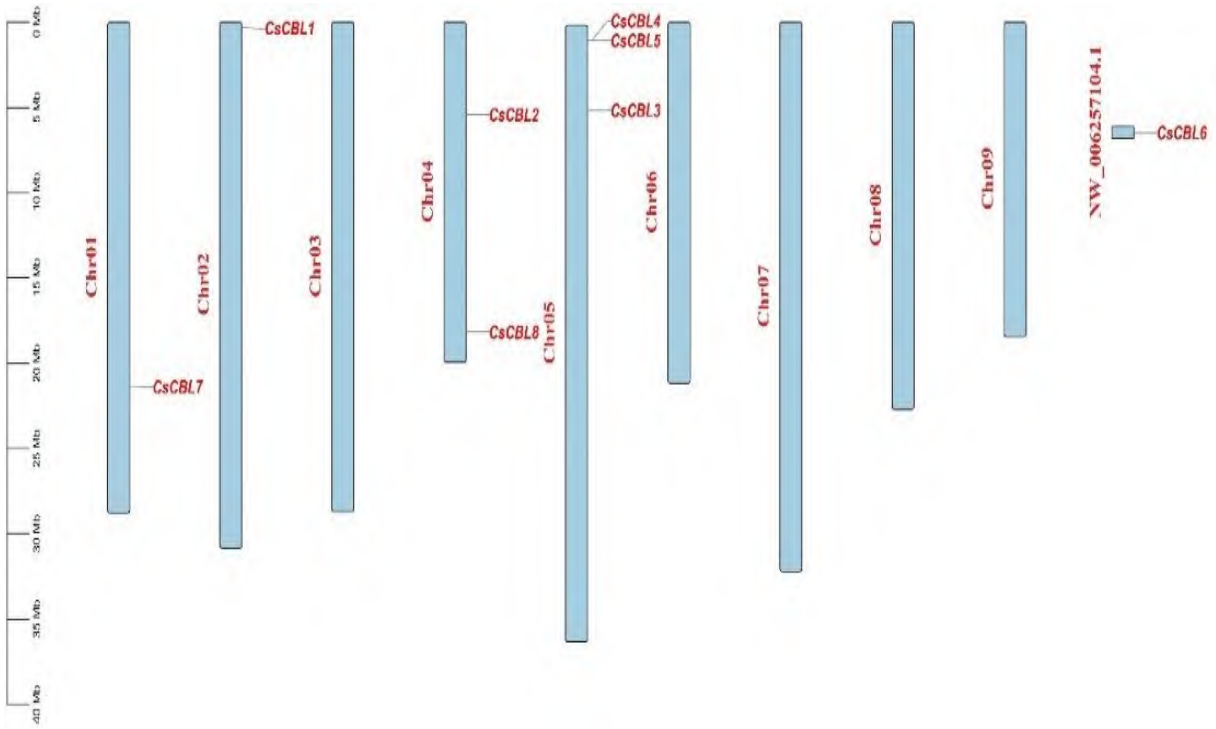

Figure 1. The chromosomal distribution of the *CBL* gene family in *Citrus sinensis*. The left side of each chromosome displays the chromosome numbers and their respective approximate sizes.

Table 2. Sequence of identified motif in eight CBL family members of *C. sinensis*.

Motif ID	Sequence	WIDTH
MEME-1	IIDKTFEDADTKGDGKIDKEEWKEFVLRNPSLLKNMTLPYLKDITTAFPS	50
MEME-2	RNGVIEFEEFVRALSIFHPNAPIEDKIDFAFRLYDLRQTGFIEREEVKQM	50
MEME-3	EIEALYELFKKJSSSIIDDGLIHKEEFQLALFKNSKKENLFADRVFDLFD	50
MEME-4	KQRPGYEDPVILAAETPFSVS	21
MEME-5	VVALLKESEMKLSDD	15
MEME-6	MLQCJEGFKHFCVVLLNCCD	20
MEME-7	MGCFCT	6
MEME-8	YWGSSSLQFGEKJCAVCIP	19
MEME-9	FVFHSEVD	8
MEME-10	MDSAAN	6

1

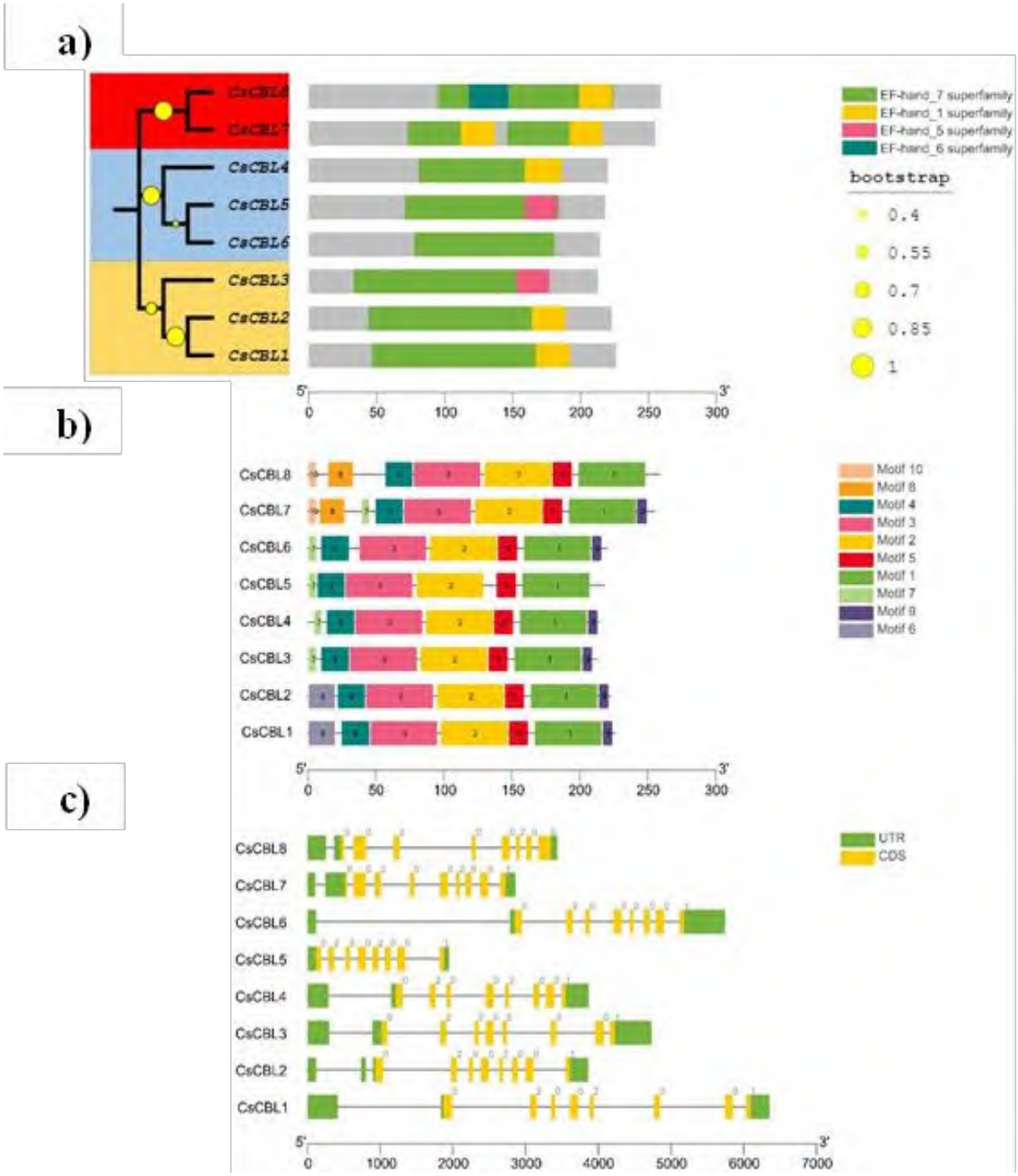

Figure 2. Schematic presentation of *CsCBL* gene structure, their domains and motifs organization. (a) Phylogenetic tree of eight predicted CsCBL as well as their EF-hands domain arrangement. (b) CsCBL motif distribution are shown in different colored boxes. (c) Gene structure of *CsCBL* gene family, and intron and exon organization are pictured. 5 and 3' untranslated -regions are marked by green boxes; the CDS is marked by yellow boxes; black lines denote introns. The bottom scale measures protein length.

Phylogenetic, conservative domains and motifs analysis of the CsCBLs

Protein sequence alignment was used to construct a phylogenetic tree, which was used to investigate the evolutionary relation between *A. thaliana*, *O. sativa*, *S. indicum* and *C. sinensis*. Three main groups (I to III) based on 37 CBL protein from different plant species could be seen in Figure 4. A total of seven, thirteen, and seventeen members were found in groups I, II, and III, respectively. In the first group, there were CsCBL7 and CsCBL8, in the second, CsCBL4, CsCBL5 and CsCBL6, and in the third, there were CsCBL1, CsCBL2, and CsCBL3. There was a disparity between the number of *C. sinensis* and *Arabidopsis* CBLs in each group, while the majority of the AtCBLs in group I clustered together. Molecular evolution is often examined at the gene or family level.

Protein families are sets of proteins that share at least 50% of their amino acid sequences. However, there are currently no models that can infer the evolution of gene families in order to estimate the ancestral state. Analysis of phylogenetic relationships and evolutionary events can be accomplished by using phylogenetic analysis.

Expression profiling of CsCBL

The RNA-seq data (TPM values) of *CsCBL* were obtained from GEO DataSets to examine the expression pattern in various sweet orange tissues, such as fruit, leaf, root, seed, flower, and stem, in order to comprehend the possible roles of the *CsCBL* family members. The expression profile of *CsCBL* genes in different bioprojects is shown in the column graph (Supplementary Figure S1). With the exception of *CsCBL4*, all seven *CsCBL* genes were found to be expressed in at least one tissue (Figure 5). The remarkable expression in most tissues, illustrating the critical functions of these CsCBL during sweet orange development and growth. The varied expression pattern of the *A. littoralus CBL* gene family in root and leaf tissues was proposed by s being associated with their functions in various biological processes and molecular functions. In this investigation, *CsCBL1* and *CsCBL8* were highly expressed in seeds, and *CsCBL5*, *CsCBL6* and *CsCBL7* was highly expressed in the stems.

Figure 3. Motif logo of CsCBL family were pictured by MEME program. MEME motifs are shown as stacks of letters. The X and Y axes reflect the motif's width and the number of bits in each letter.

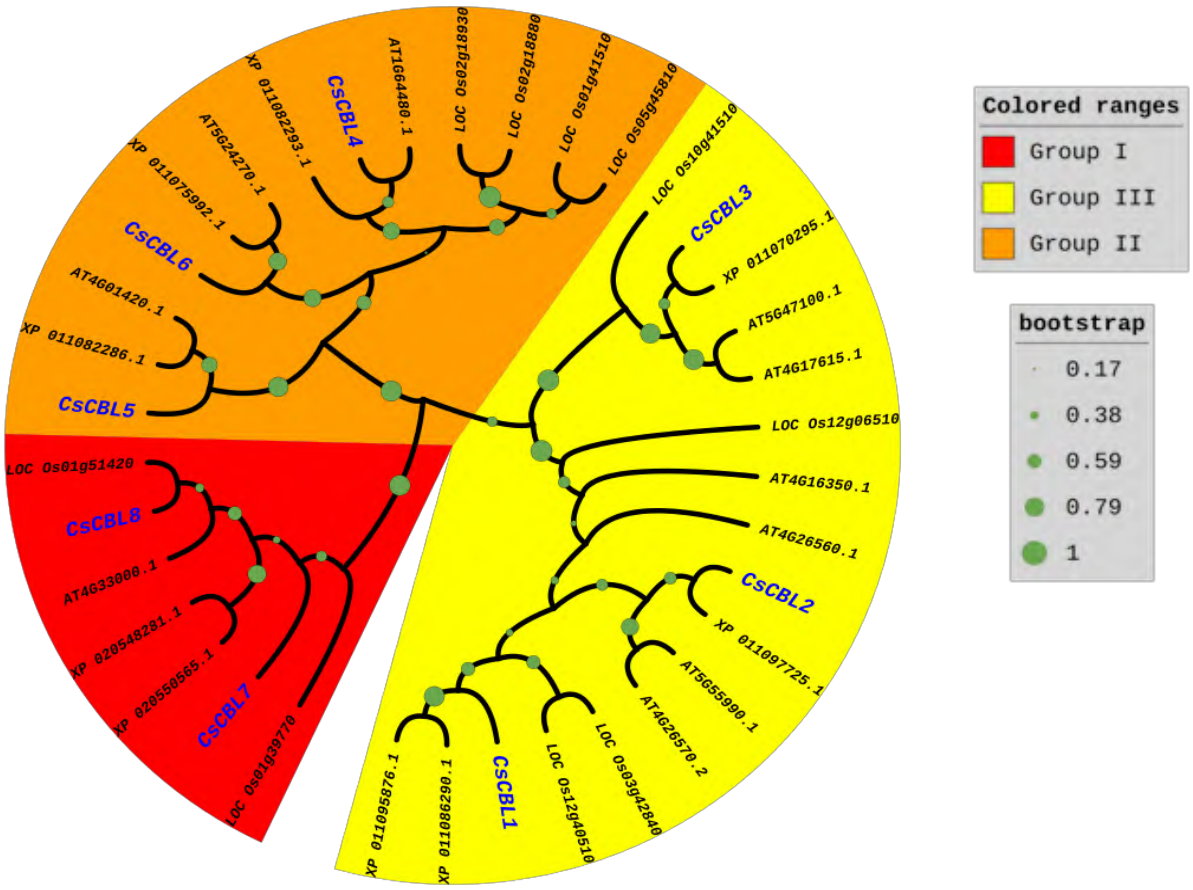

Figure 4. Phylogenetic tree of the CBL family based on an alignment of the proteins found in *Arabidopsis thaliana, Oryza sativa, sesamum indicum and C. sinensis*. Different CsCBL groups are represented by different-colored parts.

Tissue-specific expression was observed in the *CsCBL5* ortholog of the *Arabidopsis SOS3* gene (AT5G24270), with the highest levels of expression observed in stems and leaves and the lowest levels in fruit, root, seed, and flower tissues. It should be noted that, the expression of *CsCBL5*, in comparison to *CsCBL1*, *CsCBL2*, *CsCBL3*, and *CsCBL4*, was extremely low (TPM <5) in all of the specified tissues with the exception of leaves. This is likely due to the fact that *CsCBL5*, similar to *AtCBL4* (SOS3), serves regulatory functions that do not always necessitate high levels of expression.

Discussion

Abiotic and biotic stress responses are regulated by Ca^{2+} signaling in plants (Cheong et al., 2007; Ma et al., 2020). Furthermore, CDPKs, calmodulins, and calcineurin B-like proteins (CBLs) are all implicated in regulating Ca^{2+}-associated stress responses (Wang et al., 2016; Kudla et al., 2018). The availability of the *C. sinensis* genomic information (Wu et al., 2018) made it possible to conduct a genome-wide investigation of the *CsCBL* gene family. Due to their ubiquity in signaling cascades, Ca^{2+} sensor proteins have attracted increasing attention in recent years.

It was discovered in this study that there are eight CBL genes in *C. sinensis* that were found to be located on four chromosomes (Chr1, Chr02, Chr04 and Chr05 and one contig (chrNW-006257104.1).

Like *Arabidopsis*, CBLs in rice are encoded by a multigene family of at least ten members on chromosomes 1, 2, 3, 5, 10 and 12. In this study, the members of the *CsCBL* gene family share the same genetic characteristics.

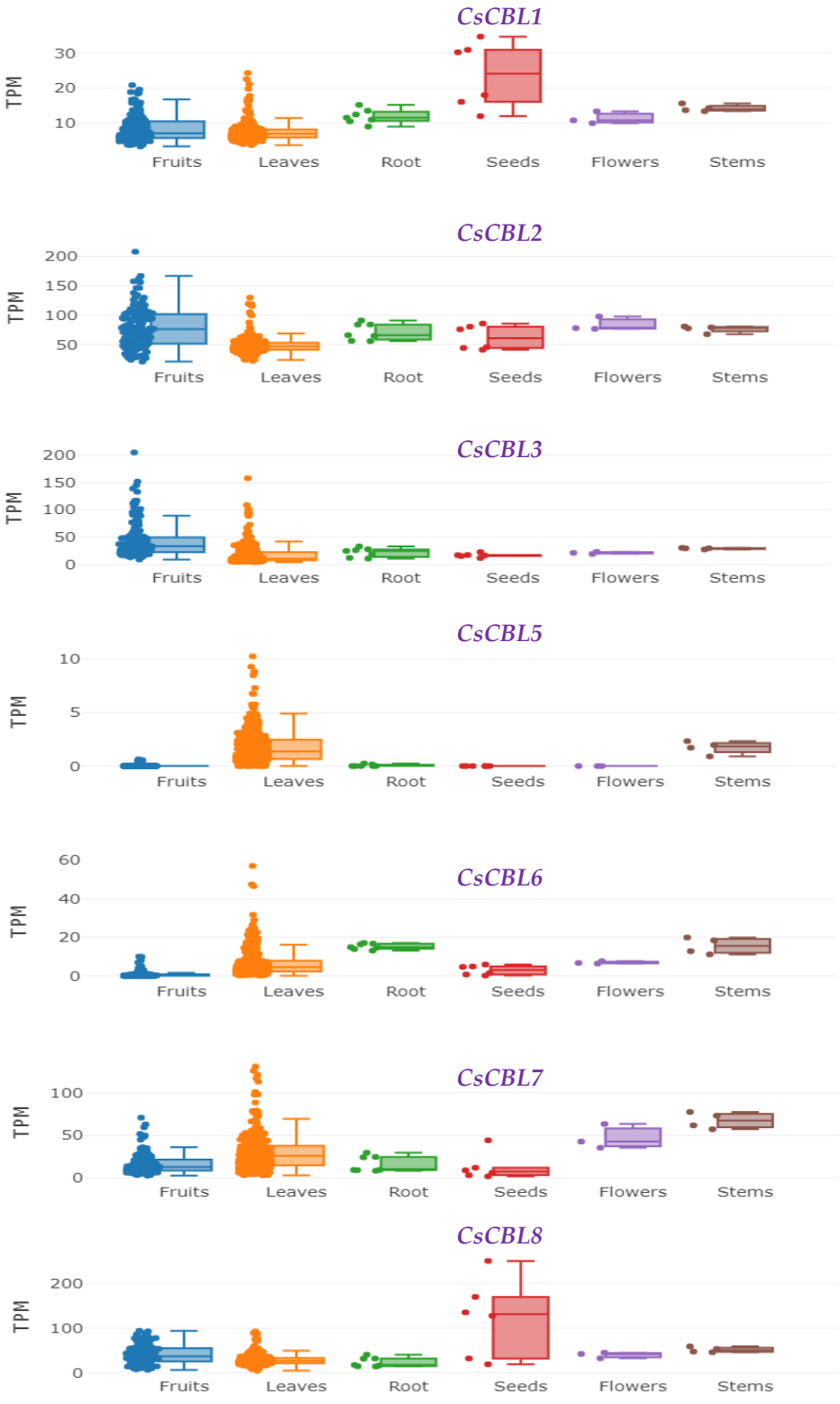

Figure 5. Meta-analysis of the *CBL* gene family's expression pattern in six distinct tissues of the sesame plant. The box plot displays expression levels in TPM (transcripts per million) format.

Among these *CsCBL* genes, polypeptides ranging from 24.42 to 29.67 kDa were predicted. The findings are comparable to those obtained from *A. thaliana* and *O. sativa*, where the majority of AtCBLs and OsCBLs had a size ranging from 23.5 to 25.9 kDa (Kolukisaoglu et al., 2004).

The coding regions of *CsCBL* gene are composed of either eight or nine exons. In other word, the majority of *CBL* genes in *C. sinensis* had seven or eight introns in their coding regions, which is very comparable to the number of introns found in *CBL* genes in *Arabidopsis*, rice, maize, canola, and eggplant (Kolukisaoglu et al., 2004; Gu et al., 2008; Zhang et al., 2014; Li et al., 2016; Zhang et al., 2016). On the other hand, the number of exons can affect the speed of gene induction and expression, and genes with fewer exons are expressed faster (Hashemipetroudi and Bakhshandeh, 2020; Hashemipetroudi et al., 2023; Yaghobi and Heidari, 2023). The junctions between their introns and exons follow the GT/AT rule (Mount, 1982). The length and position of the exons are quite consistent throughout the whole coding area. In addition to this, the majority of the CsCBLs have either three or two conserved EF hand domains in common with one another. The structures of the CsCBL proteins appear to be quite similar to one another, with each one containing four EF-hand domains. It's interesting to note that the linker region between the EF-hand domains appears to be unique to this family of calcium sensor proteins in terms of its constant size. Consequently, alterations in the size of CBL proteins are primarily associated with extension or reduction of the N- or C- terminus regions. As illustrated in Figure 2, the variation in protein size of CsCBLs can be attributed to the distinct dimensions of their amine-terminus (Gu et al., 2008). But some EF-hands are very different from the traditional EF-hand domain (Sathyanarayanan and Poovaiah, 2004; Sanchez-Barrena et al., 2005). AtCBL2 (Nagae et al., 2003) and SOS3, AtCBL4 (Sanchez-Barrena et al., 2005) also have sequences that differ significantly from the standard EF-hand sequence. These variations in the EF hand composition found in different CBLs can result in calcium ion binding affinities that are distinct from one another. Further, experimental investigations are required to determine whether or if these variations in calcium-binding affinity contribute to the decoding of the many calcium signals that are produced in response to the myriad of environmental stimuli (Gu et al., 2008).

Myristoylation of proteins and palmitoylation of proteins are two critical processes that are necessary for protein trafficking, stability, and aggregation (Linder and Deschenes, 2007). According to Smotrys and Linder (2004), the process of protein myristoylation is initiated by the addition of myristic acid to the N-terminal glycine (Gly) amino acid, whereas the protein palmitoylation process is initiated by the addition of palmitic acid to the N-terminal cysteine (Cys) amino acid. The presence of myristoylated and palmitoylated regions in numerous CBLs may have facilitated the targeting of CBL-CIPK complex to membranes. *Arabidopsis*, rice, and other plants share many of these characteristics as well (Kolukisaoglu et al., 2004; Mohanta et al., 2015). It's possible that the highly comparable modes of action and/or interactions that these CBL family members share with their target CIPKs are reflected in the highly conserved structures of these CBL family members across diverse plant species (Mohanta et al., 2015). MGCV myristoylation sequence only found in CsCBL5 and CsCBL6 (Ishitani et al., 2000). Ancestral CBLs may have originated in this realm, according to a theory (Kleist et al., 2014). In the vast majority of the CsCBLs that have been investigated, the amino acid Gly located at the N-terminus is essential for protein myristoylation and is conserved at the second position. It was discovered that the seventh position in certain other CBL proteins contains a conserved form of the amino acid Gly at the N-terminal end of the protein. In a similar manner, the N-terminal Cys amino acid is necessary for protein palmitoylation, and it is conserved at the third position in CBL proteins. Certain CBLs do not have any N-terminal Cys amino acids in their structure. According to Blaskovic et al. (2013), protein palmitoylation is an ubiquitous alteration that is seen in membrane-bound proteins. This modification is also observed in transmembrane-spanning proteins that are generated in soluble ribosomes. In general, palmitoylation of proteins increases their ability to bind to membranes, which in turn changes their location and function. RasGTPase, Rho GTPase, and CDPKs are proteins that undergo palmitoylation (Mohanta et al., 2015). Except CsCBL3, CsCBL5, and

CsCBl6, all other CsCBLs lack a second N-terminal glycine. In addition, only CsCBL3, CsCBL5, and CsCBL6 have the N-terminal Gly amino acid at the second position in addition to having the cysteine amino acid at the N-terminus. Only myristoylation confers a modest affinity for membrane attachment, but palmitoylation and myristoylation confer extremely high affinity contacts (Martín and Busconi, 2001).

Among the CsCBLs, CsCBL5 had the highest aliphatic index and CsCBL7 the lowest. Alainine, valine, isoleucine, and leucine all include aliphatic side chains, and the aliphatic index of these amino acids has been found to be correlated with their respective proteins' thermostability (Ikai, 1980). Enzymes that have a better thermostability could be used in higher reaction temperatures, which would result in an accelerated reaction rate (by decrease of diffusional limitations). According to Sharafi et al. (2017), the half-life of thermostable enzymes is often longer than that of thermolabile enzymes. Stable enzymes are of particular relevance since they can be used in biocatalysis for longer periods of time (Sharafi et al., 2017).

37 CBLs were divided into three main groups by the phylogenetic tree produced from the protein sequence alignment of four species including *A. thaliana*, *O. sativa*, *S. indicum* and *C. sinensis*. The fact that members of the group shared comparable protein sequence lengths, motifs, and exon–intron architectures hints at a strong connection between them. Therefore, it is possible that CsCBLs and their homolog AtCBLs in the same branch play similar roles in plant-microbe interactions as well as in the responses to abiotic stress. According to Mohanta et al (2015), the sequence similarity of two genes indicates structural similarity, and structural similarity indicates functional similarity. As a result, it is possible that AtCBL1 and OsCBL1 perform similar roles. The strong similarities that exist between the CBL gene sequences suggest that they originated very recently as a result of gene duplication and may have functions that overlap with one another or are comparable to one another. Segmental duplication and tandem duplication are critical in the generation of additional members during the evolution of a gene family (Cannon et al., 2004). Due to this, the likely mechanism of *CsCBL* gene family evolution was examined by looking at both segmental and tandem duplication events. New functions led to evolution of paralogous genes, which are most likely to have a role in adaptation. In evolutionary biology, gene duplication and diversification are regarded to be the most significant processes. If a gene is duplicated, its second copy has less selective constraints and can evolve to have a little altered function while the original copy retains its original function.

In the majority of the tissues tested in the meta-analysis, the expression of a certain gene was extremely low. This is most likely because these genes perform regulatory roles that do not always demand high levels of expression. According to Liu et al. (2000), the low expression levels of *AtSOS2* and *AtSOS3* are related with their regulatory function in primary signal transduction. *CBL* proteins may be able to perform similar roles in distinct pathways due to their tissue-specific expression patterns. For example, according to (Guo et al., 2001), *AtCBL4* is expressed specifically in roots, whereas *AtCBL10* is expressed exclusively in shoot tissues (Kim et al., 2007).

Conclusion

The current study discovered eight CBL genes in the *C. sinensis* genome, which were classified into three groups based on phylogenetic analysis. Examining gene structure and expression patterns of gene families could provide useful information about their activity. The utilization of RNA-seq data in the meta-analysis of *CsCBL* gene expression indicated that the expression pattern profiles of *CsCBL* genes in the five tissues under investigation—roots, leaves, fruits, and stems—were discrete. The result of this study offers a unique opportunity to investigate calcium-related sensor in *C. sinensis*. It suggests that *CsCBL* can be utilized as a tool to examine the involvement of calcium ions (Ca^{2+}) in stress signaling, as well as to explore the various interaction of CBL and CIPK proteins in CBL-CIPK signaling network. More research into the expression of these genes at different biotic and abiotic sresses is needed to learn more about *CsCBL* gene regulation in general, and how these genes are controlled spatially and temporally in particular.

Supplementary Materials

The supplementary material for this article can be found online at: https://www.jpmb-gabit.ir/article_709799.html

Supplementary Table S1. *CsCBL* orthologue genes in *Arabidopsis*.

Supplementary Figure S1. The expression profile of *CsCBL* genes in different bioprojects is shown in the column graph.

Author Contributions

Conceptualization, S.H.H.; software, S.H.H. and M.A.; formal analysis, S.H.H. and M.A.; investigation, F.S. and H.G.; data curation, S.H.H.; writing—original draft preparation, S.H.H. and H.G.; writing—review and editing, S.H.H.; All authors have read and agreed to the published version of the manuscript.

Funding

This research received no external funding.

Acknowledgments

This research is supported by the Genetics and Agricultural Biotechnology Institute of Tabarestan (GABIT) and Sari Agricultural Sciences and Natural Resources University (SANRU). The authors also gratefully acknowledge use of the services and facilities of the GABIT during this research.

Conflicts of Interest

The authors declare no conflict of interest.

References

Arab, M., Najafi Zarrini, H., Nematzadeh, G., Heidari, P., Hashemipetroudi, S.H., and Kuhlmann, M. (2023). analysis of calcium sensor families, CBL and CIPK, in *Aeluropus littoralis* and their expression profile in response to salinity. *Genes* 14(3): 753.

Blaskovic, S., Blanc, M., and van der Goot, F.G. (2013). What does palmitoylation do to membrane proteins? *FEBS J* 280(12): 2766-2774.

Cannon, S.B., Mitra, A., Baumgarten, A., Young, N.D., and May, G. (2004). The roles of segmental and tandem gene duplication in the evolution of large gene families in *Arabidopsis thaliana*. *BMC Plant Biol* 4(1): 10. doi: 10.1186/1471-2229-4-10.

Cheong, Y.H., Pandey, G.K., Grant, J.J., Batistic, O., Li, L., Kim, B.G., Lee, S.C., Kudla, J., and Luan, S. (2007). Two calcineurin B-like calcium sensors, interacting with protein kinase *CIPK23*, regulate leaf transpiration and root potassium uptake in *Arabidopsis*. *Plant J* 52(2): 223-239. doi: 10.1111/j.1365-313X.2007.03236.x.

Chow, C.N., Zheng, H.Q., Wu, N.Y., Chien, C.H., Huang, H.D., Lee, T.Y., Chiang-Hsieh, Y.F., Hou, P.F., Yang, T.Y., and Chang, W.C. (2016). PlantPAN 2.0: an update of plant promoter analysis navigator for reconstructing transcriptional regulatory networks in plants. *Nucleic Acids Res* 44(D1): D1154-1160. doi: 10.1093/nar/gkv1035.

Gao, P., Zhao, P.-M., Wang, J., Wang, H.-Y., Du, X.-M., Wang, G.-L., and Xia, G.-X. (2008). Co-expression and preferential interaction between two calcineurin B-like proteins and a CBL-interacting protein kinase from cotton. *Plant Physiol Biochem* 46(10): 935-940.

Gu, Z., Ma, B., Jiang, Y., Chen, Z., Su, X., and Zhang, H. (2008). Expression analysis of the calcineurin B-like gene family in rice (*Oryza sativa* L.) under environmental stresses. *Gene* 415(1-2): 1-12. doi: 10.1016/j.gene.2008.02.011.

Guo, Y., Halfter, U., Ishitani, M., and Zhu, J.-K. (2001). Molecular characterization of functional domains in the protein kinase SOS2 that is required for plant salt tolerance. *Plant Cell* 13(6): 1383-1400.

Hashemipetroudi, S., and Bakhshandeh, E. (2020). Expression analysis of *SiSOD* gene family during *Sesamum indicum* L. seed germination under various abiotic stresses. *J Plant Mol Breed* 8(2): 50-60.

Hashemipetroudi, S.H., Arab, M., Heidari, P., and Kuhlmann, M. (2023). Genome-wide analysis of the laccase (LAC) gene family in *Aeluropus littoralis*: A focus on identification, evolution and expression patterns

in response to abiotic stresses and ABA treatment. *Front Plant Sci* 14: 1112354. doi: 10.3389/fpls.2023.1112354.

Ikai, A. (1980). Thermostability and aliphatic index of globular proteins. *J Biochem* 88(6): 1895-1898.

Ishitani, M., Liu, J., Halfter, U., Kim, C.S., Shi, W., and Zhu, J.K. (2000). SOS3 function in plant salt tolerance requires N-myristoylation and calcium binding. *Plant Cell* 12(9): 1667-1678. doi: 10.1105/tpc.12.9.1667.

Kanchiswamy, C.N., Mohanta, T.K., Capuzzo, A., Occhipinti, A., Verrillo, F., Maffei, M.E., and Malnoy, M. (2013). Differential expression of CPKs and cytosolic Ca 2+ variation in resistant and susceptible apple cultivars (*Malus* x *domestica*) in response to the pathogen *Erwinia amylovora* and mechanical wounding. *BMC Genom* 14(1): 1-14.

Kim, B.G., Waadt, R., Cheong, Y.H., Pandey, G.K., Dominguez-Solis, J.R., Schultke, S., Lee, S.C., Kudla, J., and Luan, S. (2007). The calcium sensor CBL10 mediates salt tolerance by regulating ion homeostasis in *Arabidopsis*. *Plant J* 52(3): 473-484. doi: 10.1111/j.1365-313X.2007.03249.x.

Kleist, T.J., Spencley, A.L., and Luan, S. (2014). Comparative phylogenomics of the CBL-CIPK calcium-decoding network in the moss Physcomitrella, *Arabidopsis*, and other green lineages. *Front Plant Sci* 5: 187. doi: 10.3389/fpls.2014.00187.

Kolukisaoglu, Ü., Weinl, S., Blazevic, D., Batistic, O., and Kudla, J. (2004). Calcium sensors and their interacting protein kinases: genomics of the *Arabidopsis* and rice CBL-CIPK signaling networks. *Plant Physiol* 134(1): 43-58.

Kudla, J., Becker, D., Grill, E., Hedrich, R., Hippler, M., Kummer, U., Parniske, M., Romeis, T., and Schumacher, K. (2018). Advances and current challenges in calcium signaling. *New Phytol* 218(2): 414-431. doi: 10.1111/nph.14966.

Li, J., Jiang, M.M., Ren, L., Liu, Y., and Chen, H.Y. (2016). Identification and characterization of CBL and CIPK gene families in eggplant (*Solanum melongena* L.). *Mol Genet Genomics* 291(4): 1769-1781. doi: 10.1007/s00438-016-1218-8.

Li, L., Kim, B.G., Cheong, Y.H., Pandey, G.K., and Luan, S. (2006). A $Ca^{(2)+}$ signaling pathway regulates a $K^{(+)}$ channel for low K response in *Arabidopsis*. *Proc Natl Acad Sci USA* 103(33): 12625-12630. doi: 10.1073/pnas.0605129103.

Linder, M.E., and Deschenes, R.J. (2007). Palmitoylation: policing protein stability and traffic. *Nat Rev Mol Cell Biol* 8(1): 74-84. doi: 10.1038/nrm2084.

Liu, J., Ishitani, M., Halfter, U., Kim, C.-S., and Zhu, J.-K. (2000). The *Arabidopsis thaliana* SOS2 gene encodes a protein kinase that is required for salt tolerance. *Proc Natl Acad Sci* 97(7): 3730-3734.

Liu, L.L., Ren, H.M., Chen, L.Q., Wang, Y., and Wu, W.H. (2013). A protein kinase, calcineurin B-like protein-interacting protein Kinase9, interacts with calcium sensor calcineurin B-like Protein3 and regulates potassium homeostasis under low-potassium stress in *Arabidopsis*. *Plant Physiol* 161(1): 266-277. doi: 10.1104/pp.112.206896.

Lu, T., Zhang, G., Sun, L., Wang, J., and Hao, F. (2017). Genome-wide identification of CBL family and expression analysis of CBLs in response to potassium deficiency in cotton. *PeerJ* 5: e3653. doi: 10.7717/peerj.3653.

Luan, S. (2009). The CBL-CIPK network in plant calcium signaling. *Trends Plant Sci* 14(1): 37-42. doi: 10.1016/j.tplants.2008.10.005.

Ma, X., Li, Q.H., Yu, Y.N., Qiao, Y.M., Haq, S.U., and Gong, Z.H. (2020). The CBL-CIPK Pathway in Plant Response to Stress Signals. *Int J Mol Sci* 21(16): 5668. doi: 10.3390/ijms21165668.

Mao, J., Manik, S.M., Shi, S., Chao, J., Jin, Y., Wang, Q., and Liu, H. (2016). Mechanisms and Physiological Roles of the CBL-CIPK Networking System in *Arabidopsis thaliana*. *Genes* 7(9): 62. doi: 10.3390/genes7090062.

Martín, M.L., and Busconi, L. (2001). A rice membrane-bound calcium-dependent protein kinase is activated in response to low temperature. *Plant Physiol* 125(3): 1442-1449.

Mohanta, T.K., Mohanta, N., Mohanta, Y.K., Parida, P., and Bae, H. (2015). Genome-wide identification of Calcineurin B-Like (CBL) gene family of plants reveals novel conserved motifs and evolutionary aspects in calcium signaling events. *BMC Plant Biol* 15(1): 189. doi: 10.1186/s12870-015-0543-0.

Mohanta, T.K., and Sinha, A.K. (2016). "Role of calcium-dependent protein kinases during abiotic stress tolerance," in *Abiotic stress response plants*, eds. N. Tuteja & S.S. Gill. (USA: Wiley), pp. 185-206.

Mount, S.M. (1982). A catalogue of splice junction sequences. *Nucleic Acids Res* 10(2): 459-472. doi: 10.1093/nar/10.2.459.

Nagae, M., Nozawa, A., Koizumi, N., Sano, H., Hashimoto, H., Sato, M., and Shimizu, T. (2003). The crystal structure of the novel calcium-binding protein AtCBL2 from *Arabidopsis thaliana*. *J Biol Chem* 278(43): 42240-42246. doi: 10.1074/jbc.M303630200.

Sanchez-Barrena, M.J., Martinez-Ripoll, M., Zhu, J.K., and Albert, A. (2005). The structure of the *Arabidopsis thaliana* SOS3: molecular mechanism of sensing calcium for salt stress response. *J Mol Biol* 345(5): 1253-1264. doi: 10.1016/j.jmb.2004.11.025.

Sanyal, S.K., Pandey, A., and Pandey, G.K. (2015). The CBL-CIPK signaling module in plants: a mechanistic perspective. *Physiol Plant* 155(2): 89-108. doi: 10.1111/ppl.12344.

Sarwat, M., Ahmad, P., Nabi, G., and Hu, X. (2013). $Ca^{(2+)}$ signals: the versatile decoders of environmental cues. *Crit Rev Biotechnol* 33(1): 97-109. doi: 10.3109/07388551.2012.672398.

Sathyanarayanan, P.V., and Poovaiah, B.W. (2004). Decoding Ca^{2+} signals in plants. *Crit Rev Plant Sci* 23(1): 1-11. doi: 10.1080/07352680490273310.

Sharafi, E., Dehestani, A., and Farmani, J. (2017). Bioinformatics evaluation of plant chlorophyllase, the key enzyme in chlorophyll degradation. *Appl Food Biotech* 4(4): 167-178.

Smotrys, J.E., and Linder, M.E. (2004). Palmitoylation of intracellular signaling proteins: regulation and function. *Annu Rev Biochem* 73(1): 559-587. doi: 10.1146/annurev.biochem.73.011303.073954.

Steinhorst, L., Mähs, A., Ischebeck, T., Zhang, C., Zhang, X., Arendt, S., Schültke, S., Heilmann, I., and Kudla, J. (2015). Vacuolar CBL-CIPK12 Ca^{2+} sensor kinase complexes are required for polarized pollen tube growth. *Curr Biol* 25(11): 1475-1482.

Tamura, K., Stecher, G., Peterson, D., Filipski, A., and Kumar, S. (2013). MEGA6: Molecular Evolutionary Genetics Analysis version 6.0. *Mol Biol Evol* 30(12): 2725-2729. doi: 10.1093/molbev/mst197.

Tang, R.J., Wang, C., Li, K., and Luan, S. (2020). The CBL-CIPK calcium signaling network: unified paradigm from 20 years of discoveries. *Trends Plant Sci* 25(6): 604-617. doi: 10.1016/j.tplants.2020.01.009.

Thoday-Kennedy, E.L., Jacobs, A.K., and Roy, S.J. (2015). The role of the CBL–CIPK calcium signalling network in regulating ion transport in response to abiotic stress. *Plant Growth Regul* 76(1): 3-12.

Tuteja, N., and Mahajan, S. (2007). Calcium signaling network in plants: an overview. *Plant Signal Behav* 2(2): 79-85. doi: 10.4161/psb.2.2.4176.

Wang, J.P., Xu, Y.P., Munyampundu, J.P., Liu, T.Y., and Cai, X.Z. (2016). Calcium-dependent protein kinase (CDPK) and CDPK-related kinase (CRK) gene families in tomato: genome-wide identification and functional analyses in disease resistance. *Mol Genet Genomics* 291(2): 661-676. doi: 10.1007/s00438-015-1137-0.

Wang, Y., Tang, H., Debarry, J.D., Tan, X., Li, J., Wang, X., Lee, T.H., Jin, H., Marler, B., Guo, H., Kissinger, J.C., and Paterson, A.H. (2012). MCScanX: a toolkit for detection and evolutionary analysis of gene synteny and collinearity. *Nucleic Acids Res* 40(7): e49. doi: 10.1093/nar/gkr1293.

Wu, G.A., Terol, J., Ibanez, V., Lopez-Garcia, A., Perez-Roman, E., Borreda, C., Domingo, C., Tadeo, F.R., Carbonell-Caballero, J., Alonso, R., Curk, F., Du, D., Ollitrault, P., Roose, M.L., Dopazo, J., Gmitter, F.G., Rokhsar, D.S., and Talon, M. (2018). Genomics of the origin and evolution of Citrus. *Nature* 554(7692): 311-316. doi: 10.1038/nature25447.

Xu, J., Li, H.D., Chen, L.Q., Wang, Y., Liu, L.L., He, L., and Wu, W.H. (2006). A protein kinase, interacting with two calcineurin B-like proteins, regulates K^+ transporter AKT1 in *Arabidopsis*. *Cell* 125(7): 1347-1360. doi: 10.1016/j.cell.2006.06.011.

Yaghobi, M., and Heidari, P. (2023). Genome-wide analysis of Aquaporin gene family in *Triticum turgidum* and its expression profile in response to salt stress. *Genes* 14(1): 202. doi: 10.3390/genes14010202.

Yin, X., Wang, Q., Chen, Q., Xiang, N., Yang, Y., and Yang, Y. (2017). Genome-wide identification and functional analysis of the Calcineurin B-like protein and Calcineurin B-like protein-Interacting Protein Kinase gene families in Turnip (*Brassica rapa* var. rapa). *Front Plant Sci* 8: 1191. doi: 10.3389/fpls.2017.01191.

Yu, Q., An, L., and Li, W. (2014). The CBL-CIPK network mediates different signaling pathways in plants. *Plant Cell Rep* 33(2): 203-214. doi: 10.1007/s00299-013-1507-1.

Zhang, C., Bian, M., Yu, H., Liu, Q., and Yang, Z. (2011). Identification of alkaline stress-responsive genes of CBL family in sweet sorghum (*Sorghum bicolor* L.). *Plant Physiol Biochem* 49(11): 1306-1312. doi: 10.1016/j.plaphy.2011.08.010.

Zhang, F., Li, L., Jiao, Z., Chen, Y., Liu, H., Chen, X., Fu, J., Wang, G., and Zheng, J. (2016). Characterization of the calcineurin B-Like (CBL) gene family in maize and functional analysis of ZmCBL9 under abscisic acid and abiotic stress treatments. *Plant Sci* 253: 118-129. doi: 10.1016/j.plantsci.2016.09.011.

Zhang, H., Yang, B., Liu, W.Z., Li, H., Wang, L., Wang, B., Deng, M., Liang, W., Deyholos, M.K., and Jiang, Y.Q. (2014). Identification and characterization of *CBL* and *CIPK* gene families in canola (*Brassica napus* L.). *BMC Plant Biol* 14(1): 8. doi: 10.1186/1471-2229-14-8.

Zhang, H., Yin, W., and Xia, X. (2008). Calcineurin B-Like family in *Populus*: comparative genome analysis and expression pattern under cold, drought and salt stress treatment. *Plant Growth Regul* 56(2): 129-140.

JPMB
Journal of Plant Molecular Breeding
Published by Genetics and Agricultural Biotechnology Institute of Tabarestan
2022 | Volume 10 | Issue 2

مقاله پژوهشی

شناسایی و تجزیه و تحلیل جامع خانواده ژنی *CBL* در پرتقال (*Citrus sinensis* L.)

سیدحمیدرضا هاشمی‌پطرودی*[۱]، حمیدرضا قربانی[۲]، فیروزه سهروردی[۱]، مژده عرب[۱،۳]

۱. پژوهشکده ژنتیک و زیست فناوری کشاورزی طبرستان، دانشگاه علوم کشاورزی و منابع طبیعی ساری، ساری ایران
۲. بخش تحقیقات علوم زراعی و باغی، مرکز تحقیقات و آموزش کشاورزی و منابع طبیعی استان مازندران، سازمان تحقیقات، آموزش و ترویج کشاورزی، ساری، ایران.
۳. گروه زیست فناوری مولکولی گیاهی، پژوهشگاه ملی مهندسی ژنتیک و زیست فناوری، تهران، ایران

چکیده: پروتئین‌های شبه‌کلسینورین B (CBL)، به عنوان حسگرهای کلسیم، نقش کلیدی در پاسخ‌های گیاه به عوامل تنش‌زای غیرزیستی مختلف و در رشد و نمو از طریق تعامل با پروتئین کینازهای متقابل CBL (CIPKs) ایفا می‌کنند. با این حال، اطلاعات در مورد نقش و کارکرد CBLs در گیاه پرتقال محدود است. در این تحقیق ژنوم گیاه *Citrus sinensis* مورد بررسی قرار گرفت و هشت ژن CBL شناسایی گردید. خصوصیت دامنه، موقعیت و توزیع موتیف‌های حفاظت‌شده پروتئینی نشان داد که دامنه EF-hands به طور نسبتاً زیادی در همه هشت CsCBL شناسایی شده حفظ شده است. پروتئین‌های CsCBL در گروه CBL اسیدی طبقه‌بندی شده و در این تحقیق پنج جایگاه myristoylation و شش جایگاه palmitoylation پیش‌بینی گردید. هشت ژن *CsCBL* بر روی چهار کروموزوم Chr01، Chr02، Chr04 و Chr05 و یک کانتیگ (chrNW-006257104.1) توزیع شده است. دو ژن *CsCBL4* و *CsCBL5* بر روی کروموزوم Chr05 پیوستگی داشته، که احتمالاً از طریق تکرارهای پشت سر هم ایجاد شده‌اند. درخت فیلوژنی ۳۷ پروتئین CBL از گونه‌های مختلف گیاهی از جمله آرابیدوپسیس تالیانا، برنج، کنجد و پرتقال نشان داد که این CBLها از ارتباط نزدیکی برخوردارند. نتایج این مطالعه ویژگی‌های عملکردی خانواده ژن *CsCBL* را برجسته نموده و اطلاعات ذی‌قیمتی را برای تحقیقات آینده در مورد فعالیت‌های عملکردی این ژن‌ها ارائه دهد.

کلمات کلیدی: پرتقال، پروتئین شبه‌کلسینورین B، تنش، حسگر کلسیم، پیام‌رسانی، CBL، *Citrus sinensis*.

ویراستار علمی
دکتر جونهوا پنگ،
مدیرتکنولوژی شرکت اگری‌ساینس اسپرینگ ولی، چین

تاریخ
دریافت: ۱۶ خرداد ۱۴۰۱
پذیرش: ۱۴ دی ۱۴۰۲
چاپ: ۲۲ دی ۱۴۰۲

نویسنده مسئول
دکتر سیدحمیدرضا هاشمی‌پطرودی
shr.hashemi@sanru.ac.ir;
irahamidreza@yahoo.com

ارجاع به این مقاله
Hashemipetroudi, S.H., Ghorbani , H., Sohrevardi, F. and Arab, M. (2022). Identification and comprehensive analyses of the *CBL* gene family in sweet orange (*Citrus sinensis*). J Plant Mol Breed 10(2): 76-91. doi:10.22058/jpmb.2023.1975801.1266.

Contents:

Address:

Genetics and Agricultural Biotechnology Institute of Tabarestan (GABIT)
Sari Agricultural Sciences & Natural Resources University (SANRU)
Khazar Abad road, Sari, Mazandaran, Iran P.O.Box: 578

www.jpmb-gabit.ir Tel : +981133687744